THE FRENCH ABSORPTION SPECTROSCOPY BEAMLINE IN MATERIAL AND ENVIRONMENTAL SCIENCES

REPORT TO SAC'S

BM30B REVIEW PANEL

NOVEMBER 2014

CONTENTS

The French Absorption spectroscopy beamline in Material and Environmental Sciences

2010-2014

Report to SAC's BM30B Review Panel

1. Introduction

Scientific case

FAME is the French Absorption spectroscopy beamline for Material and Environmental Sciences at the ESRF, one of the five French Collaborating Research Group beamlines, dedicated to X-ray Absorption Spectroscopy (XAS). The aim of this beamline is to cover a wide variety of common applications of XAS in Materials Science, biophysics, chemistry and mainly in environmental and geochemical sciences. Since 2002 we have concentrated our effort on the *in situ* study of diluted elements and small samples.

One of the particularities of XAS measurements in the field of environmental sciences is that the probed element (for instance a pollutant) often exists in highly diluted form in a surrounding medium. To optimize the XAS analysis at the FAME beamline we aim at providing the highest possible photon flux on the sample together with an efficient fluorescence detection. The detection limit for XAS measurements is estimated to be ~50ppm with the 30 elements SSD detector. To improve the sensibility in detection, in accordance with the findings of the last beamline review panel (2009), we have implemented a spectrometer with five crystal analysers. This spectrometer decreases the detection limit by a factor 3, and thus allows the investigation of multi-element natural samples with enhanced precision. This prototype is now quite user-friendly and has extended the range of application of XAFS towards molecular environmental science (High Energy Resolved Fluorescence Detected X-ray spectroscopy - HERFD-XAS - and X-ray Emission spectroscopy - XES -).

Thanks to this new low detection limit linked to a sub-millimetric beam-size and the new facilities given by the spectrometer, the scientific community has expanded in particular to catalysis and Earth sciences. In addition, the experimental setup of FAME and our different sample environments are very well-adapted to *in situ* measurements. This point is particularly suitable for high pressure - high temperature measurements in Earth science, in catalysis (*in operando* analysis, as a function of temperature, gas pressure...), electrochemistry...

The technical and instrumental progresses made on FAME are illustrated by the scientific contributions highlighted in this report in geochemistry, Earth and material Sciences, catalysis and biology. The high level of the scientific activity on FAME is confirmed *i)* by a large number of publications (around 30 per year) and *ii)* by a strong attractiveness of the beamline (average oversubscription rate of 5.8 for the ESRF beamtime allocation panels).

Students and users trainings

FAME is also actively involved in training activities (European HERCULES course, teaching practicals for graduate students of the University of Grenoble) and FAME+, a dedicated CNRS users training annual school we organize since 2004. Another fundamental contribution of FAME to training activities is the successful defence between 2010 and 2014 of around 30 *PhD* theses and French HDRs based on experiments carried out on the beamline.

Development of the collaborations

In accordance with the conclusions and recommendations given by the last beamline review panel , the staff has continued to establish a wide-ranging network of collaborations, both national and international (Australia and ETH Zurich).
i) Strong collaborations are developed within our in-house research activity on hydrothermal fluids through a French National Research Agency (ANR) funding (SOUMET project), and the French Australian Science and Technology (FAST) funding scheme together with the University of Adelaide.
ii) The activity of the beamline in Nanosciences associated with the development of the new high resolution spectroscopy is carried out *via* our integration in an International Consortium for the Environmental Implications of Nanotechnology (ICEINT) and an ANR funding scheme together with CEREGE (Aix-Marseille) during the MESONNET project.

Projects and perspectives

FAME and FAME-UHD

The spectrometer developed on FAME is designed for a two-branch front end, which leads to considerable steric restrictions in the design of the components that limit the efficiency of this setup. For this reason, the new perspectives offered by the availability of the spectrometer will be exploited more efficiently on the new FAME-UHD (Ultra High Dilution) beamline currently under construction on ESRF's beam port BM16. This beamline is expected to be available to regular users by January 2016 and will offer a considerable increase of beamtime for the community.

In-house research activity on hydrothermal fluids

Raman spectroscopy. In accordance with the conclusions of the last beamline review panel, in a first step, our team has implemented a Raman spectrometer for in-house research activity on hydrothermal fluids at the Neel Institue. The high pressure/high temperature (HP-HT) autoclave of the *in situ* Raman setup is an evolution of the autoclave designed for X-ray Absorption Spectroscopy. The next step, depending the available funding, will be to develop the simultaneous measurement of Raman and XAS spectra on the beamline.

Spectroscopy at higher pressure: a 10 kbar autoclave. Our team, with the strong support of the technical staff of the Neel Institute, developed a new autoclave, dedicated to X-ray and optical spectroscopic techniques up to 10 kbar (i.e., one order of magnitude higher than the range currently available on FAME). This would extend the accessible domain of the pressure-temperature diagram to values, at which speciation measurements are available to relevant high-pressure conditions (magmatic hydrothermal conditions). Technological developments have already been done (10 kbar valve, licence CNRS-Autoclave France, Réseau technologique des Hautes Pressions; design of the HP body), but there is still work to be done in particular on the windows and the heater.

Collaborations. Our team is integrated into an Equipex project (Planex, 2013 to 2020). Planex aims at developing an (HP-HT) experimental and analytical platform allowing to perform *1) in situ* chemical, structural and isotopic analysis on fluids (molten silicates and salts, hydrous fluids) and gases, and *2)* the simulation of fluid transfer processes in geomaterials or their synthetic equivalents.
Our team has been integrated in this consortium for our strong expertise in the development of HP and HT experiments, including the study of the behavior of fluids as a function of temperature and pressure using X-ray absorption spectroscopy and Raman scattering. We also have, since several years, a renowned expertise in the study of hydrothermal fluids and supercritical fluids using small angle X-ray scattering, Inelastic X-ray Raman spectroscopy, Raman spectroscopy and X-ray absorption Spectroscopy analysis.

FAME and the ESRF upgrade.

The design of FAME has been adapted to anticipate the foreseen increase of the quality in emittance and brilliance of the source during the ESRF Upgrade Programme Phase II. Making use of a dedicated optimized source (current reflections are based on using 3 pole wiggler instead of a bending magnet) will fully exploit the beamline equipment's quality and performance.

Development of the staff

Our main requests concern the evolution of the beamline staff. Even if one of our goal is to automize the beamline as much as possible, our team will have to manage two beamlines FAME and FAME-UHD with only three permanent "local contact" positions (two Beam Line Operating Manager (BLOM) and one full time scientist) and the support of two technicians. To maintain, develop and reinforce the scientific and technical activities of the beamline portfolio, a further permanent position is needed. A position like an ESRF BLOM would be suitable, particularly for the Earth Sciences community.

The report

After a brief presentation of the beamline, selected scientific topics which are representative of results obtained at FAME in recent years will be brought to the attention of the committee: geochemistry & environmental sciences, hydrothermal fluids, mineralogy & cosmochemistry, biochemistry, materials science, catalysis and material for energy. A selection of significant papers are reprinted in the appendix, they are representative of the various scientific topics in which the beamline is clearly involved: hydrothermal fluids (Louvel et al. 2013), nano-ecotoxicology (Auffan *et al.* 2014), biochemistry (Sarret *et al.* 2010), catalysis (Gorczyca *et al.* 2014) and material science (Rodolakis *et al.* 2010), the two last papers being linked to the development of the crystal analyzer spectrometer on FAME.

2. Beamline staff

As FAME is a 'national' Collaborating Research Group (CRG) beamline, its organization differs slightly from that of ESRF beamlines. The beamline is managed by a staff of 6 CNRS[1] permanent employees and 1 junior scientist. The recommendation of the previous BLRP (2010) concerning the staff evolution was the creation of an "additional permanent engineer position". This point was solved in 2011 with the recruitment of Isabelle Kieffer as an "Ingénieur de Recherche CNRS" (new position).

	Organism	**Position**	**Time on Beamline**	**Professional degree**	from	to
Hazemann J.-L.	CNRS[1]	Senior scientist, Beamline responsible	50%	Geophysics	beginning	*
Testemale D.	CNRS[1]	Junior scientist	50%	Physics	03/2007	*
LLorens I.	CNRS[3]	Junior scientist	50%	Chemistry	09/2013	12/2014
Proux O.	CNRS[2]	BeamLine Operation Manager		Physics	beginning	*
Kieffer I.	CNRS[2]	BeamLine Operation Manager		Physics	12/2011	*
Delnet W.	CNRS[2]	Technical engineer		Electronic	08/2006	*****
Lahera E.	CNRS[2]	Technical engineer		Engineering	beginning	*****
Ulrich O.	CEA[4]	Control-command engineer	15%	Electronic and computing	beginning	*
		Former staff				
Ranieri V.[2]	CEA[4]	Post-doc. Fellow		Chemistry	03/2010	03/2012
LLorens I.	CEA[4]	Post-doc. Fellow		Chemistry	02/2008	02/2010
Nassif V.[3]	CEA[4]	Post-doc. Fellow		Chemistry	06/2004	06/2006
Palancher H.[4]	CEA[5]	Post-doc. Fellow	50%	Physics	01/2005	01/2007

Table 1: Beamline staff for the 2010-2014 period. In purple: actual staff. **1** : Institut Néel, Grenoble, CNRS; **2** : Observatoire des Sciences de l'Univers de Grenoble, UJF Grenoble – CNRS; **3** : Institut de recherches sur la Catalyse et l'Environnement de Lyon– CNRS ; **4** : CEA Grenoble - INAC/SP2M/ Nanostructure et Rayonnement Synchrotron ; **5** : CEA Cadarache - DEC/SESC/LLCC ; *****: permanent position

[1] French National Center for Scientific Research, http://www.cnrs.fr/
[2] now scientist at *Saint Gobain CREE* (Centre de Recherches et d'Etudes Européen) - permanent position
[3] now CNRS "Research Engineer" on CRG-D1B (at ILL) - permanent position
[4] now scientist at CEA-Cadarache (DEC/SESC/LLCC) - permanent position

Jean-Louis Hazemann
Beamline responsible for all scientific and technical aspects. Scientific interests include the study of aqueous solutions in sub- or supercritical conditions. This research area leads him to develop high pressure / high temperature instrumentation for *in situ* characterisations by X-ray Absorption Spectroscopy, Small Angle X-ray Scattering… Assists users to perform their experiments.

Denis Testemale
Scientific interests include the study of aqueous solutions in sub- and supercritical conditions, transport of metals in hydrothermal fluids. He also works on the development of HP/HT instrumentation. Assists users in their experimental runs.

Isabelle LLorens
Junior scientist at Institut de Recherches sur la Catalyse et l'Environnement de Lyon (end of contract: 12/2014). Assists users in performing their experiments, especially for catalysis experiments. In charge of the chemistry laboratory.

Olivier Proux
Beamline Operation Manager (CNRS "Research Engineer"), assists J.-L. Hazemann in the beamline management, upgrade and development. Engineering interests include the development of crystal analyser spectrometer projects. Assists users in performing their experiments.

Isabelle Kieffer
Beamline Operation Manager (CNRS "Research Engineer"), assists J.-L. Hazemann in the beamline management, upgrade and development. Engineering interests include the development of the detection systems. Assists users in performing their experiments.

William Delnet
Technical engineer. Responsible of all the software and hardware instrumentations on the beamline.

Eric Lahera
Technical engineer. Designs, draws and constructs mechanical apparatus (1^{st} and 2^{nd} crystals supports of the monochromator, diodes, crystal analyser spectrometer, high pressure / high temperature vessel and cells…).

Olivier Ulrich
Beamline Operation Manager (CEA "Research Engineer"). Responsible of all the software and hardware instrumentation on BM32 (CRG-IF) beamline. High level technical assistance for software and hardware instrumentation issues.

3. Statistics

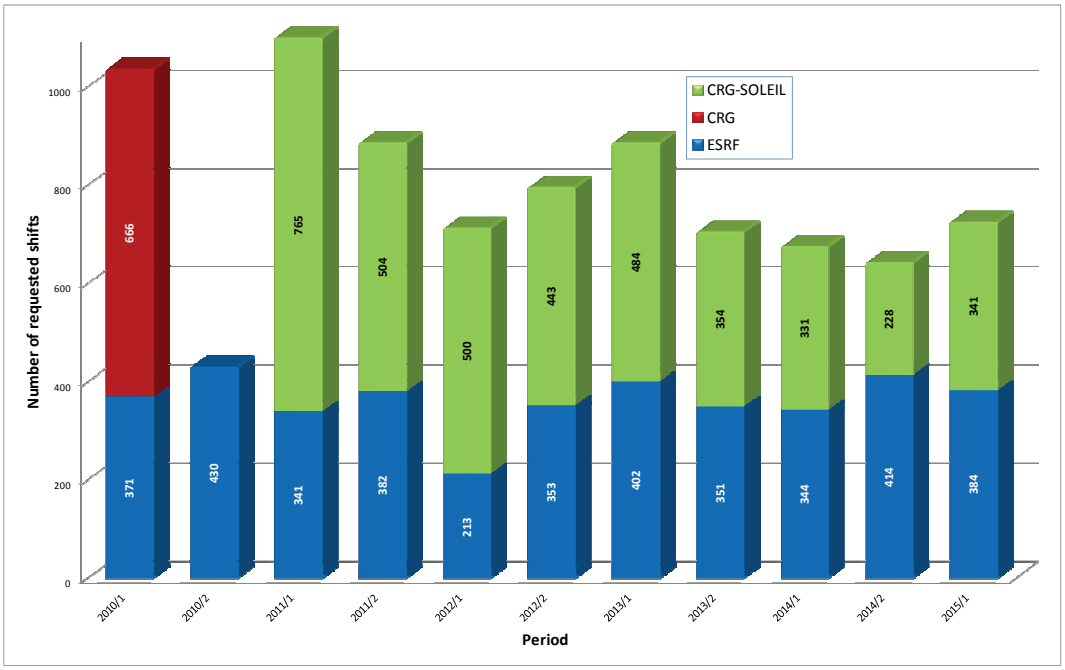

Figure 1. Requested shifts to the ESRF (blue, frequency : 1 semester), CRG (red, frequency : 1 year) and CRG-SOLEIL (green, frequency : 1 semester) committees.

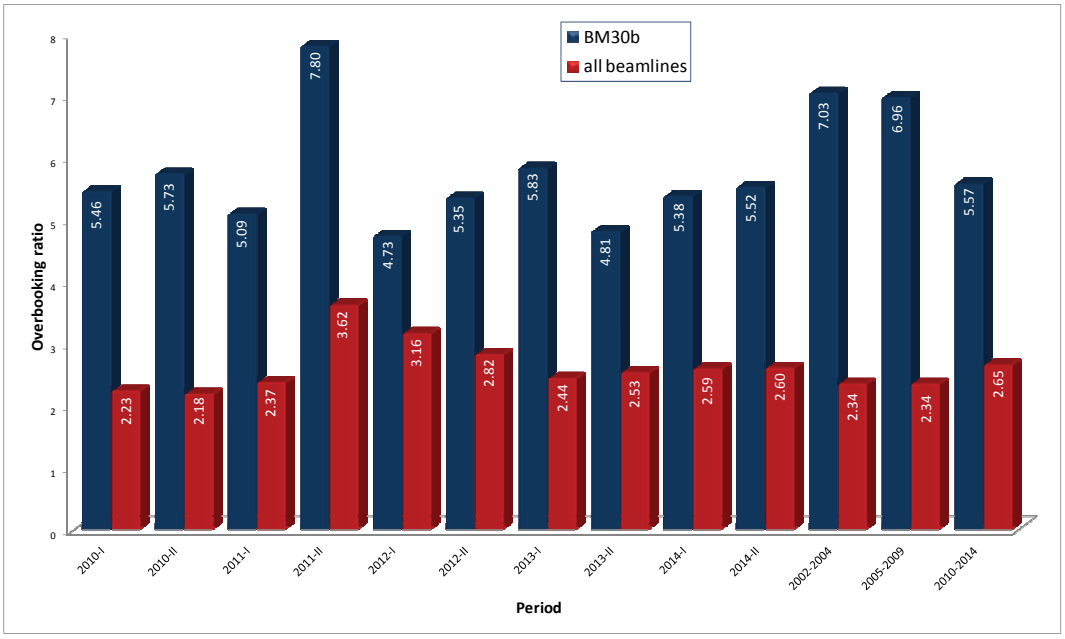

Figure 2. Evolution of the BM30B overbooking ratio (ESRF committee)

Statistics

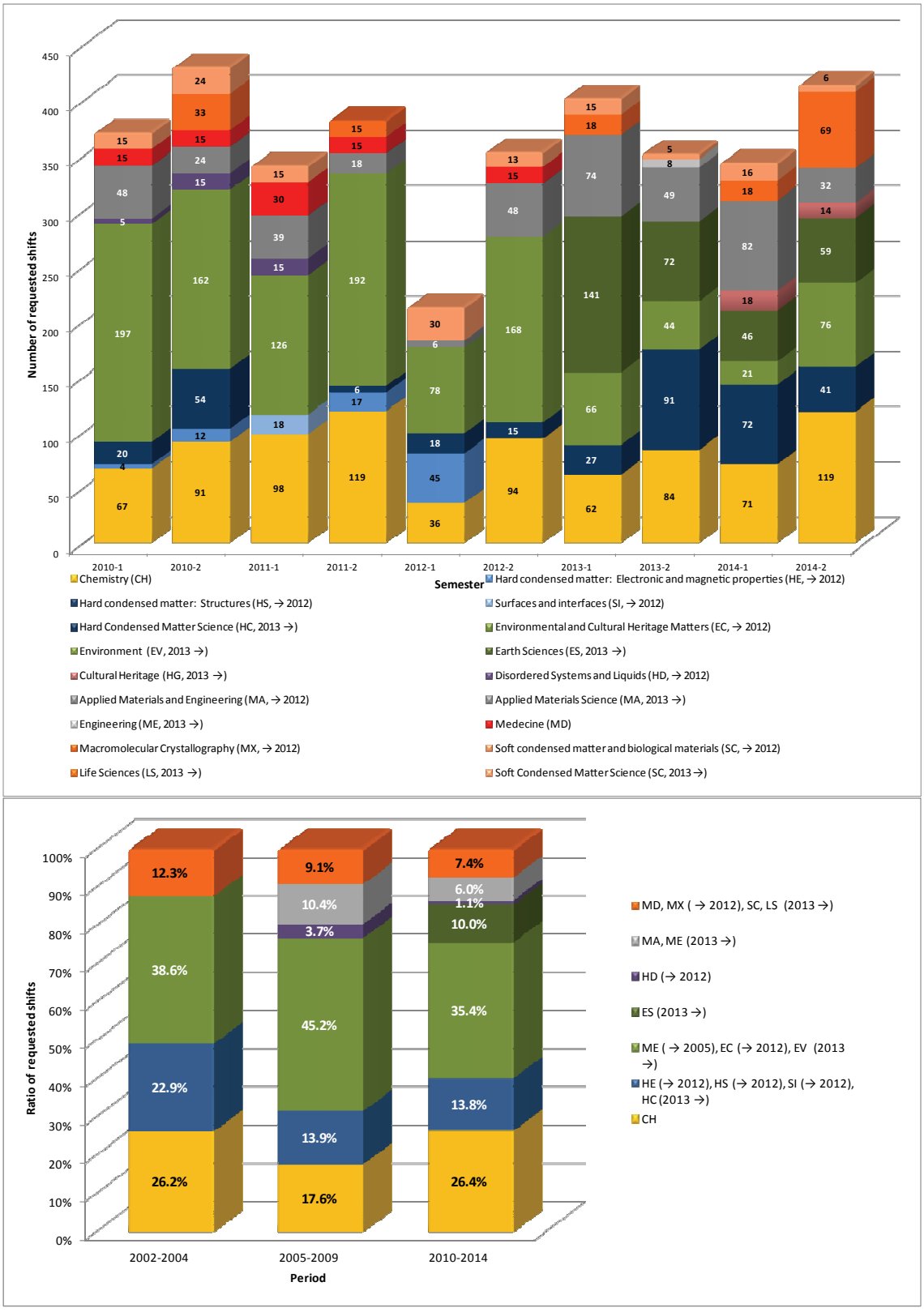

Figure 3. Repartition of the requested shifts to the ESRF scientific committees

Statistics

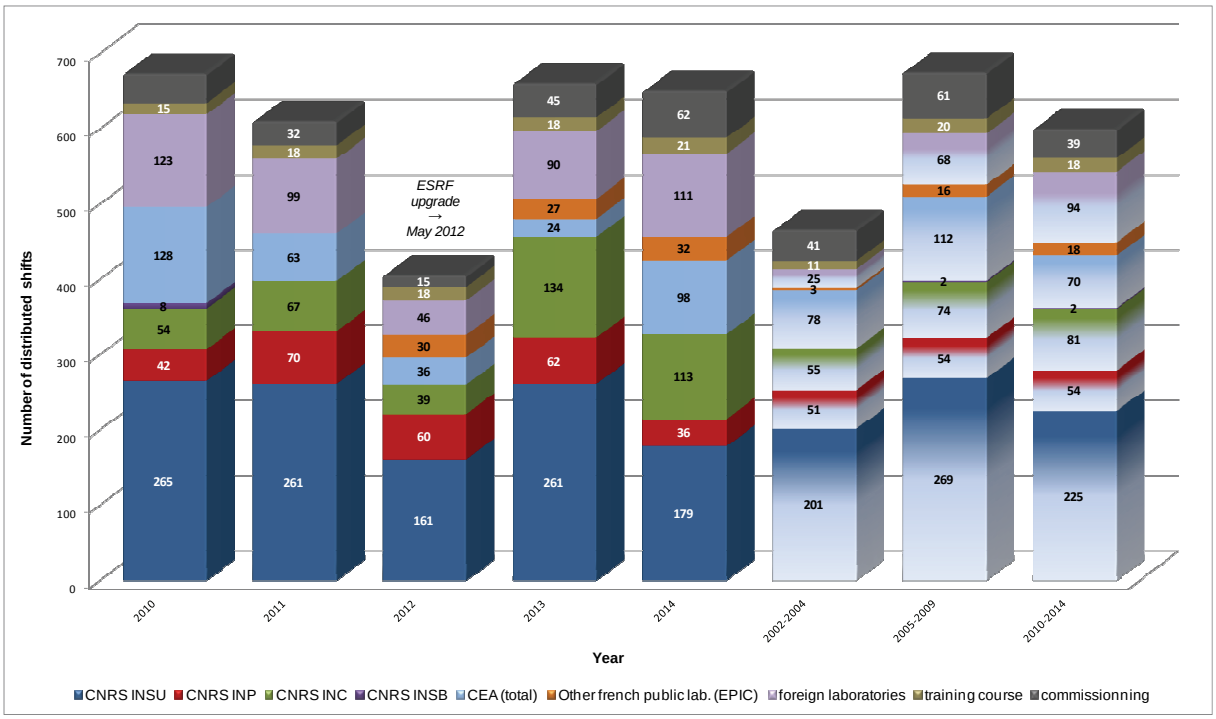

Figure 4. Repartition of the distributed shifts. CNRS: French National Center for Scientific Research. INSU: National Institute for Earth Sciences and Astronomy. INP: Institute of Physics. INC: Institute of Chemistry. INSB: National Institute for Biological Science. CEA: French Atomic Energy Center.

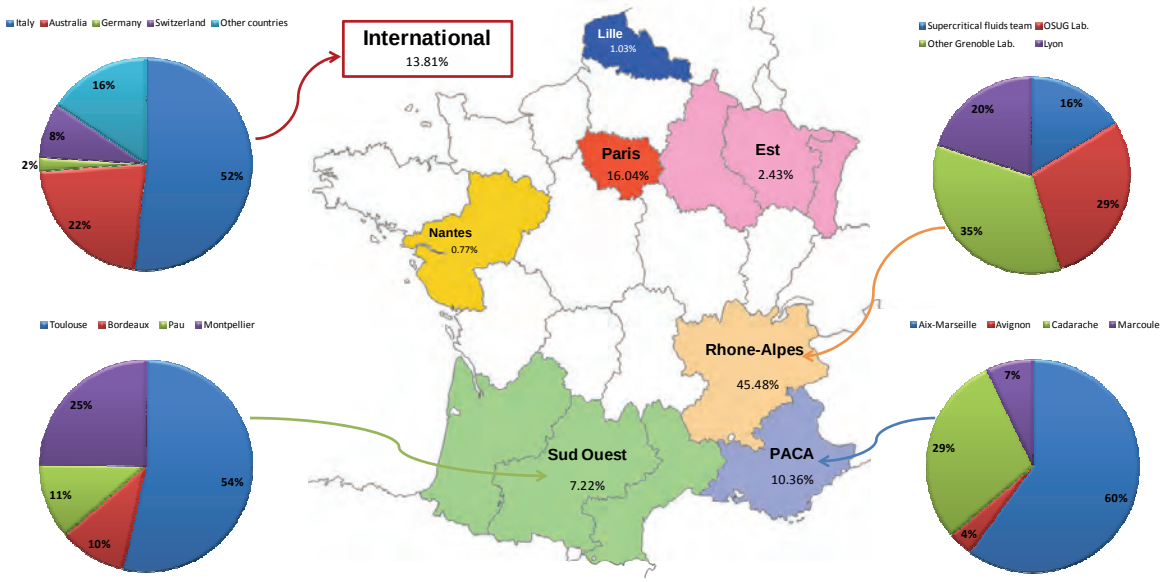

Figure 5. Repartition of the BM30B beamtime allocated by both the CRG and ESRF review committees as a function of the geographical localization of the main proposer.

Statistics

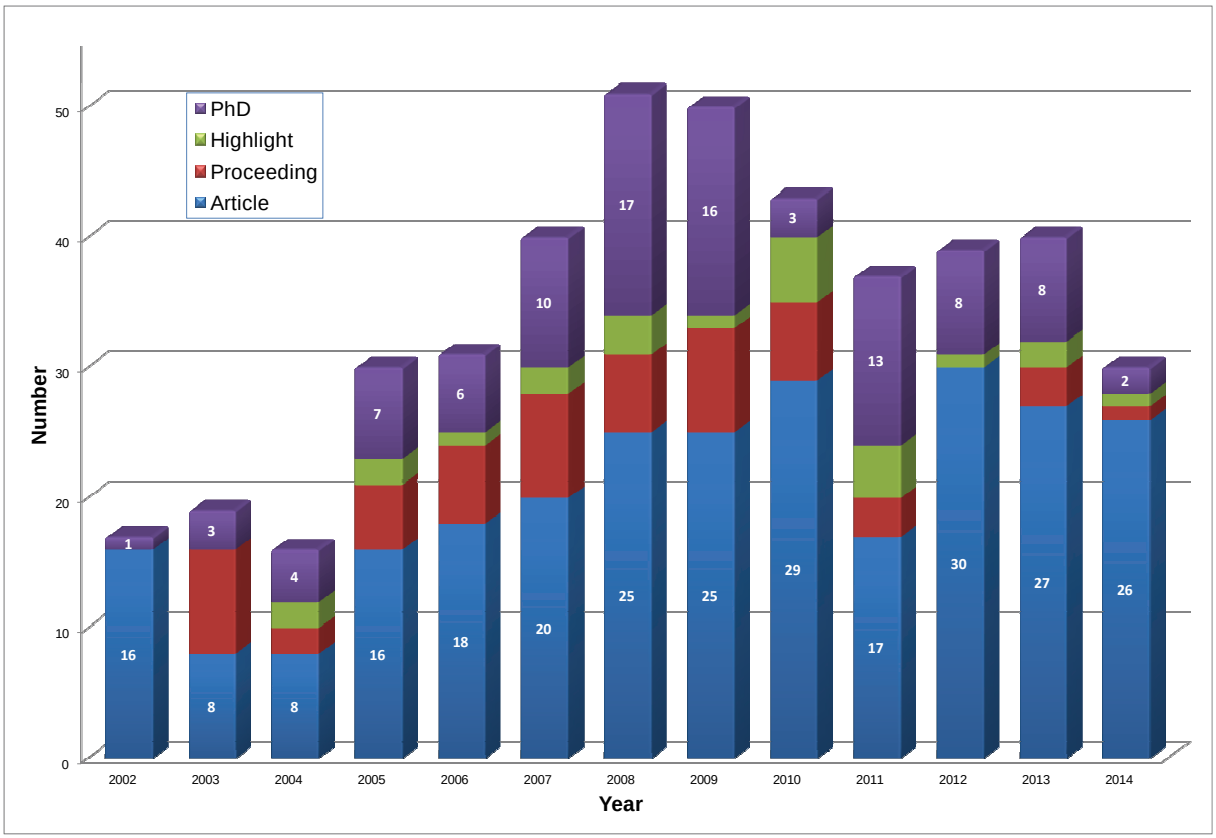

Figure 6. Evolution of the number of articles, proceedings and highlights published from results obtained on BM32 XAS station (1998-2001, 40% of the beamtime) and on BM30B (since 2002)

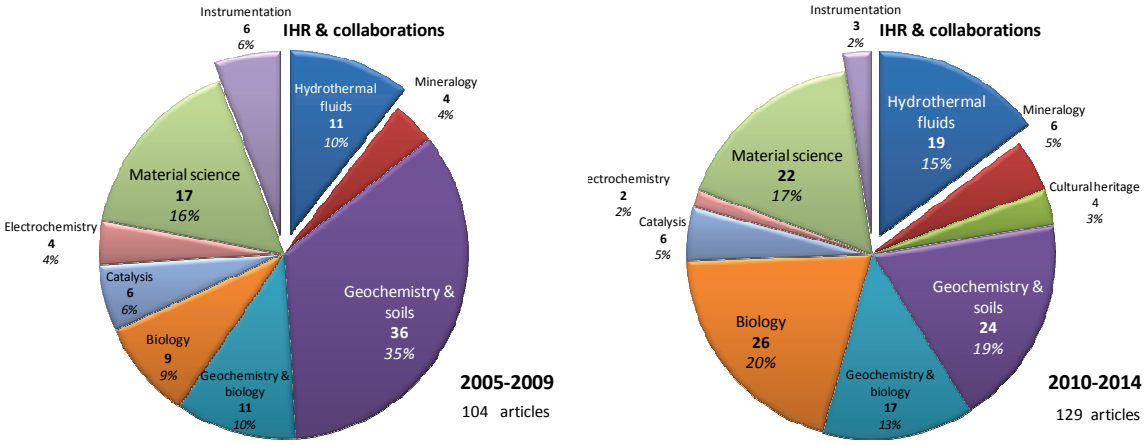

Figure 7. Evolution of the number of articles published from results obtained on BM30B between the two last BLRP periods.

Statistics

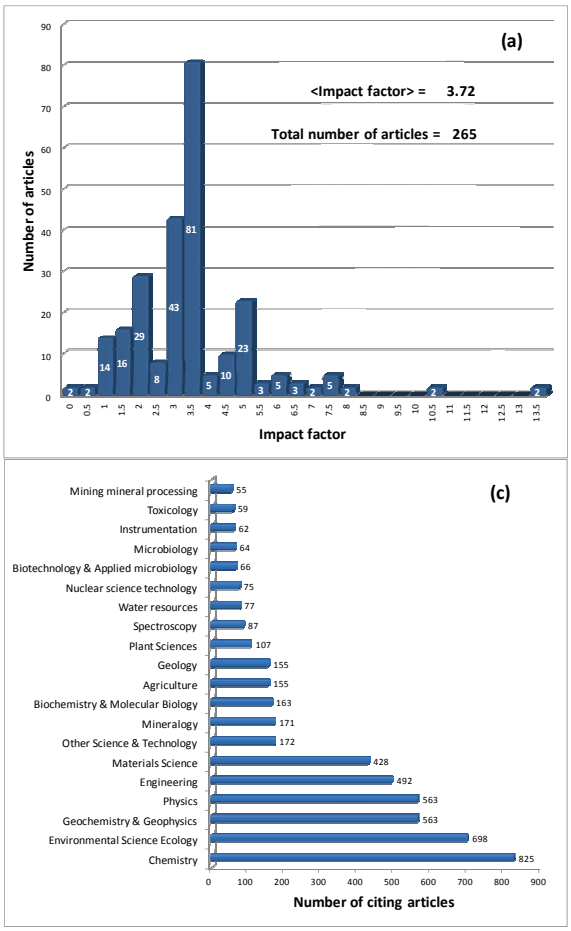

Figure 8. Bibliometric data**. (a)** Distribution of the Impact Factor of the journals (ISI Web of Knowledge 2012). **(b)** Distribution of the ranking of the journals (in order to compare journals of very different scientific fields, ISI Web of Knowledge 2012)[1]. **(c)** Distribution of the number of citing articles as a function of the scientific fields (FAME beamline Researcher ID profile, 25/07/2014)

[1] The impact factors are highly dependent on the scientific fields and are difficult to use to compare journals across disciplines. Science performed on FAME being multidisciplinary we give also distribution of the number of articles as a function of the ratio between the ranking of the current journal in its subject categories based on the journal Impact Factor and the number of journals in the same subject categories. A kind of ranking index. For example, *for Geochim. Cosmochim. Acta* (2012 impact factor : 3.88 - subject category : geochemistry & geophysics) the journal rank is 6 with 76 journals in the category, the ranking index equals 6/76, i.e. 8/100.

4. Technical specificities of the beamline

BM30B CRG-FAME is dedicated to X-ray Absorption Spectroscopy. The purpose of the beamline is the determination of the electronic and local structure of very diluted elements in materials coming from a wide range of fields such as environmental and Earth sciences, electrochemistry, catalysis, biology and solid-state physics. An important point is the possibility to analyse, with the maximum photon flux, *i)* samples in a particular environment such as high pressure cells (in this case the smaller the beam is, the higher the maximum reachable pressure is), *ii)* samples that might be sensitive to radiation damage (possibility to work below 10K) and *iii)* samples under grazing incidence to perform depth-dependent of polarization measurements. Finally, to analyse samples with complex matrices and to take benefit from the development of powerful codes to calculate XANES signals, it is also of primary importance to obtain experimental data with optimum detection energy resolution.
Schematically the three key points of the beamline are:

- a maximum and stable photon flux on the sample to probe elements at a high level of dilution producing only weak signals,
- a small spot size to probe small samples,
- a versatile focal point, so that different detectors may be used with different sample environments.

1. General features

The FAME beamline is located on a 0.85 T bending magnet (BM) of the ESRF storage ring. The basic optical design of FAME is shown in Figure 1.[1] A special liquid-nitrogen cooled two-crystal monochromator, designed and constructed by our team,[2] is located between two grazing-incidence mirrors. The monochromator allows to select the desired photon energy. The main aim of the mirrors is the rejection of the high energy harmonics. Due to the rhodium mirror coating, such a configuration is suitable for studies at energies lower than 22 keV. The beamline can also operate in a mirror-free configuration, extending the energy limit to at least 40 keV. The photon energies available on FAME range from 4 to 40 keV, allowing to probe elements starting from Ca (Z=20) to U (Z=92) combining analysis at the K and L_{III} absorption edges.[3]

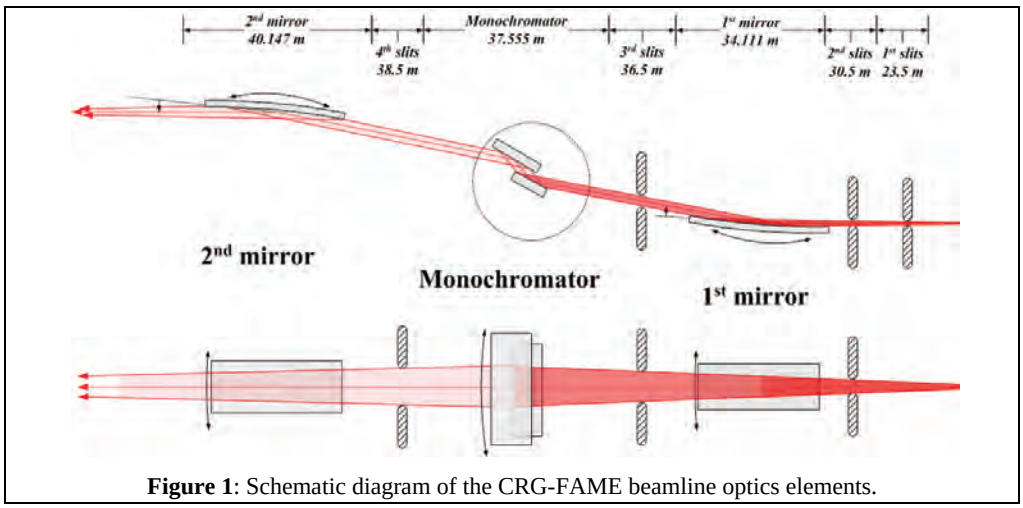

Figure 1: Schematic diagram of the CRG-FAME beamline optics elements.

[1] Proux *et al.*, *Physica Scripta* **115** (2005) 970-973
[2] Proux *et al.*, *J. Synchrotron Radiat.* **13** (2006) 59-68
[3] http://www.esrf.fr/UsersAndScience/Experiments/CRG/BM30B/Mendeleev

To **maximize the flux** on the sample, especially at low energies, the beam line was optimized such as to accept the 2 mrad horizontal (maximum divergence on a double front end BM) and 0.3 mrad vertical divergences delivered by the BM. Three factors, crucial for the **stability** of all the optical elements, were particularly optimized: *i)* the quality of the cooling devices and their thermal stability, *ii)* the suppression of vibrations due to the pumping and cooling systems and *iii)* the permanent maximization of the beamline transmittance (especially linked to the optimization of the 'parallelism' between the two crystals of the monochromator).
The monochromatic beam is **focused** on the sample in the vertical direction with the 2nd mirror (down to 100 µm) and in the horizontal one with the 2nd crystal of the monochromator (below 300 µm, even at low energies). The second crystal is dynamically curved (radius from 1m to ∞) during the XAS energy scan in order to keep the beam focused on the sample in the horizontal plane[4].
Thanks to the quality of the 1st bent mirror and the cooling of the 1st crystal of the monochromator down to 110K, the **energy resolution** of the incident beam is found to be close to the intrinsic resolution of the crystals (Darwin width).[2] Si(220) crystals were chosen instead of Si(111) ($\Delta E/E \sim 5.6\ 10^{-5}$ instead of $1.3\ 10^{-4}$). This resolution is adequate for XANES studies.
Since the beginning, fluorescence **detection** is achieved with a 30-element Canberra Ge solid state detector (SSD, Figure 2, on the right of the experimental table). With a shaping time of 0.5 µs, its average energy resolution is around 270 eV (FWHM, like all the energy resolution numerical values given in this report) as measured classically with a ^{55}Fe source (Mn Kα peak, 5.9 keV). The maximum total input count rate equals to 30 kcounts/s/element without correction of dead time. The **limit of dilution** for an EXAFS analysis is found around 100/200ppm for an element in a natural soil and is reduced for biological samples (down to 20µmol/l).
In the case of elements diluted in a complex matrix, the 5-crystal analyser spectrometer is used (Figure 2, in the middle of the experimental table). The resolution is about 1.5 eV. It enables to distinguish, for example, the Kα fluorescence line of a Z element from the Kβ fluorescence line of the Z-1 element, which is not possible with the SSD.

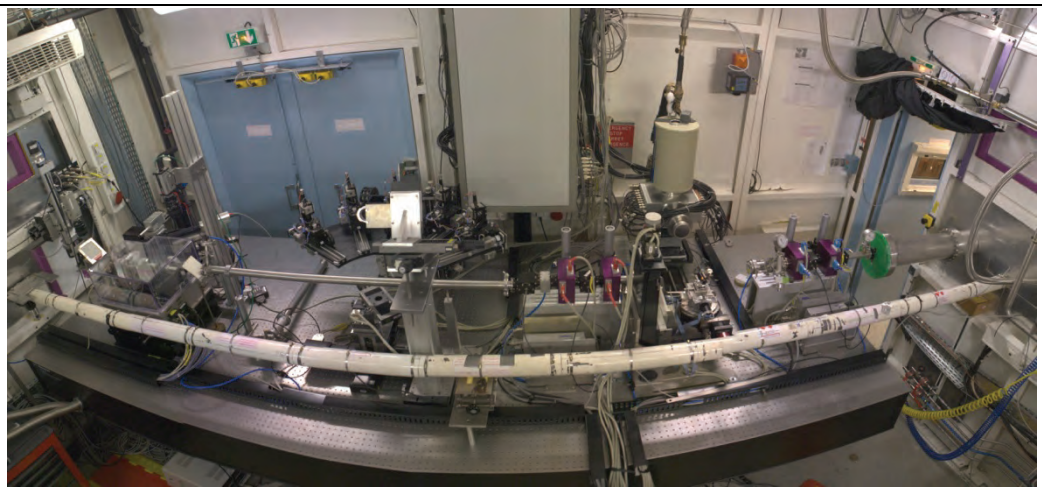

Figure 2. Experimental hutch with three experimental station, from left to right : micro-focus Kirkpatrick-Baez mirrors, 5-crystals Crystal Analyzer Spectrometer and 30-element Solid State Detector stations.

2. Main technical evolutions

2.a. Automatisation of the alignment procedures

Each time a user wants to study another absorption edge, the whole beamline has to be re-optimized: mirrors, slits, monochromator, experimental table. This optimization takes around 3 hours. In order to make this operation less time-consuming and accessible for experienced users, we started to implement routines that help to align the different optical elements. As a first step, it will ease the

[4] Hazemann J.L., Nayouf K. and de Bergevin F., *Nucl. Instr. and Meth. B*, **97** (1995) 547-550

alignment procedure, avoiding mistakes and waste of time in repetitive tasks. The main idea is to give more flexibility to the users in the organisation of their experimental plan. In a second time, we might think at teaching the procedure to the experienced users, at least in the simplest and more common cases.
The automatic alignment procedure is divided into 6 independent parts. The step-by-step sequence of the alignment, starting from the cut-off energy by the mirrors to the first spectrum acquisition (a reference for calibration) is given on Figure 3.

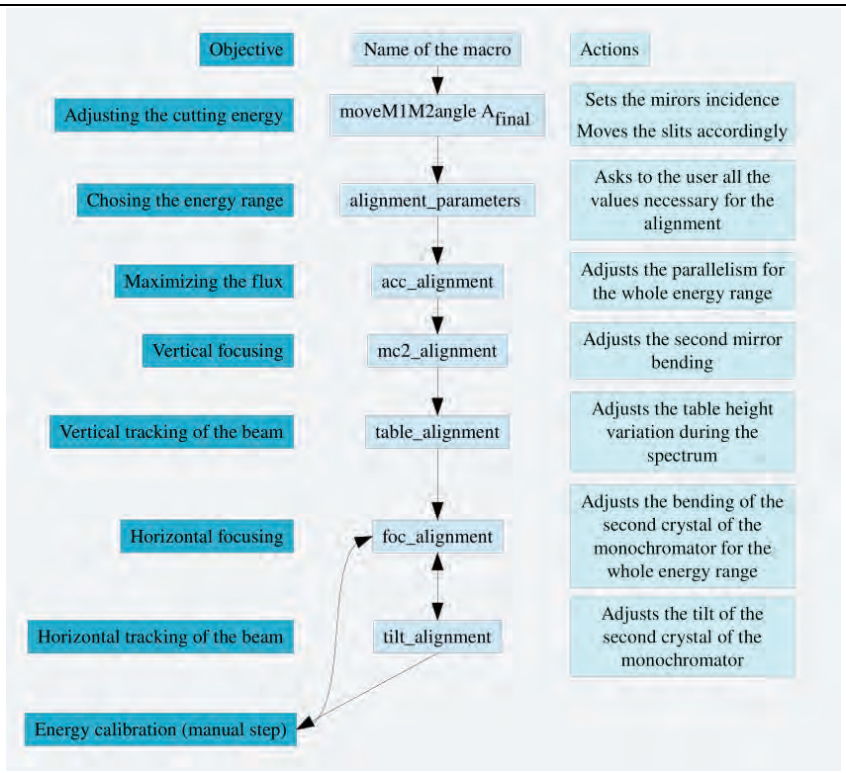

Figure 3. Automatisation of the beamline adjustments

The macros have been written so that they can be used whatever the experimental station (i.e. whatever the position of the focus point), using either the solid state detector, the micro-focus station or the crystal analyzer spectrometer.
Each time the procedure is used, a file logging all the steps and the beam characteristics is created and the positions of the motors are stored in tables. Those tables are used as a starting point for the future alignments. They can also be used to follow the evolution of the optical elements along the years.

2.b. New positioning system : ICEPAP

The positioning system was based on DPAP2 cards since the beginning of BM30B operation, that is 2002. ESRF has developed another motor control system, called Icepap and tested on the beamlines since 2006. Progressively, all the ESRF beamlines are being equipped. The Icepap system allows new possibilities such as higher power, encoder reading, closed loop operation, hardware synchronisation or high resolution positioning.

Since our system was aging, we decided to change all the positionning system : doing this, we maintain our compatibility with ESRF, we gain in reliability, in space and open new possibility (control of brushless motor should be possible in short term for example). This operation started on the beamline in January 2014 and has been finished in August 2014 for the optical hutches motors (Figure 4). The change for the experimental hutch motors will be done until the end of the year.

Figure 4. Part of the electronic installation on BM30b, actual with the new IcePap controllers (left) and old with the DPap & VPap controllers (bottom)

3. Sample environments

The experimental table is quite large on FAME (4m x 1.5m), the sample holder allows to align precisely even heavy sample (or sample environment), up to 100kg. These 2 points give us the possibility :

- to develop different experimental stations (since 2002 we successively installed a Kirkpatrick-Baez focusing mirrors station and a crystal analyzer spectrometer one in addition to the usual one linked to the solid-state Canberra detector),
- to propose to users complex sample environments, such as a liquid helium cryostat (developed at ILL and Institut Néel for the sample-holder) and a high pressure / high temperature vessel developed by the team.
- to adapt on the beamline specific *in-situ* device such as high temperature oven, catalysis oven, electrochemistry cells... depending on the user's needs.

Experiments performed on FAME are therefore done in most cases with a specific sample environment ; details in the beamtime repartition are given on Figure 5.

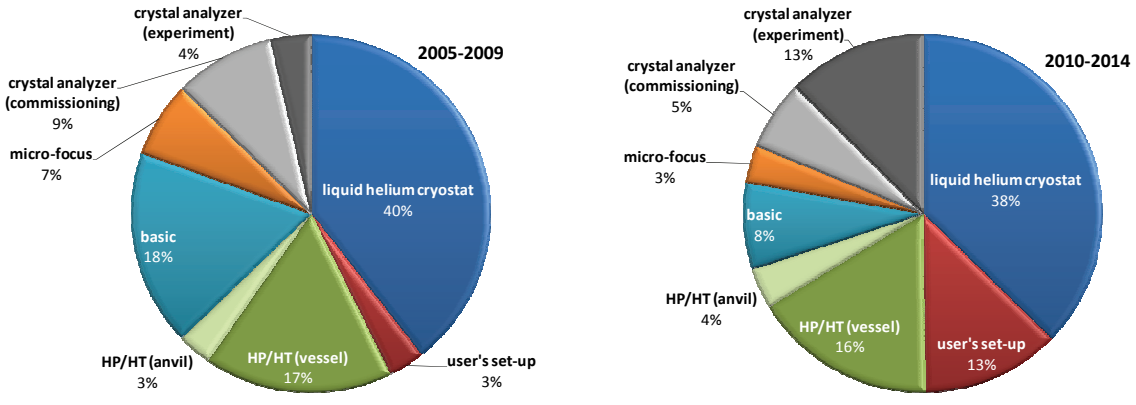

Figure 5: Beamtime ratio for the previous (left) and actual (right) BLRP periods as a function of the experimental set-up

The liquid helium cryostat, an ILL-"orange-cryostat" (Figure 6), can operate from 300 K down to liquid helium temperature. The rotation and the vertical translation of the sample-holder are motorized and up to five samples can be installed simultaneously. The main purpose of the cryostat is the protection of the samples from radiation damages. Its main features include large sample top loading capability (Ø50mm) and an isolated sample area with static exchange gas. Several improvements have been made since 2010 :

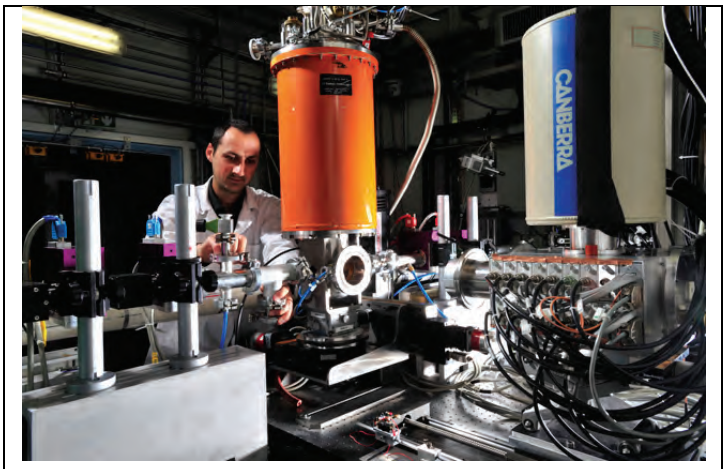

Figure 6. 30-elements Canberra Solid State Detector with the liquid helium cryostat (orange ILL cryostat)

- the complete renewal of valves and seals has been performed in 2010,
- the cryostat is associated since 2012 with a cold-valve controller (temperature adjustment is performed by adjusting the pressure of helium after the cryostat exchanger, i.e. by adjusting the helium evaporation), and LN_2 and LHe level monitors (which control automatically the cryogenic liquids refill).

Our HP/HT setup[5] has been operational on FAME since the construction of the beamline and has been used successfully by our team and our collaborators (Figure 7). As demonstrated in the chapter 6 with scientific examples, this tool is still unique in the world. Its interest in the community is even growing steadily (see figure 7, chapter 3: the number of published studies that make use of our set-up doubled in the last two BLRP periods). Our integration in the Néel Institute is a key factor to this success, with the crucial contribution to this technological development by the CNRS instrumentation and CRG technical groups.[6]

The success and resilience of an equipment installed on a synchrotron beamline and available to users rely on two factors: its constant upgrade to fulfill the changing and challenging experimental conditions targeted by users, and the polishing of its interface to make its use as reliable and smooth as possible for them. In this context, our group did improve the HP setup in the last 4 years:[7]

- better global integration on the beamline (fixed HP capillaries, better automation and control);
- new HP valves with better reliability and less maintenance;
- we designed, tested and used original glassy carbon HP windows for very high purity and low energies applications. The benefits from these original windows were immediate in the context of our collaboration with I. Daniel and A. Picard (HP respiration of deep-sea piezophilic organisms), where we could measure the XAS signal from 50ppm Fe solutions up to 1500 bar.[8]
- the design of the internal glassy carbon cell has been constantly improved for specific applications (low density fluids, phase separation, high acidity fluids, etc.).

[5] Testemale *et al., Rev. Sci. Instrum.* **76** (2005) 043905
[6] Bruyère *et al., Journal of Physics: Conference Series* **121** (2008) 122003
[7] These improvements were made possible by different external funding : High Pressure french network for the glassy carbon windows ; National Research Agency "ANR blanc" SOUMET 2011-2015 for the pressure and temperature regulations
[8] Picard et al., *Geochimica et Cosmochimica Acta* **88** (2012) 120–129

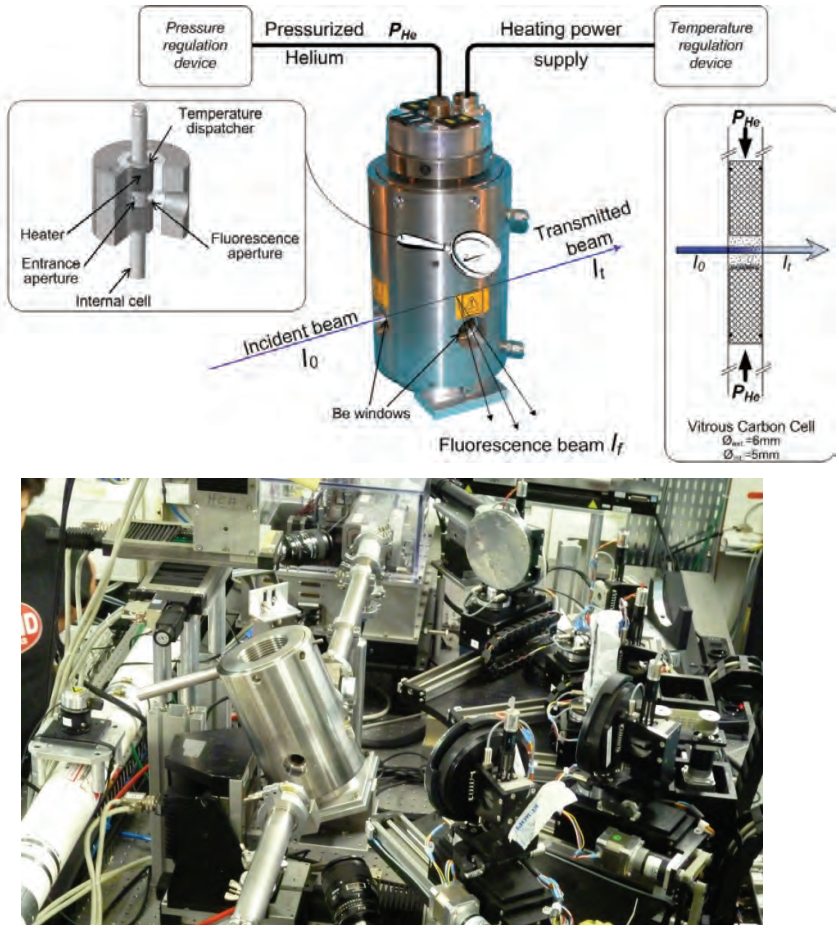

Figure 7: ***Up*** : schematic view of the high pressure / high temperature vessel used for XAS measurements. The gas pressure inside the vessel is stabilized with a special pressure regulation device. Details of the internal heating system are shown in the left inset. ***Down*** : vessel on the beamline during tests with the crystal analyzer spectrometer.

Complementarities XAS spectroscopy and visible Raman. XAS spectroscopy brings structural data about species in solution ; complementary information on the solvent itself can be given by visible Raman spectroscopy. For this reason, this high pressure/high temperature autoclave has been duplicated and adapted to perform, exactly on the same P,T conditions, Raman experiment.[9] The set-up is installed since 2012 at Neel Institute, and is regularly open to collaborators (Figure 8).

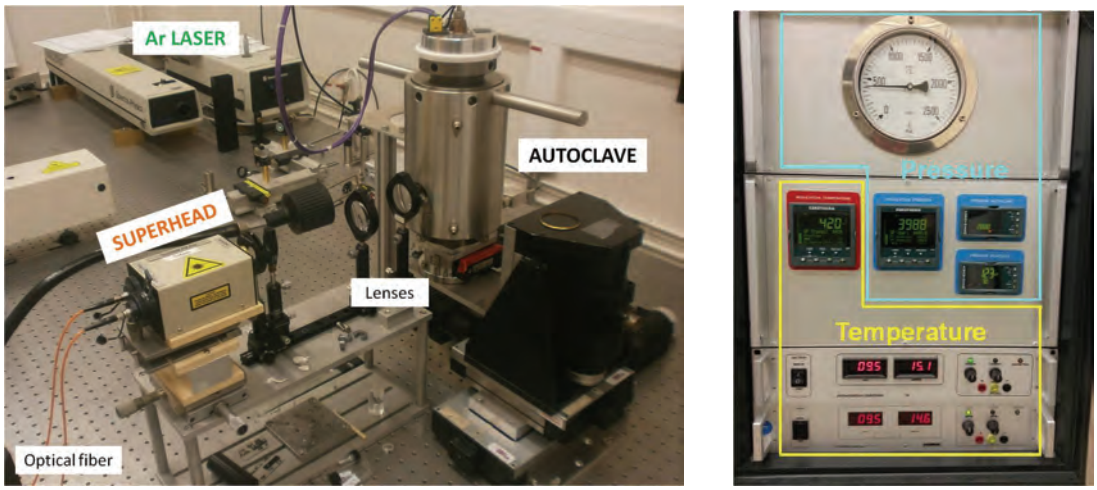

Figure 8. high pressure / high temperature set-up used for Raman measurements at Neel institute

[9] Louvel et al., *Journal of Molecular Liquids*, accepted

4. High Resolution Spectroscopies

As mentioned in the conclusions of the 2005 BLRP, the BM30B beamline team was encouraged to "implement a spherically bent analyzer for selection of fluorescence of minority species with an energy resolution of 20 eV". This project is a continuation of all the experimental tests performed on the beamline since December 2003 in order to determine if the use of a high energy resolution detector system, a bent Crystal Analyzer Spectrometer (CAS) complementary to the solid state detector, is possible on a bending magnet beamline.
This project was developed in the 2005-2009 period, with the construction and commissioning of a 5-crystals spectrometer with a 0.5m radius of curvature[10]. The achieved energy resolution is around 1-2eV. The 2009 BLRP's conclusions mentioned that "the new analyser is allowing high quality XANES spectra to be collected from complex and dilute samples with high fluorescence backgrounds". The main advantages of a measurement with an energy resolution around 1 eV are *i*) that EXAFS measurements can be achieved on complex systems (where the detection limitation is determined by the fluorescence of the main constituents of the matrix) and that *ii*) structure resolution of XANES spectra is much sharper than what could be achieved classically. Some official experiments with users were then performed[11]
In the 2010-2014 period the spectrometer was used for official experiment (13% of the beamtime, Figure 5), even if we still performed commissioning and technical developments (5% of the beamtime).

4.a Technical aspects

The multi-crystal analyzer spectrometer was first designed for crystals with a 0.5m radius of curvature (Figure 9, left).[10] This configuration allows to analyze photons emitted by the sample (fluorescence or scattered photons) on a large solid angle, with an energy resolution around 1.4eV for Cu $K_{\alpha 1}$, 3eV for Co$K_{\alpha 1}$. This set-up was used for example by Vichery *et al.* to probe Co neighbourhood in Fe oxide matrix.[12] The main advantage of the set-up is its compacity, which is a necessity on many beamlines. A second spectrometer (with only 4 crystals) was also built for beamline MARS at SOLEIL.[13]
However, the small radius of curvature of the crystals induces *i)* microstrains inside the Si wafer (and so a decrease of the energy resolution) and *ii)* technological difficulties in their elaboration process. We adapted then the spectrometer to be able to use crystals with a 1m radius of curvature (Figure 9, right). This adaptation was done keeping a maximum of part from the initial set-up.[14] The "1m spectrometer" is opened to users since November 2013. This 1m set-up was used by Gorczyca *et al.* to probe nanometric Pt clusters as a function to the hydrogen coverage.[15]

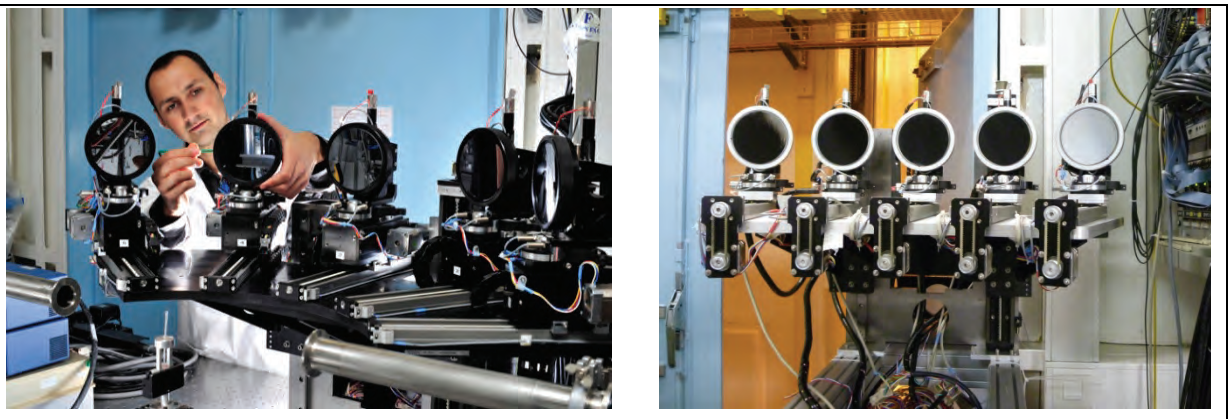

Figure 9. Crystal analyzer spectrometer installed on FAME. Left : 5 crystals @ 0.5m. Right : 5 crystals @ 1m

[10] Hazemann *et al., J. Synchrotron Rad* **16** (2009) 283-292 ; LLorens et al., *Rev. Sci. Instrum.* **83** (2012) 063104
[11] Rodolakis *et al., Phys. Rev. Lett.* **104** (2010) 047401 ; Rodolakis *et al., Phys. Rev. B* **84** (2010) 245113
[12] Vichery *et al., J. Phys. Chem. C* **117** (2013) 19672–19683
[13] Sitaud *et al., J. Nucl. Mater.* **425** (2012) 238-243 ; LLorens *et al., Radiochim. Acta* (2014) in press
[14] Financial support provided by a grant from Labex OSUG@2020 (Investissements d'avenir - ANR10 LABX56)
[15] Gorczyca et al., *Angewandte Chemie* (2014) accepted. See also the corresponding highlight.

Technical specificities

The key part of the spectrometer is the crystal. We acquired 1m bent crystals from XRS Tech company,[16] mainly Ge crystals : Ge331[14,17], Ge110[18], Ge111, Ge422[18], Si111 (diced). Energy resolution (ΔE_{CAS}) of these crystals were all measured between 1.0 and 1.5eV (Figure 10, left).
We also tested the first crystals made at ESRF with a semi-automatic system. Energy resolution of the crystals corresponds to our needs (Figure 10, right). Several parameters have still to be optimized (thickness and temperature of the wafer during the bounding operation...) but we already planned to buy 1m Si bent crystals to ESRF.

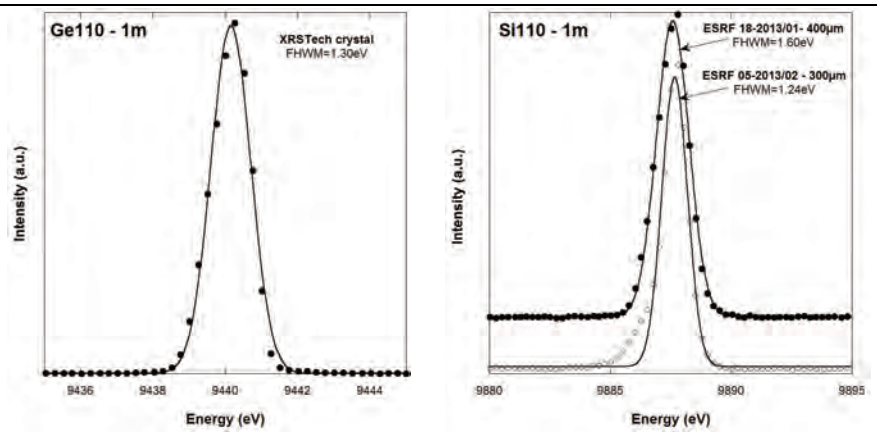

Figure 10. Determination of the energy resolution of crystals by measuring pseudo-elastic scattering energy scans

We usually use a silicon-drift detector (Vortex) to collect the photons diffracted by the bent crystals. This energy-resolved detector allows to discriminate the diffracted photons from the scattered ones, and so to better "clean" the measured signal. This detector is quite small (Ø8mm), which is a limitation especially when Bragg angle is far from 90°. For θ=75 the vertical beam size in the detector plane is around 13mm. We acquired then a 15x75mm^2 hybrid pixels detector (ImXpad).[17]

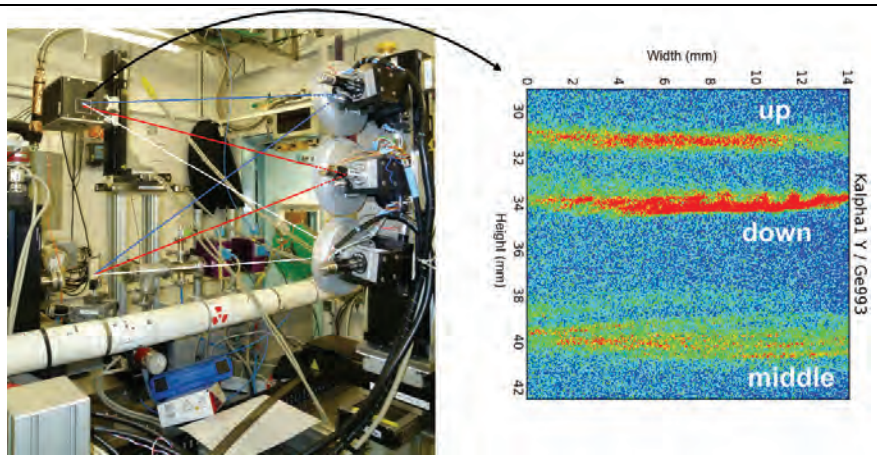

Figure 11. Tests of the spectrometer in the "3 superimposed crystals configuration". Detection is done by a hybrid pixel detector. Left : experimental set-up. Right : image of the diffracted beams on the detector.

The improvements of the spectrometer are linked to the second beamline project FAME-UHD. We have tested different configurations to increase the number of crystals. In the horizontal plane, such increase is rather limited : signal collected by crystals decreases when their angular positions with respect to the central crystal (β angle on Figure 12) increases. This is especially true when the Bragg angle θ is not around 90° (θ ranges from 90 to 64°). We found that it is not reasonable to increase the number of crystals in this direction up to β = ±30°, i.e. 7 crystals on a row. In the vertical plane we

[16] http://xrstech.com/
[17] Financial support provided by the French National Agency (ANR Mesonnet, P2N 2010)
[18] Financial support provided by Institut Français du Pétrole / CNRS Institut Néel contract

have tested the possibility to superimpose several crystals as it is already done for X-ray Raman Spectroscopy spectrometers.[19] Calculations and experiment with prototypes have shown the possibility to have several crystals rows, the focus point of each crystal depending of its "row position" (Figure 11). We decided to limit the number of rows to 2 (Figure 12).

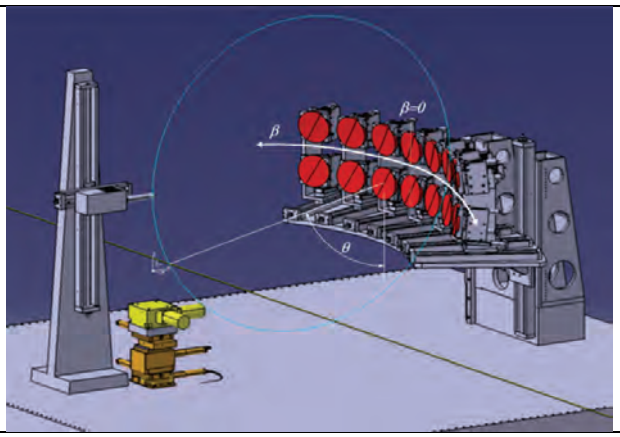

Figure 12. Project of a 14 crystals spectrometer

4.b. Scientific aspects

The main advantages of measuring fluorescence-XAS with a crystal analyzer spectrometer (ΔE_{CAS} ~1.5eV) instead of a solid-state detector (ΔE_{SSD} ~200-300eV) are :

- XAS measurements can be achieved on complex systems where the detection limitation is determined by the fluorescence of the main constituents of the matrix,
- structure resolution of XANES spectra can much sharper than what could be achieved classically (HERFD, High Energy Resolution Fluorescence Detection ; ΔE_{CAS} has to be smaller than the energy bandwidth of the probed line width),
- other spectroscopic techniques such as X-ray Emission Spectroscopy can be performed. Valence-to-core XES spectroscopy allows for example to discriminate between the different ligands in the first coordination sphere of the probed element,
- Energy position of the fluorescence lines (and expecialy the Kβ ones for the K-edges) can be sensitive to the spin-state ($K\beta_{1,3}$), to the ligands ($K\beta_{2,5}$ and its satellite lines) of the probed element. XAS spectra obtained by measuring such lines are then spin- or ligand- sensitive.

In the Environmental and Earth science fields, the main parameter which limits the ability to perform XAS experiments on diluted elements in optimal conditions may arise from the nature of the bearing phase. When the probed element is diluted in a soil (which can contain clays, silicate, iron or manganese oxides...), the fluorescence signals delivered by the main constituents of this matrix can saturate the detectors, even with the use of appropriate filters. Moreover in some cases, the fluorescence peaks of some matrix constituents can be too close in energy to the fluorescence peak of the targeted element to be discriminated by the Solid State Detector. This was the case for the studies of Co sorption on Fe oxyde (see example on Figure 13)[12,20] or Ge in Zn sulfite (sphalerite).[21]
Being only sensitive to the local order, XAS is well suitable to study either amorphous, ill-ordered or well-crystallized samples, in the solid or liquid states and has thus been quite naturally used for studies of nanomaterials, more precisely their toxicological or environmental impact[22]. In this particular field, two conditions are required. Firstly, acquisitions need to be sensitive to a very small amount of nanoparticles, in order to be as close as possible to the predictable concentration of these elements in the ecosystem. Secondly, the difference between spectra from bulk and nanostructured materials being

[19] Sokaras *et al.*, *Rev. Sci. Instrum.* **83** (2012) 043112 ; Verbeni *et al.*, *J. Synchrotron Rad.* **16** (2009) 469–476
[20] Proposal 30.02.960, Collins *et al.*, "Identification of the mineral phases controlling Co immobilisation in soils and sediments", *2010 Australian Synchrotron User meeting*, Melbourne (23-24 Novembre 2010)
[21] Proposal ES75, Bonnet *et al.*, "Characterization of the Zn-Ge substitution mechanisms in sphalerites (ZnS)"
[22] The project team is involved since 2007 in this scientific field, *via* two french ANR projects (Nanosurf, 2007-2010, Mesonnet, 2010-2013) and the iCeint (international Consortium for the Environmental Implication of Nanotechnology) research group. These ANR funds allowed to build the CAS under operation on FAME

often subtle, it is necessary to improve at the maximum the quality of the EXAFS spectra and the energy resolution of the XANES ones.

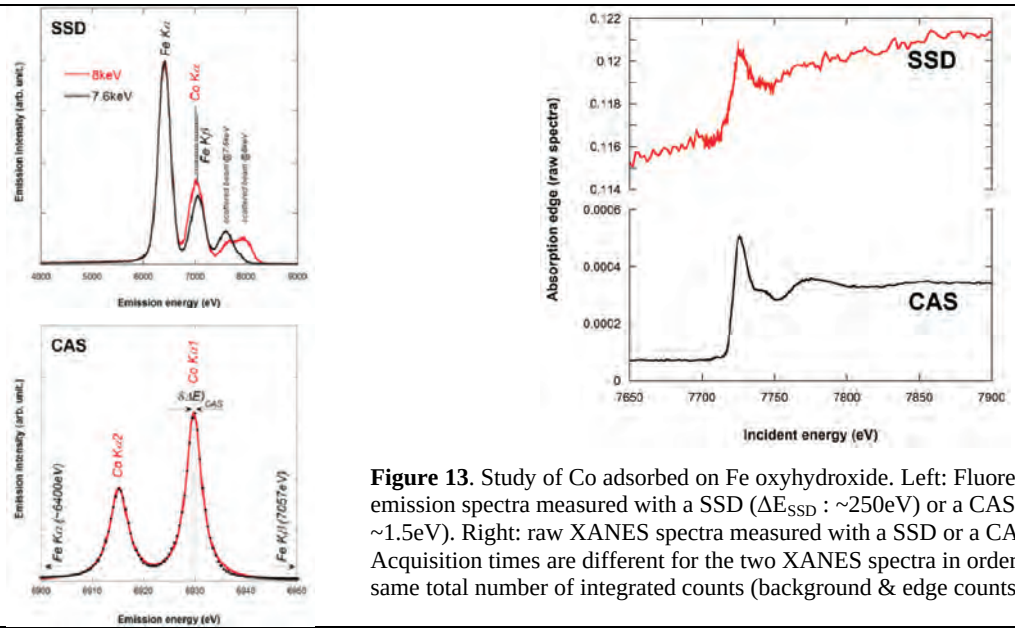

Figure 13. Study of Co adsorbed on Fe oxyhydroxide. Left: Fluorescence X-ray emission spectra measured with a SSD (ΔE_{SSD} : ~250eV) or a CAS (ΔE_{CAS} : ~1.5eV). Right: raw XANES spectra measured with a SSD or a CAS (Co K-edge). Acquisition times are different for the two XANES spectra in order to have the same total number of integrated counts (background & edge counts)

For example reduction of Ce^{4+} to Ce^{3+} in CeO_2 nanoparticles has been followed by XANES spectroscopy *in vitro* in human dermal fibroblasts. Experiment, performed on FAME few years ago, was based on linear combination of CeO_2 and Ce^{3+}-oxalate reference spectra.[23] A shoulder appeared on the XANES spectra of nano-CeO_2 suspended in the biological media at the energy of the Ce^{3+} : a contribution of 8±2% of Ce^{3+}. However, the same team showed recently[24] that this shoulder can't be attributed unambiguously to Ce^{3+}. We performed then HERFD-XANES measurement on different model compounds (Figure 14).[25] All the edge and pre-edge features are much more precisely obtained in these conditions, and two main conclusions can be already drawn : *i)* CeO_2 XANES spectra depend on the particle size and *ii)* estimation of the Ce^{3+}/Ce^{4+} ratio can be now done on the pre-edge part of the signal. Such enhanced sensitivity was used for an environmental science experiment in December 2013.[26]

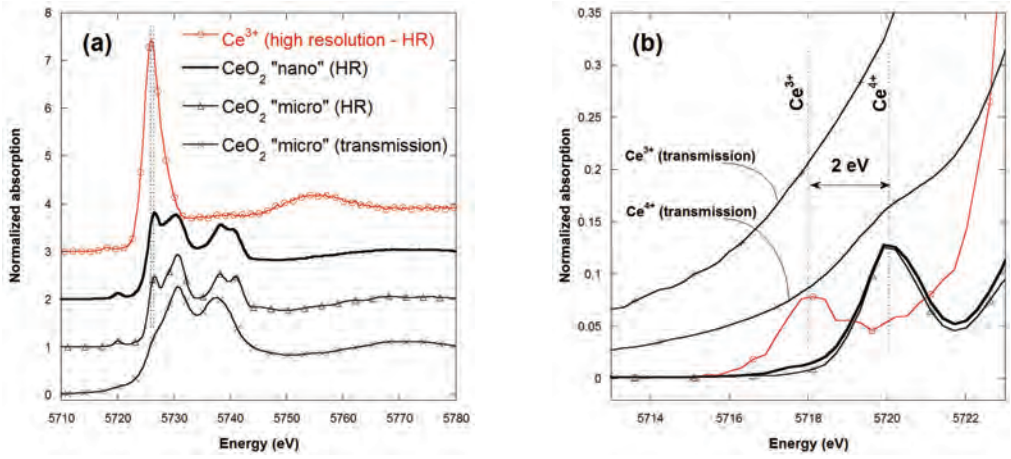

Figure 14. HERFD measurements on Ce model compounds, CeO_2 micro and nanoparticles, Ce^{3+}-oxalate. (a) : XANES. (b) : detail of the pre-edge

[23] Auffan *et al.*, *Nanotoxicology* **3** (2009) 161-171
[24] Diot M.-A., *PhD Thesis Université Aix-Marseille*, spécialité *Sciences de l'Environnement Terrestre* (2012)
[25] Proux et al., IHR proposal IH-MI-904
[26] Proposal 30.02.1061, Rose et al., "Cerium speciation in aquatic mesocosms using HERFD-XAS"

5. Training activities

Synchrotron radiation is an instrument that federates, simultaneously (around the same instrument) with similar scientific problems, different communities which are interdependent in their experimental needs. It is however necessary to create and to maintain continuously *i)* emulations around the beamline, *ii)* interactions with the users. We organized or participated to several punctual or recurrent operations since 2002 and the beginning of FAME operation.

Training courses for students

Each year, about 5 days are allocated for teaching practicals on the beamline for scientists and for University graduate students. For the 2010-2014 period we participated to several specific courses

- each year, the HERCULES course with 2 days of practicals on the beamline and 2 days of tutorials at Neel Institute,
- in 2012, the Hercules Specialized Course dedicated to Neutrons and Synchrotron Radiation in Materials for Energy (HSC14),
- since 2011, 1 day of practical for the PhD school of Grenoble Institute of Technology.

FAME+: a course dedicated to our users

Considering the technical complexity of synchrotron radiation experiments and the difficulty to obtain beamtime *via* the various program committees, few new teams having scientific problems adapted to these instruments use the FAME beamline. We decided in 2004 to organize an annual training for users (actual or potential): FAME+ (Formation en Absorption X pour la Maîtrise de l'Expérience et le Pilotage d'une Ligne Utilisant un Synchrotron). This training is organized with the help of the CNRS permanent training and very well recognized. The main goals of this training are to explain

- the technical aspects of the experiment and the various analysis possibilities,
- the optical adjustments of the beamline.

The training is conceived with lectures, praticals on the beamline and tutorials on computer.
To summarize, the training clarifying the FAME operations have several interests:

- open the beamline to the whole communities,
- make more autonomous the actual or future users, from a technical point of view,
- increase the safety on the beamline,
- give to the users a critical glance on all the important points which allow the realization of an experiment under optimal conditions,
- give to the users the up-to-date tools to analyze their data.

This project was initially reserved for the Earth sciences community but it has been quite soon opened to the other scientific communities. Since 2004, 137 trainees (mainly PhD students) issued from 53 laboratories followed this course (Figure 1).

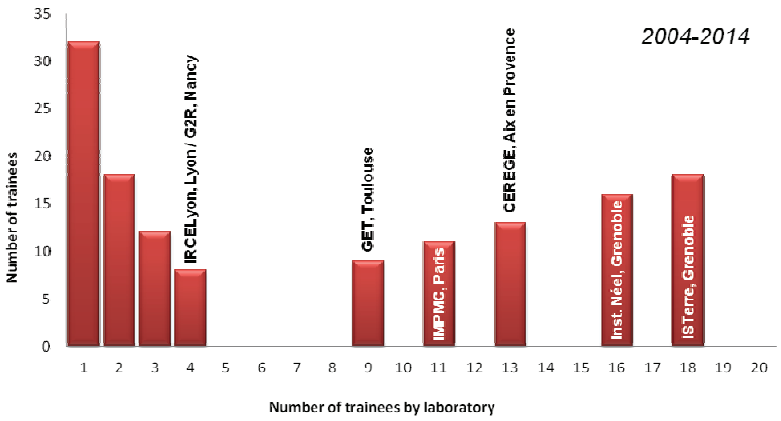

Figure 1: Repartition of number of trainees by laboratories (2004-2014)

6. Scientific results

This part of the BLRP report has been written by different users (or us for the in-house research activities) to represent the variety of topics investigated on FAME over the last years as well as their opinions and expectations on the beamline. Some results presented below are the summary of a group or laboratory activity, while others are examples that illustrate selected points. The beamtime repartition is shown on Figure 1 for the 2005-2009 (previous BLRP) and 2010-2014 periods.

Earth science still represents the main scientific activity of FAME, gathering geochemistry, hydrothermal fluids studies and mineralogy, even if the ratio of beamtime allocated to these scientific fields slightly decreases compare to 2005-2009 period (53% from 2010 to 2014, 63% from 2005 to 2009). Several laboratories are regular users since 2002: the ‘Observatoire des Sciences de l'Univers de Grenoble’ (OSUG, including ISTerre, the ‘hydrothermal fluids’ team of the Institut Néel, the ‘Laboratoire de Planétologie de Grenoble’...), the ‘Centre Européen de Recherche et d’Enseignement des Géosciences de l’Environnement’ (CEREGE, Aix en Provence), the ‘Institut de Minéralogie et de Physique des Milieux Condensés’ (IMPMC, Paris), the ‘Géosciences Environnement Toulouse’ laboratory (GET, Toulouse), the ‘Division of Mineralogy of the South Australian Museum’ & CSIRO (Adelaïde and Melbourne)... Several contributions illustrate these scientific activities in the "Geochemistry and Environmental Sciences", "Hydrothermal Fluids" and Mineralogy (including cosmochemistry) fields. If the first and last points are the fruit of external users' activity, the second one is entirely the result either of in-house research or collaborations.

Biochemistry activities on the beamline will be illustrated by examples of experiments performed by the ‘Laboratoire de Chimie Inorganique et Biologique’ of the CEA-Grenoble and by a collaboration between ISTerre and the ‘Institut de Biologie Structurale’.

The beamtime dedicated to chemistry (catalysis & electrochemistry) and material sciences represents 1/3rd of the beamtime. We select examples dealing with catalysis (mainly by the "raffinage" team of the IRCELYON and the IFPEN, with which we collaborate strongly since years), and materials for energy (Ni/Mn oxides in Lithium Ion Batteries,).

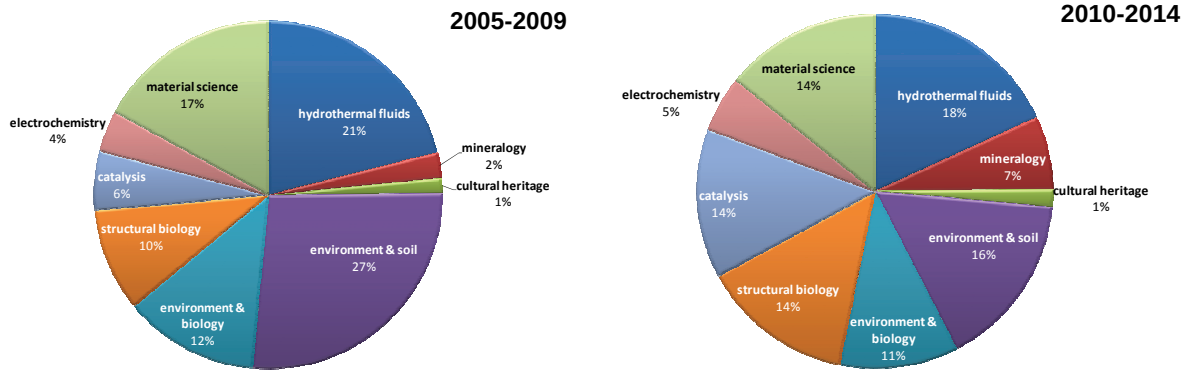

Figure 1. Distributed shifts as a function of scientific fields for the previous (left) and actual (right) BLRP periods

Geochemistry and Environmental Sciences

Interaction of plants with metallic contaminants : uptake and detoxification processes

Plants play a key role in the biogeochemical cycle of trace elements and metallic contaminants. On one hand they act as an entry point into trophic chains and route of human exposure due to consumption of crops. For example, the consumption of rice in southeast Asia at current consumption rates constitutes a significant excess cancer risk to these populations due to the accumulation of arsenic contained in soils and pore-water in the plant, particularly in rice grains.[1] Plant uptake of contaminants also occurs by foliar uptake. In urban areas and particularly in rapidly growing regions of Asia, Africa and Latin America regions where air pollutant emissions have been increasing, this process may lead to a threat to crop production and quality. On the other hand, plants act as stabilizing agents of contaminants in soils due to complexes biogeochemical processes taking place in the rhizosphere. They contribute to the natural attenuation of contamination in soils, and are used in phytoremediation processes such as constructed wetlands[2] or phytostabilization.[3] A better understanding of the mechanisms controlling metal homeostasis in plants and of key processes for metal uptake, hyperaccumulation, detoxification, and prevention against nutrient deficiency in the case of low-nutrient soils are needed for a better risk evaluation and food quality, optimization of phytoremediation techniques, and for plant biofortification of crops.

Classical methods to assess gene functions and physiological processes in plants involve molecular biology and molecular genetics, and UV, visible light and electron microscopy. Synchrotron techniques have emerged as powerful and highly complementary techniques, particularly to study the distribution and the speciation of metals in plants.[4] The major advantages of these techniques are their high sensitivity, and lateral or spatial resolution for microfocused techniques, the limited sample preparation and nondestructive character, and the possibility to work on hydrated samples, in vivo in some cases. Although hyperspectral imaging is very attractive, bulk techniques such as bulk XAS remain an essential approach to determine the speciation of trace elements in plants and plant organs.

Two case studies will be presented, including cadmium accumulation and detoxication in Cd hyperaccumulating and non accumulating plants, and foliar uptake of lead in crop species exposed to atmospheric contaminations.

G. Sarret [1], M.P. Isaure M.P [2], S. Huguet [1,2], E. Schreck [3], G. Uzu [3], V. Magnin [1], C. Dumat [3]
[1] ISTerre Grenoble, [2] LCABIE Pau, [3] EcoLab Toulouse

Localization and speciation of cadmium in the model plant Arabidopsis halleri

Metal hyperaccumulation by plants is an interesting and still misunderstood phenomenon. Arabidopsis halleri is a model plant to investigate metal tolerance and hyperaccumulation. This species hyperaccumulates Zn and Cd. It is phylogenetically close to the model plant Arabidopsis thaliana, and interspecific crossings between *A. halleri* and its non tolerant and non hyperaccumulating relative Arabidopsis lyrata ssp petraea can be done to obtain progenies with various traits of tolerance and accumulation. The overexpression of metal transporters including HMA4 for Zn and Cd loading into the xylem, MTP1 for Zn transfer in the leaves were evidenced for *A. halleri*, and other ones including ZIP for metal soil-to-root uptake, NAS2 for root-to-shoot translocation, and HMA3 transporter for vacuolar sequestration in shoots have been suggested. Concerning the detoxification of cadmium, two processes have been proposed. The first one, supposed to prevail in hyperaccumulating species, involve the sequestration in the vacuole and complexation by simple organic acids (citrate, malate, etc…). This compartmentalization is a way to cope with metal toxicity by limiting metal interactions with metabolically active cells. The second one, supposed to prevail in other species, consist in the chelation by thiol-containing molecules such as glutathione, phytochelatins and

[1] Meharg *et al.*, *Environmental Science & Technology* **43** (2009) 1612-1617.
[2] Garcia *et al.*, *Critical Reviews in Environmental Science and Technology* **40** (2010) 561-661.
[3] Bolan, N.S., Park, J., Robinson, B., Naidu, R., Huh, K, *Adv. Agron.* **112** (2011) 145-204.
[4] Sarret *et al.*, *Adv. Agron.* **119** (2013) 1-82 / **Article 2013-24**

metallothioneins in the cytoplasm. It is energetically more expansive because it requires the production of chelating agents for each atom of metal.

We have studied the accumulation form of Cd in *A. halleri* exposed for 9 weeks to different Cd concentrations in the nutrient solution (5 and 20 µM). Since *A. halleri* hyperaccumulates both Zn and Cd and Zn level in soils and in the plant being one to two orders of magnitude higher than Cd, the influence of this co contaminant on Cd uptake and speciation was studied as well. 30 and 300 µM Zn were applied. Cd K-edge bulk EXAFS spectra for the plant leaves and reference compounds were recorded on the Beamline FAME. After harvesting, plant leaves were flash frozen and ground in liquid nitrogen, and pressed as pellets in frozen state. Pellets of frozen-hydrated leaves and reference compounds were transferred in a He cryostat cooled to 15 K. Spectra were recorded in fluorescence mode using a 30-element solid-state Ge detector. EXAFS spectra were treated by linear combination fits and shell fitting (Figure 2). Cd was predominantly bound to COOH/OH groups belonging to organic acids and/or cell wall components. Cd bound to thiol groups was found as a secondary species (less than 25%) in leaves of plants exposed to the low Zn concentration, regardless of Cd concentrations, and in young leaves. Thiols ligands might correspond to glutathione found in significant amount in aerial parts. Thus, in these experimental conditions and in conditions of Zn sufficiency (300 µM Zn), *A. halleri* acts as a real Cd hyperaccumulator and sequesters Cd in the vacuoles and possibly in the cell walls. In conditions of Zn deficiency and in young leaves, the chelation by thiol-containing molecules appears as secondary detoxification process. In parallel, Cd distribution at the plant and leaf scale was studied by ^{109}Cd autoradiography after 3 and 9 weeks of exposure (Figure 3). At the rosette scale, there was no clear trend in Cd localization in young or mature leaves. At the leaf scale, an enrichment of the petiole, central vein and trichomes was observed after 3 weeks. After 9 weeks, leaf edges were the most Cd-enriched tissues, and regions along leaf vascular bundles appeared less concentrated.

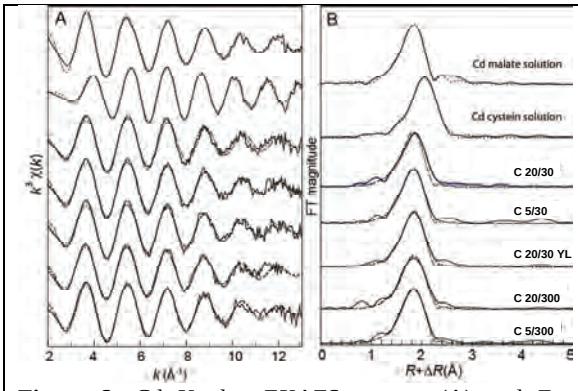

Figure 2. Cd K-edge EXAFS spectra (A) and Fourier transforms (B) for the leaf samples and linear combination fit (dashed lines).

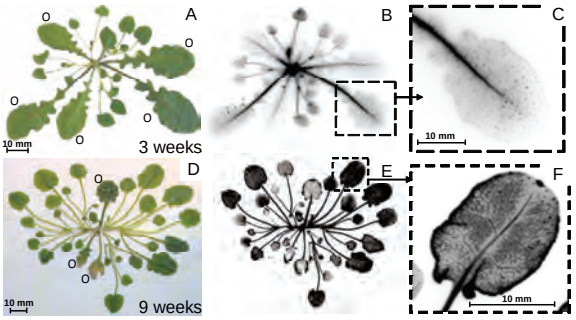

Figure 3. Photographs (A, D) and autoradiographs (B, E) of *A. halleri* exposed for 3 and 9 weeks to 20 µM Cd and 30 µM Zn.

In a following study, we have investigated Cd speciation in *A. halleri*, in the non tolerant and non hyperaccumulating relative *A. lyrata*, and F2 progenies exposed to 10 µM Cd for one and three weeks using the same approach. Cd content in the leaves ranged from 60 to 800 mg kg^{-1} dw, *i.e.*, a few ppm to a fem tens of ppm in the frozen hydrated samples. As observed previously, in A. halleri Cd was mainly present as Cd-O complexes and to a minor extent as Cd-S species, but the proportion of Cd-S species decreased with exposure time. In *A. lyrata*, Cd was mainly present as Cd-S species, and again the proportion of Cd-S slightly decreased with exposure time. These results suggest that chelation is the major detoxification mechanism in the non tolerant and non accumulator plant. In the hyperaccumulator, it is a short term response to metal exposure, progressively replaced by vacuolar sequestration (and possibly efflux to the apoplasm). In parallel, Cd distribution in the leaves was studied by µXRF on ID21 beamline. In *A. halleri*, Cd was mainly located in xylem and phloem and in mesophyll tissue with a sequestration both inside cells and in cell walls/apoplast. The edge of the leaves were richer in Cd, as observed by autoradiography. The presence of Cd in the phloem suggests a reallocation of Cd within the plant after transit in the leaves. Contrary to other Cd hyperaccumulators, the epidermis of *A. halleri* contained very little Cd. In *A. lyrata*, Cd-concentrated

regions were the vascular bundles and the epidermis. Cd was also identified in trichomes of both species. Finally, Cd tolerant and Cd sensitive progenies from an interspecific crossing between *A. halleri* and *A. lyrata* were studied. Results showed the exclusive presence of Cd-S species in sensitive plants. On the contrary, tolerant progenies contained a mixture of Cd-O and Cd-S species. Therefore, these results highlight a link between Cd speciation and tolerance trait. There was no correlation between Cd accumulation and Cd speciation.

Overall, these studies showed complex responses of the plants to Cd exposure. The same detoxification mechanisms, chelation, vacuolar sequestration and possibly efflux in the apoplasm, were used in *A. halleri* and *A. lyrata* but at very different levels. Chelation was the major mechanism in *A. lyrata* whereas vacuolar sequestration and possibly efflux in the apoplasm dominated in *A. halleri*. In both species, the extent of chelation decreased with exposure time. Finally, reallocation processes within the plant were suggested. Finally, this study illustrates the interest of combining imaging and spectroscopic techniques with a sub micron resolution with bulk analyses to obtain a global view of metals status in biological samples.

Main publications

Isaure M.P., Huguet S., Meyer C.L., Castillo-Michel H., Testemale D., Vantelon D., Saumitou Laprade P., Verbruggen N., Sarret, G., Evidence of various mechanisms of Cd sequestration in the hyperaccumulator *Arabidopsis halleri*, the non accumulator *Arabidopsis lyrata* and their progenies by combined synchrotron-based techniques. *New Phytol. in revision.*

Huguet S., Bert V., Laboudigue A., Barthes V., Isaure M.P., Llorens I., Schat H., Sarret G., Cd speciation and localization in the hyperaccumulator Arabidopsis halleri. *Environmental and Experimental Botany* **82** (2012) 54-65 / **Article 2012-13**

Sarret G., Willems G., Isaure M.P., Marcus M.A., Fakra S., Frérot H., Pairis S., Geoffroy N., Manceau A., Saumitou-Laprade P. (2009) Zn localization and speciation in *Arabidopsis halleri* x *Arabidopsis lyrata* progenies presenting various Zn accumulation capacities. *New Phytol.* **184**, 581-595 / **Article 2009-19** (BLRP 2009)

Foliar versus root exposure: consequences on Pb accumulation and speciation in crop species

In urban areas with high fallout of airborne particles, metal uptake by plants mainly occurs by foliar pathways and can strongly impact crop quality. However, there is a lack of knowledge on the mechanisms of foliar uptake, and on the fate of metals once they are trapped by plant leaves. In this study, two contrasting crops, lettuce (*Lactuca sativa* L.) and rye-grass (*Lolium perenne* L.), were exposed to Pb-rich particles emitted by a Pb-recycling factory via either atmospheric or soil application. Pb accumulation in plant leaves was observed for both ways of exposure. The mechanisms involved in Pb uptake were investigated using a combination of microscopic and spectroscopic techniques (electron microscopy, laser ablation, Raman microspectroscopy, and X-ray absorption spectroscopy).

For EXAFS, plant leaves were prepared as described above, and Pb L_{III}-edge EXAFS spectra were recorded on FAME beamline at 10°K in fluorescence mode. Pb content in plant samples ranged from 80 to 700 mg kg^{-1} dw, *i.e.*, a few ppm to a fem tens of ppm in the frozen hydrated samples. Both XANES and EXAFS parts were treated by linear combination fits.

The results showed that Pb localization and speciation were strongly influenced by the type of exposure (root or shoot pathway) and the plant species. Foliar exposure was the main pathway of uptake, involving the highest concentrations in plant tissues. Under atmospheric fallouts, Pb-rich particles were strongly adsorbed on the leaf surface of both plant species. In lettuce, stomata contained Pb-rich particles in their apertures, with some deformations of guard cells. In addition to PbO and $PbSO_4$, chemical forms that were present in pristine particles, secondary species were identified including organic compounds (minimum 20%) and hexagonal platy crystals of $PbCO_3$ (Figure 4, Figure 5 & Figure 6). In rye-grass, the changes in Pb speciation were even more egregious: Pb-cell wall and Pb-organic acid complexes were the major species observed. For root exposure, identified here as a minor pathway of Pb transfer compared to foliar uptake, another secondary species, pyromorphite, was identified in rye-grass leaves.

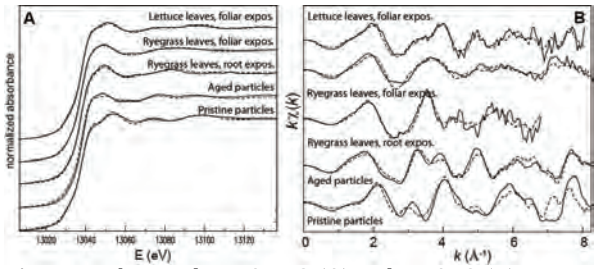

Figure 4. Pb L_{III}-edge XANES (A) and EXAFS (B) spectra for the particles and leaf samples and linear combination fit (dashed lines).

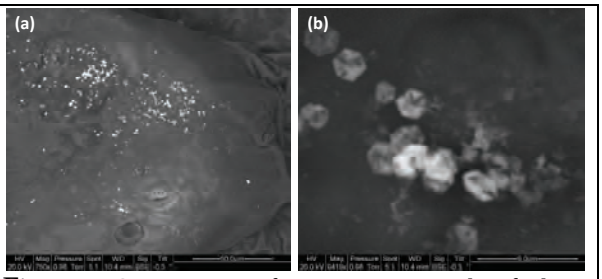

Figure 5. SEM images of a necrotic area identified on lettuce leaf containing hexagonal PbCO3 particles (a); Detailed view of PbCO3 crystals (b).

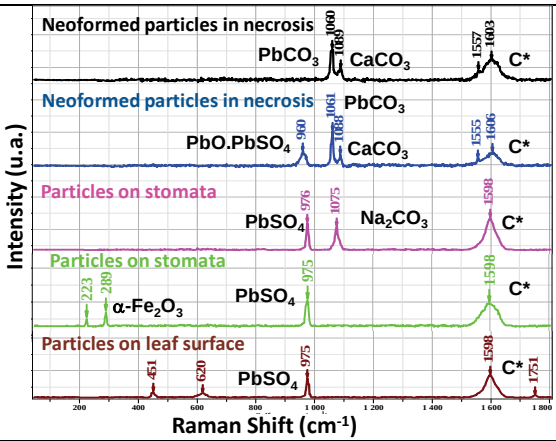

Figure 6. Typical micro-raman spectra recorded on lettuce leaf

The complementarity between bulk XAS, which provided the overall Pb speciation and was sensitive to diffuse Pb–organic complexes present in the leaf tissue, and Raman microspectroscopy and SEM–EDX, which could detect additional Pb mineral species present on the leaf surface, was essential to clarify the fate of metal in plants. Indeed, minor species may be highly reactive and possibly the most toxic ones. The accuracy of human health risk assessment in the case of ingestion of polluted vegetables might be considerably improved by taking into account the compartmentalization and speciation of metals in edible parts of plants. Thus, such type of information is essential to better understand the mechanisms of contaminant uptake and detoxification, and is of high interest to improve health risk assessment models.

Main publication

Schreck, E., Dappe, V., Sarret, G., Sobanska, S., Nowak, D., Nowak, J., Stefaniak, E.A., Magnin, V., Ranieri, V., Dumat, C. Foliar or root exposures to smelter particles: Consequences for lead compartmentalization and speciation in plant leaves. *Science of the Total Environment* **476–477** (2014) 667-676 / **Article 2014-23**

First evidence for amorphous ZnS particles as major Zn species in suspended matter from the Seine River

Zn is one of the most widespread trace metal in Earth environments because of anthropogenic and natural inputs over millennia. Furthermore, Zn is the most concentrated trace metal in the Seine River watershed downstream the Paris conurbation. In order to better identify the sources and fate of Zn in this large urbanized watershed, the chemical speciation of this element was investigated in the suspended particulate matter collected by filtration of large volumes of Seine surface water. Samples were collected monthly over a one year period upstream and downstream the Paris conurbation. Zn K-edge Extended X-ray Absorption Fine Structure (EXAFS) analysis of these finely divided solids that can contain up to 1000 mg/g Zn revealed the occurrence of significant amounts of amorphous ZnS particles, which accounts for more than 40 at% of total Zn in this particulate matter. The relative proportion of zinc sulfide with respect to total Zn speciation in the samples investigated was found to dramatically increase dowstream of the Paris conurbation. Although the sources of these reduced mineral forms of Zn is still poorly constrained, they could originate from resuspension of bottom

sediments and sewer overflow during storm events. These results emphasize the possible occurrence of sulfide metal species in the suspended load of oxic rivers, and thus provide new constraints for modeling Zn cycling in such rivers, including the interpretation of Zn isotopic tracing. They also highlight the importance of preserving environmental conditions (especially oxidation state) for metal speciation studies in continental waters and sediments where oxic/anoxic boundaries are common.

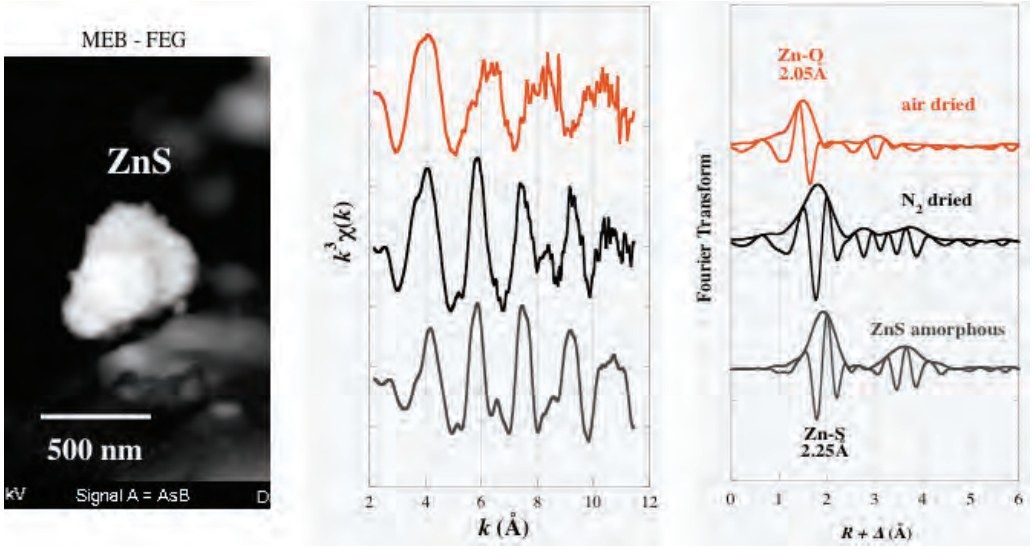

Figure 7. MEB images of zinc sulfide particles (left), EXAFS spectra (center) and corresponding Fourier Transform (right) of air dried, nitrogen dried and ZnS reference compound samples.

EXAFS Analysis of suspended matter samples dried under pure nitrogen atmosphere indicated that sulfur dominate the first coordination environment around Zn in the form of amorphous/poorly crystalline ZnS. In contrast, an oxygen first coordination environment around Zn was systematically observed in the samples dried under ambiant oxygenated atmosphere. The occurrence of ZnS solid phases in nitrogen dried samples was confirmed by scanning electron microscopic observations coupled with energy dispersive x-ray spectroscopy analyses.

Authors and principal publication:

Priadi C.[1], Morin G.[2], Ayrault S.[1], Maillot F.[2], Juillot F.[2], Alliot I.[3], Testemale D.[4], Proux O.[5], Brown Jr G. E.[6,7], XAFS Evidence for Amorphous Zinc Sulfide as a Major Zinc Species in Suspended Matter from the Seine River Downstream of Paris, Ile-de-France, France. *Environ. Sci. Technol.* **46** (2012) 3712–3720 / **Article 2012-20**
[1]LSCE/IPSL, UMR 1572, Gif-sur-Yvette, France / [2]IMPMC, UMR 7590, (CNRS/UPMC), Paris / [3]CEA DRFMC/SP2M/IRS, Grenoble / [4]Institut Néel MCMF, Grenoble / [5]OSUG, Grenoble / [6]Surface & Aqueous Geochemistry Group, Dpt of Geological and Environmental Sciences, Stanford Univ. / [7]SSRL

Nano-ecotoxicology

Nanotechnology is no more an emerging technology. More than 2000 nanoproducts are already on the market. The variety of products is large going from cosmetics to electronic, paints to food and health. Nevertheless, nanotechnologies are at the heart of societal interest and also fear since more than 15 years. One of the first reasons of this fear is the size of the nanoparticles that is seen as the parameter that could induce health and environmental problems. In this regards, governments and politic organizations have decided to fund national and European scientific projects about the risk assessment of nanotechnology in order to decide normalization politics through OECD countries.
Compared to nano-toxicology, nano-eco-toxicology is seen as a new discipline. The challenge in nano-eco-toxicology is to work with an interdisciplinary approach with only weak information available concerning the quantities of nanomaterial which could be released all along their life-cycle and to take into account the complexity of the environmental matrices. This requires to evaluate the exposure, (bio)transformation, bio(distribution) and hazards of the nanomaterials at environmentally relevant doses and on the long term.

The research developed at the CEREGE is part of a dynamic network of academic research laboratories and industries to design tomorrow's nanomaterials that will be safer for both humans and the environment (GDRi iCEINT[5] and the LABEX SERENADE[6]).

The recent improvements of the FAME beamline especially with the crystal analyzer spectrometer were essential to understand the aging, physico-chemical transformations, exposure, and impacts of nanoparticles and nano-composite. This helped us to provide reliable exposure (and impacts) input data to build an environmental risk assessment model related to nanotechnologies. Several examples will be presented in this section highlighting the surface transformation of nanoparticles in complex matrices as biological tissues, aquatic mesocosms, but also during interactions with others pollutants.

Mélanie Auffan & Jérôme Rose
Centre de Recherche et d'Enseignement de Géosciences de l'Environnement, Aix-en-Provence

Co-contamination of human cells by magnetic nanoparticles and arsenite

Once nanoparticles (NPs) are released in natural systems they may react with pollutants, cross biological barriers and modify the bioavailability/bioaccessibility of the associated pollutants. Then the issue of NPs as contaminant carriers needs to be investigated. This biological effect also known as 'Trojan horse' effect has been mentioned in the literature but remained poorly investigated, except for intentional effects as drug delivery. By combining viability assays, and structural analysis by XAS at the As K-edge, we assessed how γFe_2O_3 NPs affect the cytotoxicity (toward human dermal fibroblasts), the intra- and extracellular speciation of As^{III}. Two co-contamination scenarios were studied: a simultaneous co-injection of the NPs and As, and an injection of the NPs after 24h of As adsorption in water. We demonstrated that the co-injection of γFe_2O_3 NPs and As in the cellular media strongly affects the complexation of the intracellular As with thiol groups (Figure 8). This significantly increases at low doses the cytotoxicity of the As non-adsorbed at the surface of the NPs. However, once As is adsorbed at the surface (through double-corner-sharing, As^{III}-O-Fe distance of 3.33±0.02Å) the desorption is weak in the culture medium. This fraction of As adsorbed at the surface is significantly less cytotoxic than As itself. Based on XAS data and the thermodynamics, we demonstrated that any disturbance of the biotransformation mechanisms by the NPs (as a surface complexation of -SH groups with the Fe surface atoms) is likely to be responsible for the increase of the As adverse effects at low doses.

Main publication
Auffan M., Rose J., Proux O., Masion A., Liu W., Benameur L., Ziarelli F., Botta A., Chaneac C., Bottero J.-Y., *Environmental Science & Technology* **46** (2012) 10789–10796 / **Article 2012-3**

[5] **G**roupement **d**e **R**echerche **i**nternational : **i**nternational **C**onsortium for the **E**nvironmental **I**mplication of **N**ano**T**echnology / http://www.i-ceint.org/
[6] **Lab**oratory of **Ex**cellence for **S**afe(r) **E**codesign **R**esearch and **E**ducation applied to **NA**nomaterial **DE**velopment / http://www.labex-serenade.org/

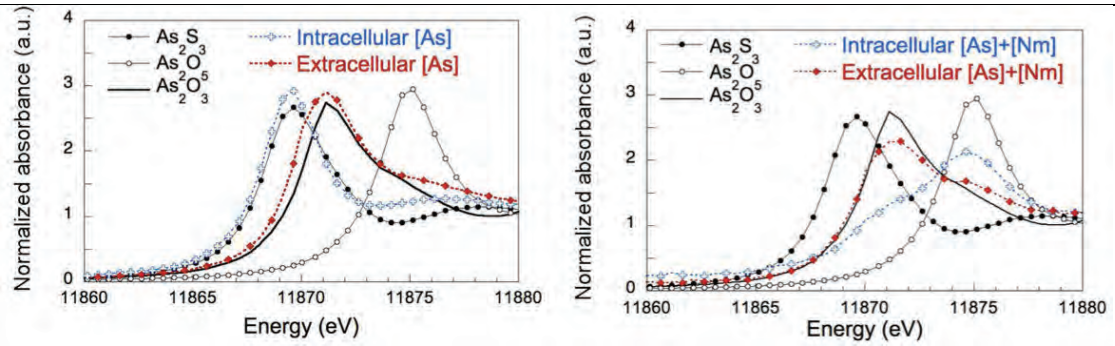

Figure 8. Arsenic K-edge XANES spectra of (left) As in the extra- and intracellular media of human dermal fibroblasts following 24h exposure to 20 µM of As(III) and (right) of As localized in the extra- and intracellular media of fibroblasts following 24h exposure to 500 µM As(III) and 50 mg/L of Nm coinjected simultaneously ([As]+[Nm]). The experimental data are compared to XANES spectra of reference compounds (As_2O_3, As_2O_5, and As_2S_3).

Salinity-Dependent Silver Nanoparticle Uptake and Transformation by Atlantic Killifish (Fundulus heteroclitus) Embryos

In 2012, 117 products containing zero valent silver nanoparticles (Ag NPs) were commercialized in Europe, while a knowledge deficit as to the safety of these products still exists. A recent review focused on the toxicity of Ag NPs concluded that an adequate evaluation of Ag NPs toxicity, biodistribution and biotransformation has yet to be performed. This lack of information is mainly related to the technical challenges of imaging, quantifying, and determining the biodistribution and biotransformation of Ag NPs in complex matrices and at realistic doses (~ µg/L).

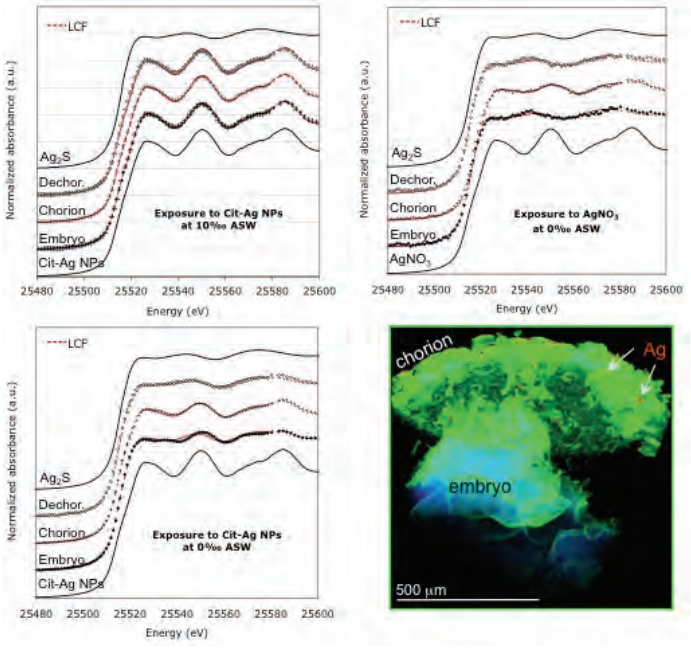

Figure 9. Silver K-edge XANES spectra of Ag taken up by fish embryo and localized in the chorion (external membrane of the egg) and the dechorionated embryo ('dechor.') following 48h exposure to $AgNO_3$ (0.2 mg/L) and coated-Ag^0 NPs (5 mg/L). Red dotted lines: linear combination fits of reference compounds (Ag^0 NPs, Ag_2S, $AgNO_3$, AgCl, Ag_3PO_4, and Ag_2O). A 3D X-ray microscopic image of the embryo is shown with false colors adjusted to reveal possible silver-rich area (measurement with a laboratory X-ray tomographic system MicroXCT-200, Xradia, at 40 kV and 4 W).

In collaboration with the Equipex nanoID platform, the FAME and ID21 beamlines, we developed a methodology based on 2D and 3D X-ray imaging and *in situ* characterization of Ag within fish embryos. We demonstrated the importance of the salinity on the uptake and in situ speciation of Ag. The Ag uptake was reduced by 2.3-fold for Ag NPs, and 2.9-fold for $AgNO_3$ in estuarine water (10‰ ASW) compared to freshwater (0‰ ASW). Between 58 to 85% of the silver was localized in the chorion and formed patches of 20-80 µm. More than a physical barrier, the chorion was found to be a chemically reactive membrane controlling *in situ* the Ag speciation. A strong complexation of the Ag NPs with the thiolated groups of proteins or enzymes of the chorion was responsible of the oxidation of 48 ± 5% of the Ag^0 into $Ag^{(I)}$-S species at 0‰ ASW. This oxidation/complexation is even more intense once the Ag crossed the chorion and was localized inside the embryo. However, at 10‰ ASW

the presence of Cl^- ions at the surface of Ag NPs reduced the oxidation/complexation with S atoms.

For the dissolved silver, we demonstrated that 69 ± 7% of Ag^+ taken up by the chorion was complexed by the thiolated functions of proteins while the others 30 ± 3% interacted with the hemiacetal-reducing ends of polysaccharides of the chorion to form Ag^0. It is the first time that such a bio-reduction of dissolved silver in the chorion of embryo has been demonstrated.

Main publication

Auffan M., Matson C. W., Rose J., Arnold M., Proux O., Fayard B., Liu W., Chaurand P., Wiesner M. R., Bottero J.-Y., Di Giulio R. T., *Nanotoxicology* **8** (2014) 167-176 / **Article 2014-3**

Transfer, Transformation, and Impacts of Ceria Nanomaterials in Aquatic Mesocosms Simulating a Pond Ecosystem

Physical-chemists, (micro)biologists, and ecologists need to conduct meaningful experiments to study the environmental risk of engineered nanomaterials with access to relevant mechanistic data across several spatial and temporal scales. This requires to develop experimental strategy to understand the interactions between the nanoparticles and naturally occurring (in)organic colloids (heteroaggregation *vs* homoaggregation), or the flux between compartments of the ecosystems (aqueous phase, sediments, biota), as well as the speciation of the nanoparticles in the different compartment of an ecosystem. Indoor aquatic mesocosms (60L) that can be tailored to virtually mimic any ecosystem appear as a particularly well-suited device.

Here, this concept is illustrated by a study that assess the distribution of CeO_2-based nanomaterials within a pond ecosystem at low concentration. In this study, we determine the transfer, redox transformation, and impacts of 1 $mg.L^{-1}$ of bare and citrate coated CeO_2 nanoparticles toward an ecologically relevant organism (snail, *Planorbarius corneus*) exposed 4 weeks in a complex experimental system mimicking a pond ecosystem. Over time, both CeO_2 nanoparticles tend to homo- and heteroaggregate and to accumulate on the surficial sediments. The kinetics of settling down were coating-dependent and related to the coating degradation. A transitory oxidative stress was observed for bare CeO_2 nanoparticles lipid peroxidation and change in the antioxidant defense capacity. After 4 weeks, Ce was observed in the digestive gland of benthic organisms and associated with 65−80% of Ce^{IV} reduction into Ce^{III} for both bare and coated CeO_2 NPs. With the high energy resolution of the XANES obtained using the crystal analyzer spectrometer, we were able to thoroughly studied this redox transformation and to attribute them to the digestive activity of the snails, and not to an interaction with the biofilm present on the surficial sediments.

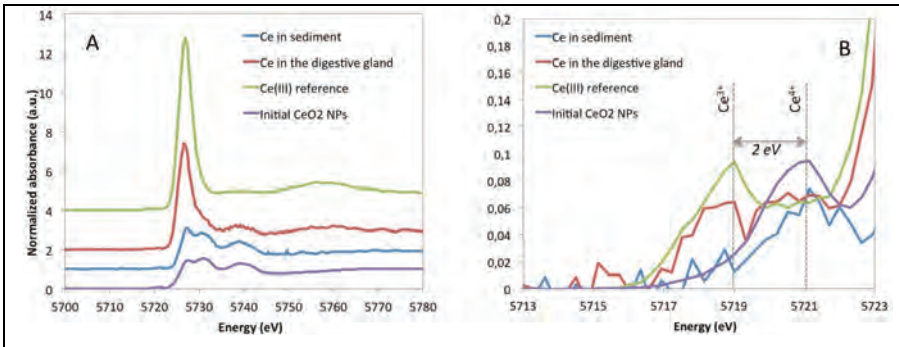

Figure 10. (A) Ce L_3-edge XANES spectra (HERFD measurements) of CeO_2 nanoparticles accumulated at the surface of the sediment or taken up by benthic snails in aquatic mesocosms after 4 weeks. (B) Details of the pre-edge.

Main publication

Tella M., Auffan M., Brousset L., Issartel J., Kieffer I., Pailles C., Morel E., Santaella C., Artells E., Rose J., Thiéry A., Bottero J.-Y., *Environmental Science and Technology* **48** (2014) 9004–9013 / **Article 2014-21**

Other publications

Auffan M., Rose J., Orsière T., De Méo M., Thill A., Zeyons O., Proux O., Chaurand P., Spalla O., Botta A., Wiesner M. R., Bottero J.-Y., "DNA damage generated by redox processes occurring at the surface of cerium dioxide nanoparticles", *Nanotoxicology* **3** (2009) 161-171 / **Article 2009-4** (BLRP 2009)

Rose J., Auffan M., Proux O., Nivière V., Bottero J.-Y., "Physical-chemical properties of nanoparticles in relation with toxicity", *Encyclopedia of Nanotechnology*, Springer **16** (2012) 2075-2085 / **Article 2012-24**

Yang X., Gondikas A., Marinakos S. M., Auffan M., Liu J., Hsu-Kim H., Meyer J., "The mechanism of silver nanoparticle toxicity is dependent on dissolved silver and surface coating in *Caenorhabditis elegans*", *Environmental Science and Technology* **46** (2012) 1119–1127 / **Article 2012-30**

Hydrothermal Fluids

The investigation on hydrothermal fluids is the main research topic of our staff and consequently has always been very active on FAME beamline. The previous Beamline Review Panel Report (period 2005-2009) detailed all the elements that constitute the foundations of this research : the FAME beamline itself (high flux, very good fluorescence detection, stability), the high temperature/high pressure (HT-HP) autoclave developped at Institut Néel, and our XAS expertise (classical EXAFS analysis and novel XANES ab initio calculations). In the last period (2010-2014), the trend in the research area of hydrothermal fluids is to conduct a more global analysis that integrates multiple tools and methods to obtain a more complete view. It is a path we followed in our own activity and our in-house research is definitely collaborative nowadays, with the interplay of absorption spectroscopy techniques, high pressure technology, molecular dynamics calculations and geochemical analysis.

In this context, and as illustrated by the following scientific examples, our previous collaborations are still active and strengthened. In particular, we maintained a very solid and successful scientific relationship with the team of G. S. Pokrovski GET (Toulouse, France), the team of J. Brugger (Monash University, Australia) and the group of I. Daniel and A. Picard (LGL, Lyon, France). The next chapters demonstrate that :

- these collaborations benefit from the tools and methods developed previously and that are well established now. Indeed, XANES calculations (initiated 10 years ago in our team) are almost 'routine' now and included in most XAS studies of hydrothermal fluids. Also our HP/HT setup is used routinely and reliably by users of FAME beamline but still is unique in the world (two international HP laboratories contacted us with the goal to install our technology on their premises : Edinburgh University/Diamond synchrotron in UK, and Münster University/DESY in Germany). Finally, the FAME micro-beam set-up is still occasionally requested by user (see Louvel et al. below) and makes it possible to scale our XAS methods (EXAFS analysis and XANES calculations) down to the micrometric scale (in this case in a Diamond-Anvil cell).
- new tools and methods are integrated in our research : with the increase of computing power, ab initio molecular dynamics calculations are a very useful complement to XAS structural results but they need the expertise of dedicated research groups (see Pokrovski et al. and Brugger et al.).
- the collaborations we are involved in have now a global integrated approach to understand things by using the physical-chemical results from XAS and DM (typically the local molecular structure) to understand 'real-life' Earth Sciences problems, whether it be the role of sulfur in metal hydrothermal transportation (SOUMET project, Pokrovski et al.), the fate of metals in hydrothermal fluids (Louvel et al. from ETH Zürich, and australian collaboration, Brugger et al.) or the role of deep-sea piezophilic organisms on the carbon and iron geochemical cycles (I. Daniel & A. Picard).
- finally there is a constant need for further technological development to fulfill the ever challenging experimental conditions. This point is detailed in chapter 4 of this report.

Another facet of our internal research activity of the last 4 years is based at Institut Néel with the installation of a Raman spectrometer (Horiba JY T64000). This was anticipated in the previous BLRP report and has been successfully done. Its use is shared between I. Néel users and ourselves. For our in-house research we fitted the spectrometer with a dedicated HP-HT set-up, similar to the one installed on FAME (see §4 of this report). The topics of investigation are the study of hydrothermal fluids H2O-CO2-NaCl and the role of co-solvents and solutes on the structure of water itself, the hydrogen bonding network in particular. It was decided not to detail exhaustively these studies in the present report (they are concisely evoked by G. S. Pokrovski below), because they are not conducted on FAME, but the connection of Raman spectroscopy with our beamline is obvious for two reasons :

- there still exist the project to install a Raman spectrometer on the beamline for parallel Raman and XAS measurements ;
- with the future Crystal Analyzer Spectrometer of FAME-UHD, the study of low Z elements K edges will be realistically do-able by inelastic scattering, which will open possibilities for solvent molecular investigation, as it is done with Raman.

Denis Testemale & Jean-Louis Hazemann

Impact of sulfur on the fate of metals of high technological value in geological fluids (ANR blanc SOUMET 2011-2015)

The metal crisis in the last years has provoked an urgent need for better understanding the processes of metal ores formation, for developing geochemical tools for identifying new mineral resources, and for improving ore treatment and extraction technologies in environmentally-responsible ways for metallic elements. In particular, base and noble metals are the first in this growing demand, nowadays raising a rapidly increasing economic concern (e.g., Au, Ag, Pt, Cu, Zn, Mo, Sn). The most remarkable common feature of these metals is the association with *sulfur - a ubiquitous component in magmatic-hydrothermal systems*. Paradoxically, very little is known about how metals and sulfur behave and interact *in the fluid and vapor phases, which are the primary transporting media for metals to the deposits*. Sulfur may affect the metals behavior in geological fluids in different ways: it can lead to metal deposition as sulfide minerals; it can, in contrast, enhance the metal mobility in the fluid and vapor phase via formation of soluble complexes; it can affect the acidity and redox potential of the metal-bearing fluid[7,8,9]. The understanding of the geochemical and economic role of metal-sulfur interactions requires an integrated approach, from molecular to geological scale, and taking account of the other important constituents of geological fluids (salts, volatiles, solvent). Such an approach has been developed in the framework of an ANR multidisciplinary project SOUMET that brings together four French research teams of geochemists, economic geologists, physicists, and chemists (GET, G2R, IMPMC, and FAME) working together on the wide range of complementary tasks: a) measurements of metal solubility and partitioning in model S, salt and CO_2-bearing fluids, b) in situ spectroscopic investigations of metals, sulfur and solvent molecular structures, c) molecular and thermodynamic modeling and d) analytical developments for tracing ore formation processes. The FAME team is a key player in this multidisciplinary research program, applying in-situ spectroscopic methods (XAS and Raman) to probe hot and deep hydrothermal fluids that cannot be studied unambiguously using ex-situ techniques. Below is a brief summary of the major contributions of the FAME team to this project. All of them are based on the use of a high-pressure high-temperature spectroscopic cell unique in the world enabling accurate measurements of element concentrations (i.e. mineral solubility) and local molecular structure of solutes and solvent using different spectroscopic methods such as XAS, Raman, and SAXS.

Gleb Pokrovski
Géosciences Environnement Toulouse

Silver and gold speciation in hydrothermal fluids

These two metals of high economic value have a contrasting affinity for the main ligands of natural fluids, Cl and S; Ag loves chloride and Au loves sulfide (and potentially other S-reduced forms); therefore it is critical to know the stability and composition of their main complexes to understand Au/Ag fractionation and economic ore formation. By combinining EXAFS and XANES spectra analyses of Ag chloride bearing solutions to 450°C and 1 kbar (FAME & BM29) with molecular dynamics simulations (IMPMC) and thermodynamic modeling (GET), our teams have unambiguously revealed, for the first time, the identity, structure and stability of Ag-chloride complexes responsible for Ag transport by hydrothermal fluids[10]. Our results show that the tri- and tetra-chloride species ($AgCl_3^{2-}$ and $AgCl_4^{3-}$), which have been a matter of discussions for 30 years, are important only in moderate-temperature (<250°C) concentrated (>20-30 wt% NaCl) salt brines, whereas the di-chloride ($AgCl_2^-$) is the major Ag carrier in typical hydrothermal fluids above 300°C (Figure 11). This species has an angular geometry (Cl-Ag-Cl angle ~160±10°) offering stronger interactions with outer-sphere

[7] Kouzmanov K., Pokrovski G.S. Hydrothermal controls on metal distribution in Cu(-Au-Mo) porphyry systems. In: 'Geology and Genesis of Geology and Genesis of Major Copper Deposits and Districts of the World: A Tribute to Richard H. Sillitoe' (eds. J.W. Hedenquist, M. Harris, and F. Camus). *Society of Economic Geologists Special Publication*, **16** (2012) 573-618.
[8] Pokrovski G.S., Borisova A.Y., Bychkov A.Y. Speciation and transport of metals and metalloids in geological vapors. *Reviews in Mineralogy & Geochemistry* **76** (2013) 165-218.
[9] Pokrovski *et al.*, Gold speciation and transport in geological fluids: insights from experiments and physical-chemical modeling. In: *Geological Society of London Special Publication* "Gold-transporting fluids in the Earth's crust" (eds. P. Garofalo, E. Ripley) **402** (2014) 9-70 / **Article 2014-21**.
[10] Pokrovski *et al., Geochim. Cosmochim. Acta* **106** (2013) 501-523.

water molecules and Na and Cl ions, compared to Cu and Au that form linear di-chloride complexes[11,12]. This structural control explains Ag fractionation from Au and Cu in S-poor vapor-brine systems. In S-rich fluids, both Ag and Cu stay as chlorides, but Au forms S-bearing species[12]; this difference further contributes to the fractionation of these three elements in their economic deposits[10].

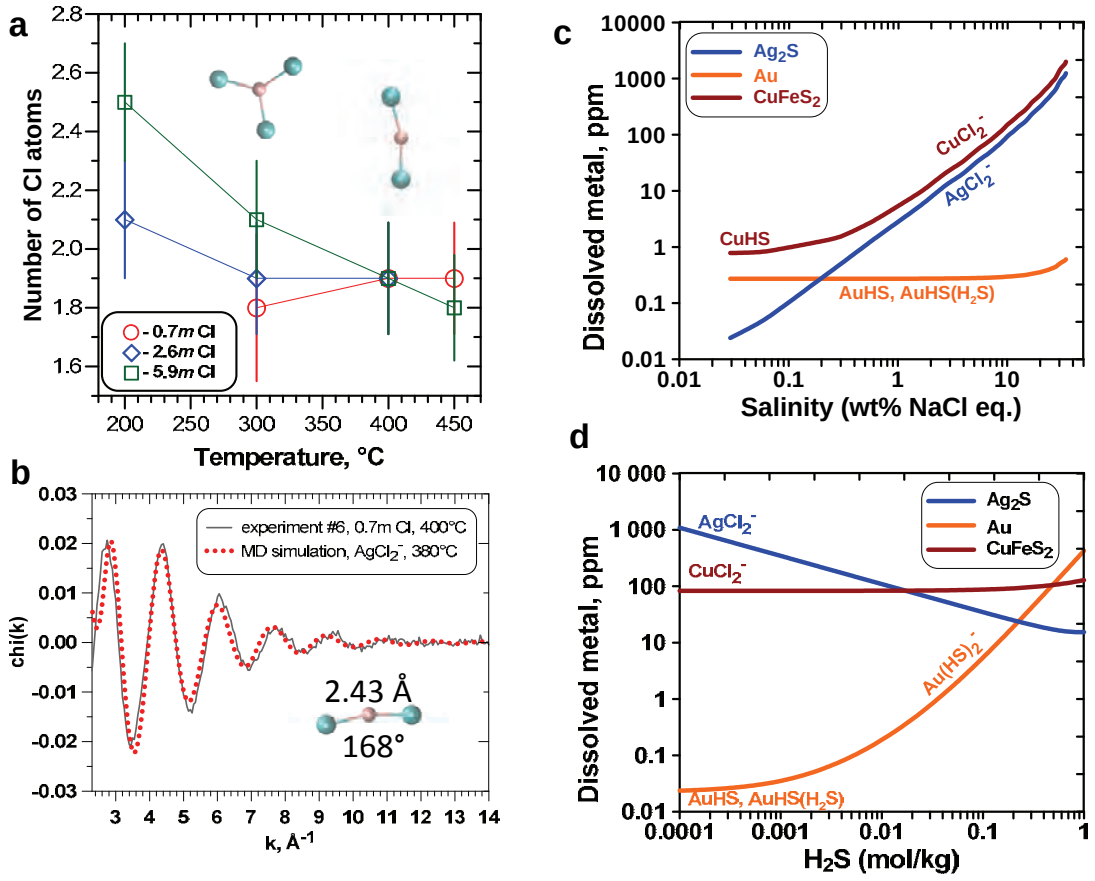

Figure 11. Speciation and solubility of Ag in Cl hydrothermal solutions as reveals by combination of XAS spectroscopy, MD and thermodynamic modeling. (a) Average numbers of Cl atoms in the nearest atomic shell of Ag as function of chlorinity and temperature. The structures of the dominant $AgCl_3^{2-}$ and $AgCl_2^-$ species are also shown. (b) comparison of MD calculated and experimental EXAFS spectrum of $AgCl_2^-$ (Ag-Cl distance and Cl-Ag-Cl angle are indicated). (c and d) Ag, Cu and Au concentrations in equilibrium with their principal ore minerals (Ag_2S, $CuFeS_2$ and native Au) in typical hydrothermal fluids at 400°C and 500 bar as a function of chlorinity (c) and H_2S concentration (d). The contrasting speciation of Cu and Ag (dominated by Cl) and Au (dominated by sulfide) accounts for the fractionation of these metals in their hydrothermal ores.

However, one of the key unknowns remains the speciation of sulfur itself in geological fluids. Until now, all models of gold and accompanying metals transport and ore-deposit formation have been based on a fundamental assumption that sulfate and sulfide (and sulfur dioxide in the gas phase) are the only sulfur forms in geological fluids, vapors and melts, and that the hydrogen sulfide (H_2S/HS^-) is the major carrier of gold in these environments[7,8,9,12]. The recent discoveries of another sulfur reduced form, the trisulfur radical ion S_3^-, may change this long-standing view[13,14,15]. In this ANR project, we have combined in situ X-ray absorption spectroscopy (XANES and EXAFS) and gold solubility measurements with molecular dynamics and thermodynamic simulations on model Au-sulfate-sulfide aqueous solutions, representative of ore-forming hydrothermal fluids, to show the formation, between S_3^- and Au^+, of stable soluble complexes of the likely stoichiometry $Au(HS)S_3^-$ (Figure 12). These

[11] Brugger *et al. Geochim. Cosmochim. Acta* **71** (2007) 4920-4941 / **Article 2007-4** (BLRP 2009)
[12] Pokrovski *et al. Geochim. Cosmochim. Acta* **73** (2009) 5406-5427 / **Article 2009-18** (BLRP 2009). Pokrovski *et al. Chem. Geol.* **259** (2009) 17–19 / **Article 2009-17** (BLRP 2009)
[13] Pokrovski G.S., Dubrovinsky L.S, *Science* **331** (2011) 1052-1054.
[14] Jacquemet N., Guillaume D., Zwick A., Pokrovski G.S, *American Mineralogist* **99**(2014) 1109-1118.
[15] Pokrovski G.S., Dubessy J. (2014) Stability and abundance of the trisulfur radical ion in hydrothermal fluids. *Earth & Planetary Science Letters* (under review).

species enable a far more efficient extraction, transport and precipitation of gold by geological fluids than believed based on our knowledge of hydrogen sulfide Au complexes (AuHS and $Au(HS)_2^-$), and may account for gold and associated metals tenors in major porphyry-epithermal Cu-Au-Mo and Carlin-type and orogenic Au deposits. The discovery of gold-trisulfur ion complexes requires a revision of Au speciation and transport models in S-bearing magmatic-hydrothermal fluids and, possibly, hydrous silicate melts. The formation and breakdown of the S_3^- ion during the fluid generation and evolution is thus one of the key factors controlling gold distribution and concentration in the Earth's crust[16].

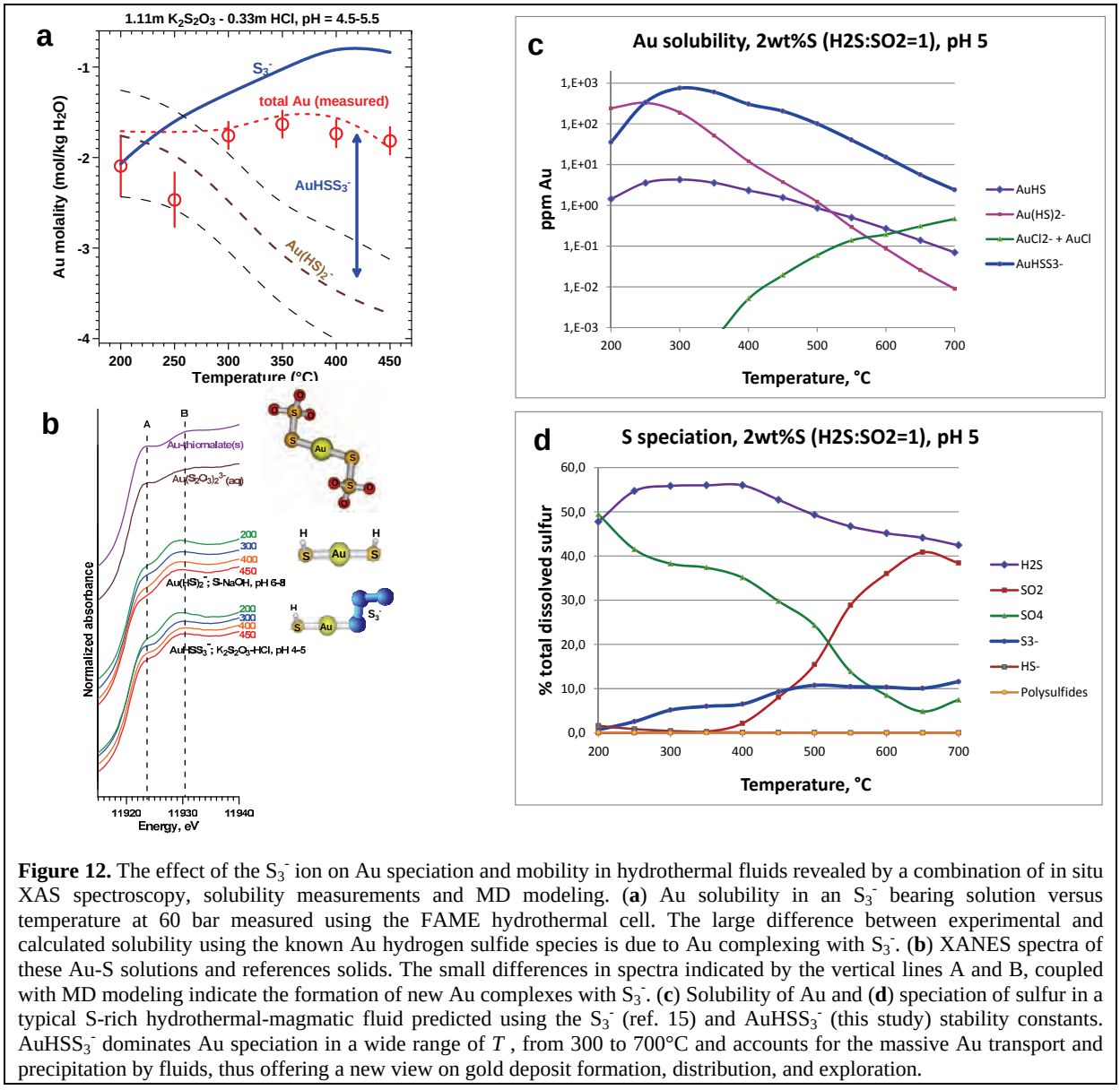

Figure 12. The effect of the S_3^- ion on Au speciation and mobility in hydrothermal fluids revealed by a combination of in situ XAS spectroscopy, solubility measurements and MD modeling. (**a**) Au solubility in an S_3^- bearing solution versus temperature at 60 bar measured using the FAME hydrothermal cell. The large difference between experimental and calculated solubility using the known Au hydrogen sulfide species is due to Au complexing with S_3^-. (**b**) XANES spectra of these Au-S solutions and references solids. The small differences in spectra indicated by the vertical lines A and B, coupled with MD modeling indicate the formation of new Au complexes with S_3^-. (**c**) Solubility of Au and (**d**) speciation of sulfur in a typical S-rich hydrothermal-magmatic fluid predicted using the S_3^- (ref. 15) and $AuHSS_3^-$ (this study) stability constants. $AuHSS_3^-$ dominates Au speciation in a wide range of T , from 300 to 700°C and accounts for the massive Au transport and precipitation by fluids, thus offering a new view on gold deposit formation, distribution, and exploration.

These findings, which may have only been achieved via unprecedented combination of experimental, spectroscopic and modeling approaches centered around the unique FAME research facility, open a number of perspectives for studying ore-formation processes. In particular, the approaches developed in our ANR program may contribute to resolving one of the long-standing enigmas in Metallogeny, which is the ubiquitous Au association with pyrite in almost all types of

[16] Pokrovski G.S., Kokh M.A., Guillaume D., Borisova A.Y., Gisquet P., Hazemann J-L., Lahera E., Del Net W., Proux O., Haigis V., Ferlat G., Vuilleumier R., Saita A.M., Boiron M.-C., Dubessy J. The role of the trisulfur radical ion S_3^- in the formation of hydrothermal gold deposits (in preparation).

deposits[9,17]. Revealing the molecular state of Au in pyrite, which may have multiple S-ligand environments (e.g., Au-S and Au-S_3) and is complicated by the presence of other trace elements (e.g., As, having similar absorption edge energies) will require in-situ XAS spectroscopy with a high-resolution setup (crystal analyzers). Such a setup is under development at FAME and will be tested on natural and synthetic Au-bearing pyrite samples in the framework of the SOUMET project. In the future, this setup may also be used in combination with high *T-P* spectroscopic cells thus offering a great step forward in our understating of hot and deep fluids that operate in the interiors of our planet.

In situ Raman spectroscopy of sulfur, water, and H_2O-CO_2 solvents

Understanding metal speciation and transport in hydrothermal fluids is impossible without knowledge of the molecular speciation of ligands themselves and the solvent structure. The outstanding advantage of the FAME hydrothermal cell is to enable such measurements using laser Raman spectroscopy on the same model high *T-P* fluids that those used in the studies of metal speciation by XAS described above. The Raman spectroscopy set up with a dedicated autoclave with optically transparent windows and inner cell (made of alumina) is on operation at the Institute Néel. It allowed first measurements of sulfur speciation in aqueous solution, which perfectly confirmed our recent findings of S_3^- using different Raman designs [13-15].

Systematic measurements of aqueous (H_2O and D_2O) and mixed CO_2-H_2O supercritical fluids using this set up reveal the persistence of hydrogen bonds in water along the critical isochore (density ~0.35 g/cm^3), and unexpected effect of CO_2 on these bonds, as manifested by changes in the CO_2 Fermi diad Raman bands (Figure 13). Critical to accurate interpretation of the solvent Raman spectra is molecular modeling conducted in coll. with the IMPMC/ENS team. The molecular data on hydrothermal solvents obtained using this unique technique will be critical for developing new physical-chemical models of hydrothermal fluids combining both macroscopic (density, dielectric constants) and molecular (hydrogen bond, solvation structures) information. A logic and necessary evolution of this Raman set up is its incorporation into the FAME beamline environment that will enable unprecedented research combining XAS and Raman spectroscopy on the same sample during the same experimental session.

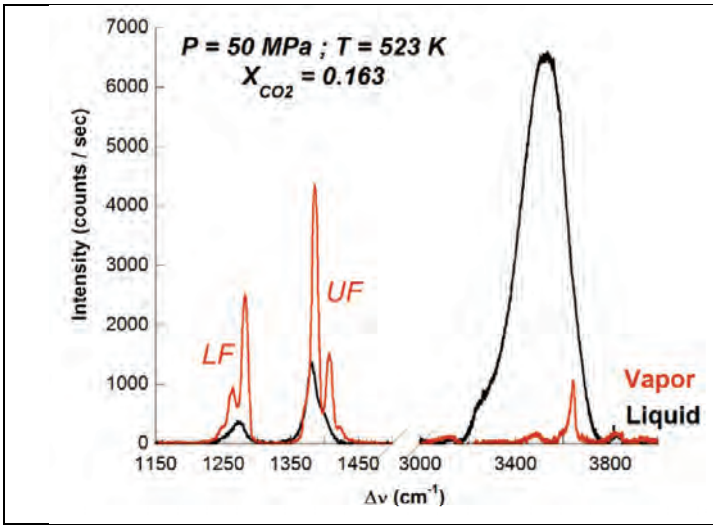

Figure 13. Raman spectra collected in coexisting CO_2-rich vapor phase and H_2O-rich liquid phase at 523 K and 50 MPa, for a 16.3 mol% CO_2 concentration. Both the CO_2 Fermi diad (1150-1500 cm^{-1}) and the OH stretching band (3000-4000 cm^{-1}) are presented.[18]

Main publications and authors:

Pokrovski G.S.[1], Roux J.[2], Ferlat G.[3], Jonchiere R.[3,5], Seitsonen A.P.[4], Vuilleumier R.[5], Hazemann J.-L.[6] Silver in geological fluids from in situ X-ray absorption spectroscopy and first-principles molecular dynamics. *Geochimica et Cosmochimica Acta* **106** (2013) 501-523.

[17] Velásquez *et al.* Formation and deformation of pyrite and implications for gold mineralization at the El Callao Mining District, Venezuela. *Economic Geology* **109** (2014) 457-486.

[18] Louvel M., Bordage A., Da Silva-Cadoux C., Testemale D., Lahera E., Del Net W., Geaymond O., Dubessy J., Argoud R., Hazemann J.-L., *Journal of Molecular Liquids*, accepted

Pokrovski G.S., Kokh M.A., Guillaume D., Borisova A.Y., Gisquet P., Hazemann J-L., Lahera E., Del Net W., Proux O., Haigis V., Ferlat G., Vuilleumier R., Saita A.M., Boiron M.-C., Dubessy J. The role of the trisulfur radical ion S_3^- in the formation of hydrothermal gold deposits (in preparation)
[1] Geosciences Environnement Toulouse (GET, ex-LMTG), Observatoire Midi-Pyrénées, Université de Toulouse, CNRS, IRD, Toulouse, France / **[2]** Equipe PMM, Institut de Physique du Globe de Paris, France
[3] Institut de Minéalogie et de Physique des Milieux Condensés, Université P. & M. Curie (UPMC), UMR CNRS-UPMC-IPGP 7590, Paris, France / **[4]** Physikalisch-Chemisches Institut der Universität Zürich, Switzerland / **[5]** Département de Chimie, Ecole Normale Supérieure, UMR CNRS-ENS-UPMC 8640, Paris, France / **[6]** Institut Neél, CNRS, Grenoble, France

Towards a molecular-level understanding of ore-forming processes: Hydrothermal experiments by the Aussie-FAME team 2009-2014

Aqueous metal complexes play a fundamental role in controlling metal transport and mineral solubility in natural and industrial hydrothermal systems. In the past five years, our collaborative team (CNRS, Adelaide University and CSIRO) has used *in situ* X-ray Absorption Spectroscopy techniques developed at the FAME beamline to investigate the speciation of Mn[19], Fe[20], Co[21], Ni[22], Cu[23], Zn[24], As[25,26], Au[27], Bi[28,29] and Te[30,31] in hydrothermal fluids. These studies provide crucial structural information and thermodynamic data for predicting the behaviour of these metals through the complex processes involved in ore formation, geothermal energy production, or mineral processing.
For the first-row transition metals (Me), the structure of the chloride complexes changes from octahedral to tetrahedral with increasing temperature and/or halide concentration, accompanied with dehydration and increased number of chloride ligands, with a general reaction of

$$Me(H_2O)^{2+}_{6(octahedral)} + mCl^- = MeCl_m(H_2O)_{4\text{-}m(tetrahedral)} + (m+2)H_2O, \qquad (1)$$

We used XANES to obtain thermodynamic properties of the predominant species, enabling numerical modelling of behaviour of these metals in hydrothermal fluids. As an example the solubility of cobalt sulfide in chloride brines is shown in Figure 14.a. The change of coordination structure leads to solubility drop and deposition of cobalt from hydrothermal fluids upon cooling.

Our XAS experimental studies of copper in sulphur-bearing brines and vapours provided evidence that copper does not preferentially partition into the vapour phase, in contrast to the view at that time; this result was later confirmed by new fluid inclusion studies. Our XAS study of Bi and Te in chloride fluids, and As in natural fluids inclusions identified important species for Bi, Te and As transport in hydrothermal fluids. Study of gold complexation in mixed-ligand solutions revealed that sulphur outcompete chloride, bromide and ammonia for transporting gold in reduced S-bearing fluids.

Recently our group has focused on combining state-of-the-art molecular dynamics (MD) simulations with XAS experiments to improve our understanding of solvation processes and provide more accurate thermodynamic models of mass transfer at high P,T. Based on case studies on Cu^I, Au^I and Zn^{II}, we have demonstrated that first principle MD predict reliably the speciation and complex geometry observed experimentally. This exciting result led to detailed MD studies of the energetics of the complex-forming reactions (Figure 14) and the demonstration that accurate free energies can be derived from first principles. Experiment on Zn-chloride complexing confirmed the MD predictions.
The collaboration has resulted in 13 joint papers.[19-31] Brugger and Testemale also obtained joint funding from the Australian Research Council of A$1,200k (two grants over 2008-2015). FAME remains the only place in the world to conduct high P-T experiments on aqueous fluids routinely. The

[19] Tian *et al., Geochimica et Cosmochimica Acta* **129** (2014) 77-95 / **Article 2014-25**
[20] Testemale *et al., Chemical Geology* **264** (2009) 295-310 / **Article 2009-22** (BLRP 2009)
[21] Liu *et al., Geochimica et Cosmochimica Acta* **75** (2011) 1227-1248 / **Article 2011-8**
[22] Tian *et al., Chemical Geology* **334** (2012) 345-363
[23] Etschmann *et al., Geochimica et Cosmochimica Acta* **74** (2010) 4723-4739 / **Article 2010-14**
[24] Mei *et al.,* submitted to *Geochimica et Cosmochimica Acta*
[25] James-Smith *et al., American Mineralogist* **95** (2010) 921–932 / **Article 2010-17**
[26] Qian *et al., Geochimica et Cosmochimica Acta.* **100** (2013) 1–10 / **Article 2013-21**
[27] Liu *et al., Chemical Geology* **376** (2014) 11-19
[28] Tooth *et al., Geochimica et Cosmochimica Acta* **101** (2013) 156-172 / **Article 2013-26**
[29] Brugger *et al., J. Sol. Chem.*, **43** (2014) 314-325 / **Article 2014-5**
[30] Brugger *et al., American Mineralogist* **97** (2012) 1519-1522 / **Article 2012-5**
[31] Grundler *et al., Geochimica et Cosmochimica Acta* **120** (2013), 298-325 / **Article 2013-14**

team is working of bringing some of these capabilities (P≤600bar) to the Australian Synchrotron, which will allow to extend the scope of the collaboration.

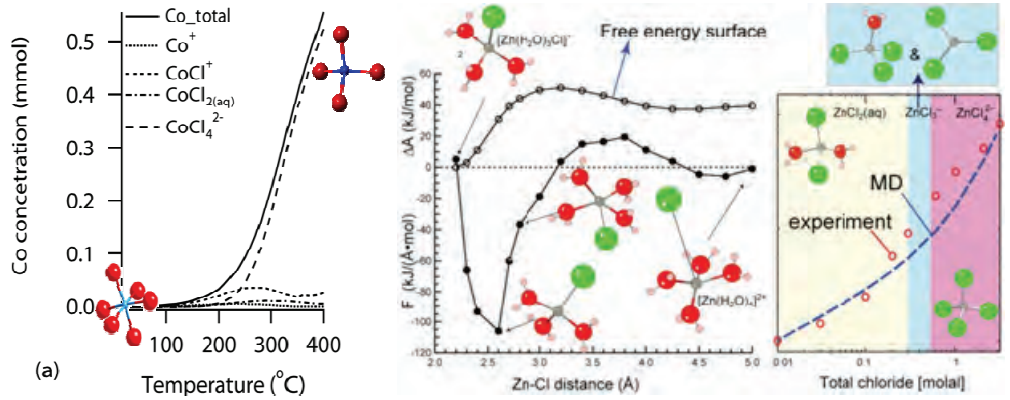

Figure 14. Thermodynamical properties deduced from XAS results. **(a)** solubility of cobalt sulfide in chloride brines as a function of the temperature and Co-Cl molecule geometry. **(b)** Free energies Zn-Cl complexes formation deduced from XAS measurements and MD calculations

Authors
Brugger J.,[1,2] Etschmann B.,[1,2] Liu W.,[3] Grundler P.V.,[1] Tian Y.,[1] Mei Y.[1] Qian G.,[1] Tooth B.,[1] James-Smith J.,[1,4] Testemale D.,[4] Hazemann J.-L.[4]
[1] South Australian Museum, Adelaide, Australia / [2] School of Earth and Environmental Sciences, The University of Adelaide, Australia / [3] CSIRO Earth Science and Resource Engineering, Clayton, Australia / [4] Institut Néel, Grenoble, France

In situ investigation of Zr speciation in high P-T fluids and melts in Hydrothermal Diamond-Anvil Cell. Implications for mobilization of HFSE in subduction zones

Magmas erupted in volcanic arcs display are characterized by a strong enrichment in large ion lithophile elements (Sr, Rb, Th, U) and a depletion in high-field strength elements (HFSE: Nb, Ta, Zr, Ti, Hf) compared to mid-ocean ridge basalts. This distinct geochemical signature carries critical information about the petrogenesis of arc magmas, and in particular about the contribution of a slab-derived metasomatic agent (aqueous fluid, silicate melt or a supercritical liquid of intermediate composition) to the source of arc magmas in the mantle wedge.

For instance, it is generally accepted that the HFSE depletion of arc magmas arises from their low solubility in H_2O [32] and selective segregation in minerals from the slab or the mantle wedge [33]. On the opposite, relative HFSE-enrichment recorded in high-Nb basalts or adakitic magmas in volcanic arcs such as Kamtchatcka, Cascades, or Lesser Antilles[34] have been attributed to a significant contribution of slab melts to their source, in regards of the high solubility of HFSE in silicate melts[35]. However, the occurrence of rutile or zircon-rich veins in UHP metamorphic rocks[36] attests that high temperature aqueous fluids also have the potential to mobilize and transport nominally insoluble HFSE and hence question the importance of slab melts in HFSE recycling in subduction zones.

Recent experimental studies provided evidences that the addition of Cl, F, Si or Na significantly enhances the solubility of HFSE-bearing phases as zircon in high P-T aqueous fluids[37]. It was hence proposed that complexation of HFSE with alkalis and/or halogens could favour the incorporation and transport of nominally insoluble HFSE in subduction zone fluids. In this context, we conducted high P-T experiments to determine *in situ* the influence of P-T conditions and composition on the speciation of Zr in aqueous fluids and silicate melts.

[32] Antignano A. and Manning C. E. *Chem. Geol.* **255** (2008) 283–293.
[33] Rubatto D., Hermann J. *Geochimica et Cosmochimica Acta* **67** (2003) 2173–2187 / Scambelluri M., Philippot P. *Lithos* **55** (2001) 213–227
[34] Munker C., Worner G., Yogodzinski G., Churikova T. *Earth Planet. Sci. Lett.* **224** (2004) 275–293
[35] Linnen R. L., Keppler H. *Geochimica et Cosmochimica Acta* **66** (2002) 3293–3301
[36] Gao J., John T., Klemd R., Xiong X. M. *Geochimica et Cosmochimica Acta* **71** (2007) 4974–4996
[37] Hayden L. A., Manning C. E. *Chem. Geol.* **284** (2011) 74–81 / Rapp *et al. Geology* **38** (2010) 323–326.

The experiments were conducted in hydrothermal diamond anvil cells (HDAC) that enable *in situ* spectroscopic analyses of high P-T fluids and melts up to 800-900 °C and 2-3 GPa [38]. Despite stringent spatial constraints, an optimal experimental configuration was achieved at BM30B (Figure 15). The set-up comprised a set of mirrors that ensures the focusing of the monochromatic X-ray beam down to 10 x 15 (VxH) μm^2 with a flux of ~1.10^9 photons/s for *in situ* measurements. XAS spectra were collected in fluorescence mode using a Si drift detector. A CCD camera was used to collect XRD pattern from the pressure calibrant ($Au+Al_2O_3$) before and after each heating step. A microscope placed on the side of the KB mirrors completed the micro-set-up to visually monitor the compression chamber during heating stage. In addition, reference spectra could be acquired on macroscopic mineral and glass standards conducting XAS measurements *ex situ* with a 300 x 150 (FWHM HxV) μm^2 size beam and a flux of 10^{11} photons/s. These reference spectra were collected in transmission or fluorescence modes using either diodes or a Canberra solid-state 30 element Ge detector (Figure 15).

In situ XAS spectra were collected up to 800°C and 2.4 GPa in Zr-bearing 2.5 wt% HCl aqueous solutions, homogeneous fluid phases containing from 35 to 60 wt% dissolved Si and Na and hydrous haplogranite melts (up to 33 wt% H_2O) to investigate the effect of dissolved silicates on Zr speciation in high P-T fluids. The likeliness of Zr-Cl and Zr-F complexation was tested on the Zr-bearing 2.5 wt% HCl aqueous solutions and F-bearing $Na_2Si_2O_5$ and haplogranite glasses. The quality of the spectra attests that high resolution µXAS can be conducted in high P-T fluids and melts on FAME.

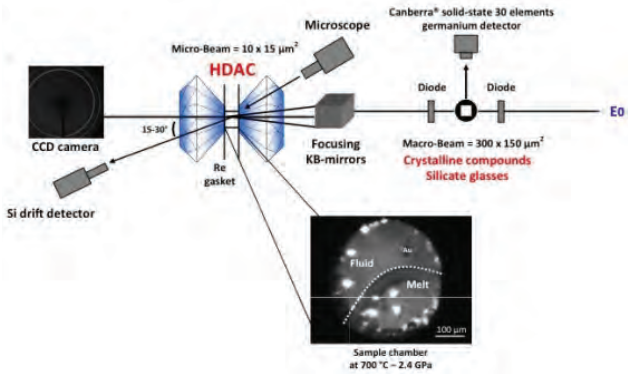

Figure 15. Experimental set-up for in situ XAS data collection at the BM30B beamline

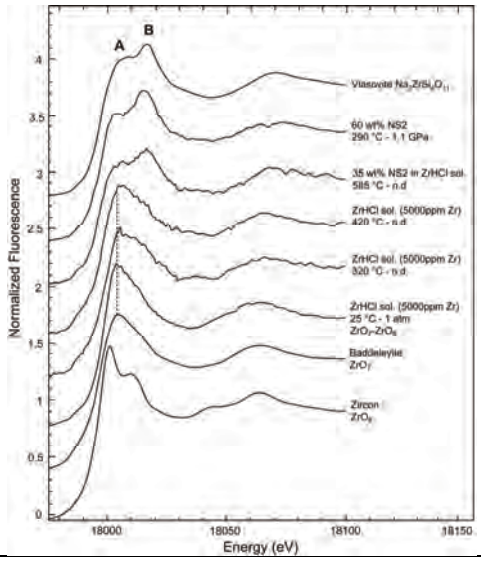

Figure 16. Comparison between the XANES spectra collected on reference minerals and Zr-bearing high P-T fluids.

Experimental XANES provide evidence for the formation of Zr–O–Si/Na polymeric species in high pressure fluids with the addition of dissolved Si and Na (Figure 16). Indeed, while the strong resemblance between the XANES spectra of reference baddeleyite and the ZrHCl solution attest that Zr^{4+} speciation in dilute fluids is dominated by 8-fold-coordinated $[Zr(H_2O)_8]^{4+}$ hydrated complexes, the addition of Si and Na dissolved species into the fluid favors the formation of octahedral alkali-zirconosilicate clusters Zr–O–Si/Na similar to those found in vlasovite ($Na_2ZrSi_4O_{11}$). Similar environment is observed in hydrous haplogranite and F-free and F-bearing NS2 and haplogranite glasses. EXAFS analyses confirm the octahedral coordination of Zr in silicate-rich fluids, hydrous melts and silicate glasses with Zr–O distance of 2.09 ± 0.04 Å and the presence of ≈ 6 Si (Na) second neighbors at a mean distance of 3.66 ± 0.06 Å.Comparison of experimental XANES spectra to *ab initio* XANES calculations provide no evidence for extensive Zr–Cl complexation in high P-T aqueous fluids and are not conclusive concerning the extent of Zr–F complexation in hydrous granitic melts.

The formation of Zr-O-Si/Na clusters as those identified in this study provide a favorable mechanism for the efficient mobilization of nominally insoluble HFSE by subduction zone fluids (aqueous fluids, supercritical liquids or slab melts). Thus, the characteristic HFSE depletion of arc magmas must arise from complex fluid/melt/rock interactions that could affect the stability of these

[38] Bassett *et al.* (1993) *RSI* **64**, 2340–2345 / Sanchez-Valle *et al. J. Phys. Cond. Matter* **16** (2004) S1197–S1206.

complexes and trigger the precipitation of HFSE-bearing accessory phases at the slab interface and within the mantle wedge

Authors and principal publication:
Louvel M.[1,2], Sanchez-Valle C.[1], Malfait W. J.[1], Testemale D.[2], Hazemann J.-L.[2], "Zr complexation in high pressure fluids and silicate melts and implications for the mobilization of HFSE in subduction zones", *Geochimica et Cosmochimica Acta* **104** (2013) 281-299
[1] Institute for Geochemistry and Petrology, ETH, Zurich, Switzerland/ [2] Institut Néel, Grenoble, France

Microbial Fe transformations under deep-subsurface pressure conditions

Microorganisms influence biogeochemical cycles from the Earth's surface to the greatest depths of marine sediments. In deep surbsurface environments, pressure increases as a function of depth and certainly has a great influence on the distribution of microbial life. Yet the influence of pressure on survival and subsurface microbial activities has hardly been investigated. We recently developed a protocol to monitor microbial metal and metalloid transformations under pressure using XANES spectroscopy.[39] We used this protocol to investigate bacterial Fe(III) reduction kinetics under pressure at the FAME beamline. We performed XANES measurements in bacterial cultures to monitor Fe(III) reduction as a function of pressure in the autoclave available at the beamline[40] (Figure 17). The bacterium *Shewanella oneidensis* MR-1 grows optimally at atmospheric pressure and stops growing at 50 MPa (*i.e.* MR-1 is pressure-sensitive). Nevertheless it can reduce Fe(III) to Fe(II) up to a pressure of 110 MPa. More importantly iron reduction rates are higher in the range 30-70 MPa than at 0.1 MPa (Figure 18). Above 70 MPa reduction rate and extent concomitantly decrease with survival rate.[41] The results of this study have implications for the functioning of deep subsurface microbial communities. "Surface" microorganisms transported to depth are potentially active and are able to take part to Fe and C transformations at moderate pressures. Unfortunately it is still unknown what the proportion of pressure-sensitive microorganisms is as opposed to the pressure-adapted ones. This study sets the stage for further studies of pressure-adapted microbes isolated from deep-subsurface environments.

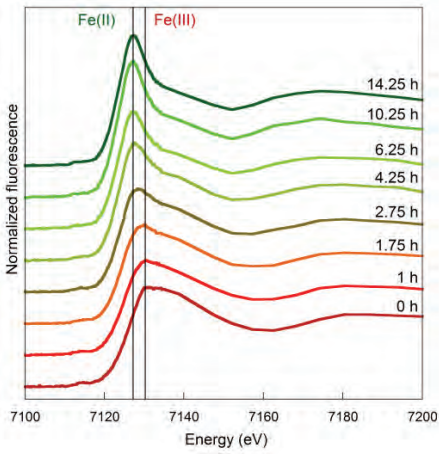

Figure 17. Fe K-edge XANES spectra measured in a culture of *Shewanella oneidensis* MR-1 incubated in the autoclave at 70 MPa and 30°C.

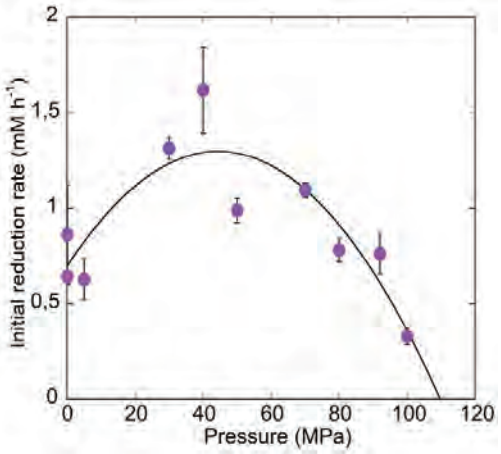

Figure 18. Initial iron reduction rates by *Shewanella oneidensis* MR-1 as a function of pressure. MR-1 is more active in the reange 30-70 MPa than at 0.1 MPa.

Authors and principal publication:
Picard A.[1,2], Testemale D.[3], Hazemann J.-L.[3], Daniel I.[2], The influence of high hydrostatic pressure on bacterial dissimilatory iron reduction, *Geochimica Cosmochimica Acta*, **88** (2012) 120-129
[1]Max Planck Institute for Marine Microbiology & MARUM Center for Marine Environmental Sciences, Bremen, Germany / [2] Lab. de Géologie de Lyon, Lyon / [3] Institut Néel & FAME Beamline, Grenoble, France

[39] Picard *et al.*, *Geobiology* **9** (2011) 196–204 / **Article 2011-13**
[40] Testemale *et al.*, *Review of Scientific Instruments* **76** (2005) 043905 / **Article 2005-15** (BLRP 2009)
[41] Picard *et al.*, *Geochimica et Cosmochimica Acta* **88** (2012) 120-129 / **Article 2012-18**

Mineralogy & cosmochemistry

Iron Redox Reactions in Nuclear Waste Glasses and Melts

Borosilicate glasses are privileged materials for nuclear waste storage because they allow a wide variety of elements to be incorporated in a stable and compact matrix. These glasses include various multivalent elements (Ce^{4+}/Ce^{3+}, Cr^{4+}/Cr^{3+}, Fe^{3+}/Fe^{2+}…) whose redox state influences the melts during the vitrification process as well as the properties of the final material. For iron, the multivalent element which is most readily amenable to experimental studies, this influence is complex because not only the abundance but also the structural role of Fe^{2+} and Fe^{3+} ions depend markedly on temperature, chemical composition and oxygen fugacity.[42] In this work, our goal was to determine how the presence of boron in silicate melts affects the equilibrium redox state and the kinetics of iron redox reactions to gain information on the mechanisms of these reactions through determination of rate limiting parameters.

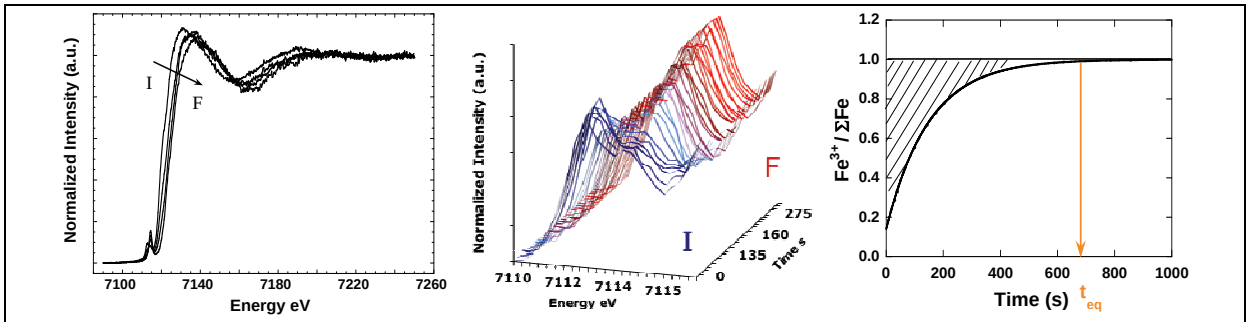

Figure 19. Time evolution of the XANES spectra at the iron K-edge (a) and of the pre-edge feature (b) of a sodium borosilicate melt at 1370 K with the oxidation evolution associated (c); I: initial state; F: final state at redox equilibrium; t_{eq} time need to reach 99% of redox equilibium.

As a matter of fact, it has long been assumed that at superliquidus temperatures, redox reactions are rate limited by diffusion of either molecular or ionic oxygen.[43] However, at supercooled liquid temperatures (*i.e.* near the glass transition temperature range), extensive work has shown that oxygen diffusion is a too slow process. The kinetics of redox reactions are then limited instead by diffusion of network-modifying cations toward the melt interface where crystallization of metastable phases takes place.[44] But this mechanism cannot operate at superliquidus temperatures (*i.e.* viscosities ranging from 10^1 to 10^3 Pa.s) where crystallization of metastable phases, which provides the driving force for cation diffusion, becomes impossible and oxygen diffusion thus represents the rate-limiting parameter.[45] These results have been mainly obtained for iron-bearing alkaline earth silicate and aluminosilicate melts.[44,45] To investigate the influence of boron, we have measured for iron-bearing sodium borosilicate melts the time evolution of the iron redox state as a function of temperature by XANES.

We determined the kinetics of the oxidation reaction between 700 and 1570K for initially reduced samples with different B_2O_3/Na_2O ratio and 67 mol % of SiO_2. To obtain the redox kinetics, we focused our attention on the pre-edge feature of the XANES spectra, which is sensitive to the iron redox state[45] (Figure 19). Comparisons between the kinetics of redox reactions were made by introducing the so-called redox diffusivity, D, which take into account the time needed to reach 99 % of the equilibrium redox ratio (Figure 19c) and the sample thickness.[45] At superliquidus temperatures, where oxygen diffusion is the rate-limiting factor of the iron redox reactions, the slowdown of the redox kinetics observed in the present work (Figure 20a) indicate that oxygen diffusion becomes slower upon addition of boron. Such an effect is expected from the polymerization reaction that is induced by introduction of boron. Also, iron redox kinetics were found to depend on the B_2O_3/Na_2O ratio as indicated on Figure 20b by the changes in activation energies of the redox diffusivities.

In summary, this work illustrates that FAME beamline is a powerful beamline to provide *in situ* knowledge of redox reactions and mechanisms as a function of temperature and chemical composition

[42] B.O. Mysen, P. Richet, 2005. Silicate Glasses and Melts: Properties and Structure. Elsevier
[43] D.S. Goldman, P.K. Gupta, *J. Amer. Ceram. Soc.*, **66**, 188-190 (1983).
[44] G.B. Cook, R.F. Cooper, T. Wu, *J. Non-Cryst. Solids*, **120**, 207-222 (1990).
[45] V. Magnien *et al.*, *Geochim. Cosmochim. Acta*, **72**, 2157-2168 (2008) / **Article 2008-13** (BLRP 2009)

of silicate melts. The results obtained on borosilicate melts will be compared with those previously derived for simpler systems.[45] Insights on redox mechanism will thus be obtained, especially on how addition of boron in silicate affects the redox reactions mechanisms.

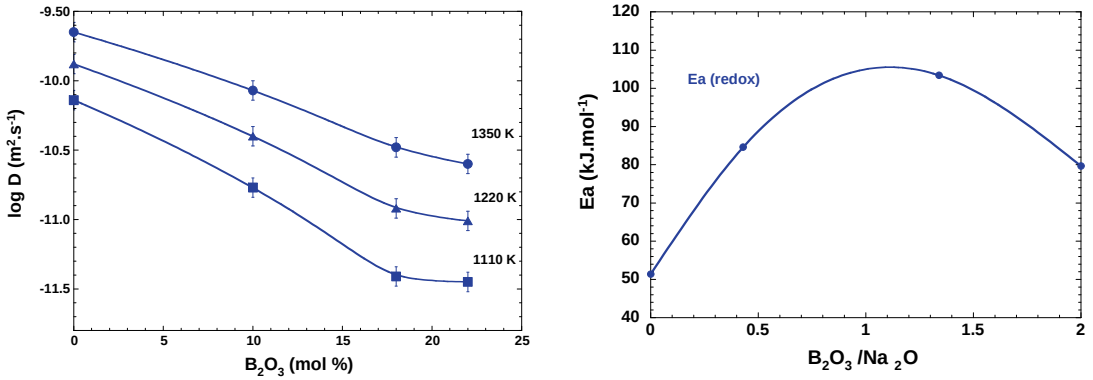

Figure 20. Redox diffusivity (left) and iron redox (right)

Authors and principal publication:
B. Cochain[1,2], D. R. Neuville[2], D. de Ligny[3], J. Roux[2], D. Testemale[4], O. Pinet[1] and P. Richet[2]
[1]CEA-DEN, DTCD, SECM, LDMC, Bagnols-sur-Cèze / [2]CNRS-IPGP, Physique des Minéraux et des Magmas, Paris / [3]LPCML, UCBL, 12 rue Ampère, 69622 Villeurbanne / [4]Institut Néel et FAME, Grenoble.
Cochain B. *et al.*, Iron Redox Reactions in Model Nuclear Waste Glasses and Melts, *Mater. Res. Soc. Symp. Proc.* **1124**, 1124-Q03-02 (2009).

Cr ligands and local environment in low-phonon glasses and glass-ceramics

Oxysulfide glass-ceramics constitute a new luminescent low phonon-energy material group for optical application accommodating the advantages of both crystals (good optical and mechanical properties) and glasses (good formability). Its conversion efficiency and emission intensity increase greatly when transition elements or rare earth ions are embedded into the sulphide-containing microcrystalline phases.[46] In particular, chromium can confer promising optical properties to the materials such as high quantum efficiency of luminescence and broad near-infrared emission in the range from 1 to 1.7 μm.[47] Cr is also an important element as it can act as nucleating agent for promoting nanocrystals. However, chromium can take different redox states with different coordination and ligands environments as a function of the chemical composition of the parent glass. Because the glass-ceramics optical properties depend on the chromium structural environment, a good control and knowledge of both its redox state and local environment is highly desirable.
We therefore performed valence-to-core XES spectroscopy[48] on FAME beamline to discriminate between the different ligands in the first coordination sphere of the chromium atom in Cr^{3+}-doped oxide and oxysulfide glasses of chemical composition: $45SiO_2$ - $3Al_2O_3$ - $30Na_2O$ - (22-x)CaO - xCaS - $0.5Cr_2O_3$ with x=0 and 2 respectively. To help the interpretation of the data, we also recorded the XES spectra of Cr^{3+}-bearing reference compounds and calculated them using DFT simulations.
Figure 21 shows the fine structure of the Kß satellite lines of Cr_2O_3 and Cr_2S_3 reference compounds (Figure 21 left) and of an oxide and oxysulfide glasses (Figure 21 right). The experimental spectra of the reference compounds are very well reproduced by the simulation allowing a better interpretation of the different features. The spectrum of the Kß satellite lines consists of two main contributions called the Kß'' and Kß2,5. The positions of the Kß satellite lines are very sensitive to the Cr ligands while the Kβ″ intensity depends on the Cr-ligand distance.[48] The substitution of O with S in the Cr^{3+} doped glasses is clearly visible through the shift of the Kß satellites emission lines to higher energies as observed between Cr_2O_3 and Cr_2S_3 but also by the decreasing intensity of the two Kβ satellite line. It can be concluded that S replaces O in the first coordination shell of Cr^{3+} in the glasses investigated.

[46] Q. Luo *et al.* (2011) *J. Am. Ceram. Soc.* **94**, 1670 / D. Chen *et al.* (2009) *J. Phys. Chem. C* **113**, 6406 / Y. H. Wang, and J. Ohwaki (1993) *Appl. Phys. Lett.* **63**, 3268
[47] T. Suzuki, Y. et al. (2008) *Journal of Luminescence* **128**, 603
[48] Eeckhout et al. (2009) *J. Anal. At. Spectro.*, **24**, 215-223 / U. Bergmann & P. Glatzel (2009) *Photosynthesis Research* **102**, 255-266

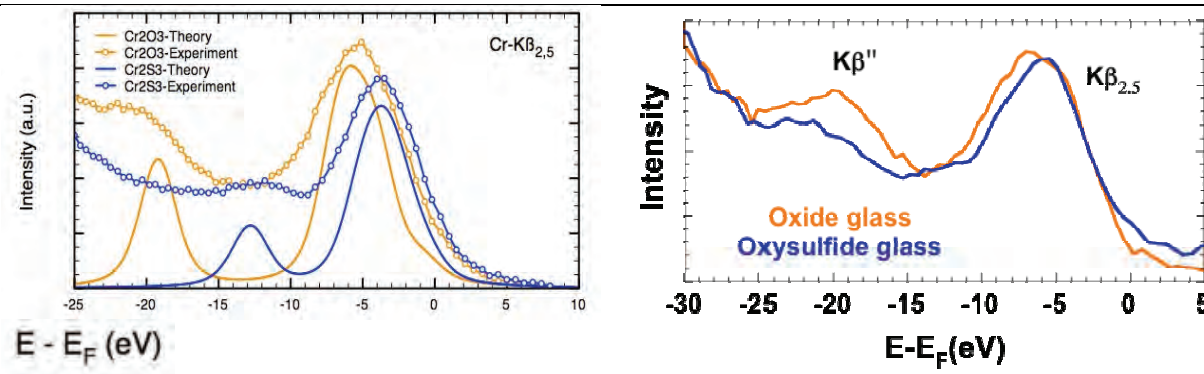

Figure 21. Experimental and DFT simulated Kß" and $Kß_{2,5}$ satellites emission lines of Cr_2O_3 and Cr_2S_3 reference compounds (a) and experimental Kß" and $Kß_{2,5}$ satellites emission lines of Cr^{3+} doped oxide and oxysulfide glasses (b).

Authors
Cochain B.[1], Cormier L.[1], Radtke G.[1], Proux O.[2], Hazemann J.-L.[3]
[1] Institut de minéralogie et de physique des milieux condensés, Paris, France / [2] Observatoire des Sciences de l'Univers de Grenoble, France / [3] Institut Néel, Grenoble, France

The redox state of iron in primitive, aqueously altered, and thermally metamorphosed chondrites by XANES

Chondrites are primitive meteorites originating from undifferentiated asteroids. Their mineralogy record presolar, nebular and asteroidal histories. On their parent body, they may have experienced important physico-chemical modifications through geological events, such as thermal metamorphism and aqueous alteration, transforming primary minerals into secondary phases.[49]

Iron is a major chemical element in planetary materials and its various valence states can be used to fingerprint geological processes.[50] Iron in fresh meteorites can exist as Fe0 in Fe-Ni metal, Fe2+ in silicates and sulfides and Fe^{3+} in phyllosilicates and magnetite. During fluid/rock interaction, iron as Fe^0 and Fe^{2+} are transformed into Fe^{3+}-rich phases. In the other hand, during thermal events, a reduction of iron is likely to occur.

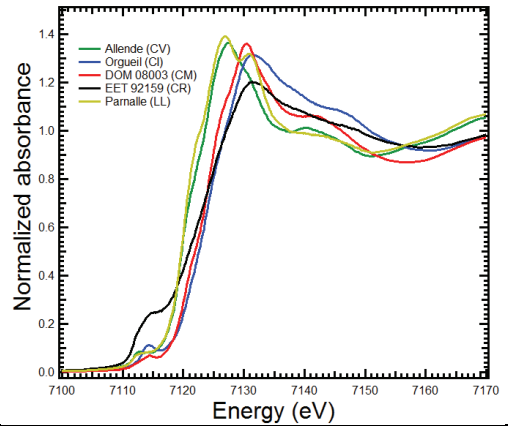

Figure 22. XANES spectra of 5 types of chondrites. The beamline energy was calibrated by setting the maximum of the derivative of a Fe^0 foil spectrum to 7112 eV. A minimum of 3 spectra were measured for each meteorite at different positions on the pellet in order to probe the inhomogeneity and variability of the preparation. For each sample, an average spectrum was calculated before performing a baseline correction and normalization (0 at the minimum pre-edge intensity and 1 at the average post-edge intensity).

X-ray Absorption Near-Edge Spectroscopy (XANES) is a very sensitive method to constrain redox states and local coordination environment of iron in natural materials including meteorites.[51] This valence state can also be used to follow the origin of D/H fractionation in aqueously altered meteorites and ultimate-ly of terrestrial water.[52] In the present study, we performed XANES on 90 chondrites belonging to 6 different families, and on 10 terrestrial standards with well-known redox statew. Clear

[49] McSween H. Y. *Geochimica et Cosmochimica Acta* **41** (1977) 477. McSween H. Y. *Geochimica et Cosmochimica Acta* **43** (1979) 1761. Brearley A.(2006) *Meteorites and the Early Solar System II*. 587
[50] Wilke M. et al. (2001) *Am. Min.* 86, 714
[51] Beck *et al.*, *Geochimica et Cosmochimica Acta* **74** (2010) 4881
[52] Sutton *et al.*, *44th Lunar and Planetary Science Conference* (2013) *abstract* #2357

variations in the redox state of iron and its crystallographic environment are observed and the Fe^{3+}/Fe_{total} ratio could be quantified. These results are discussed in the light of parent body processes.

Figure 22 presents 5 "typical" spectra of 5 different families of chondrites (CI, CM, CR, CV and LL). This figure shows the variability of the pre-edge intensity, of the edge position and of the energy of the first maximum for these different chondrites. Position, intensity and spectral shape can be used to constrain the Fe state. Also, following Wilke et al.[50], the pre-edge peak was analysed to quantify the Fe^{3+}/Fe_{total} ratio. After baseline substraction, the energy of the pre-edge centroid was calculated as well as its integrated intensity (Figure 23 & Figure 24).

The valence state between falls and finds among CM chondrites is compared on Figure 23. It allows to assess the possible consequences/impact of terrestrial residence. When comparing the pre-edge features of 25 Antartica CM chondrites and 11 fall CM chondrites, an overlap is observed rather than an increased oxidation for the finds. This implies similar Fe^{3+}/Fe_{total} ratio for all CM finds and falls. Thus, terrestrial oxidation did not significantly modify the redox state of Fe in Ant-arctic finds.
Figure 24 presents the energy at maximum intensity for the different groups of chondrites. This diagram reveals a clear dichotomy between chondrites having experienced hydrothermal alteration (CR, CI, CM) and thermal metamorphism (CV, LL). Some exceptions are present within each family of meteorites. Among CMs, PCA 02010 and PCA 02012 are distinct and present a reduce mineralogy (Figure 24). Both have been considered as thermally metamorphosed.[53] Among CRs, RBT 04133 and GRA 06100 appears different. Both have been considered as anomalous in comparison to other CRs, and evidence of thermal metamorphism has been found for GRA 06100.[54]

Kaba appears different from the other CVs, by a signif-icant amount of Fe^{3+}. In our dataset, it is the only relatively low metamorphosed (3.1) oxidised CV chondrite.[55] In the case of LL chondrites, MET 00452 appears unusual with a high-amount of Fe^{3+}.

Fe K-edge XANES is an efficient method to characterize the redox state of iron atoms in chondritic meteorites. Our dataset reveals a clear dichotomy between the aqueously altered and the thermally processed meteorites. Such a dichotomy might be related to the thermal buffer effect of water phase transitions on the parent body.

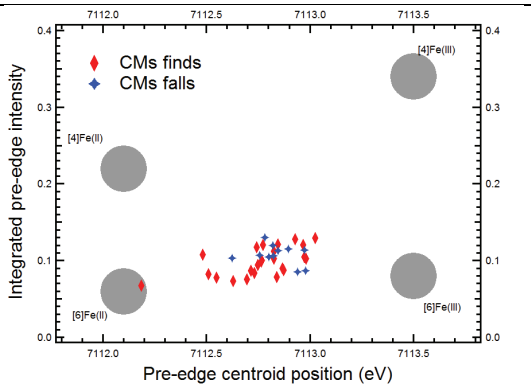

Figure 23. The pre-edge feature of CMs (finds and falls) plotted in the Wilke et al. (2001)[50] diagram

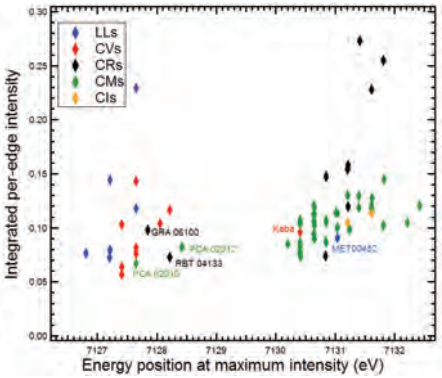

Figure 24. Maximum energy position of K-edge for the different kind of chondrites

Authors and principal publication:
A. Garenne[1], P. Beck[1], G. Montes-Hernandez[2], L. Bonal[1], E. Quirico[1], B. Schmitt[1], O. Proux[3], JL Hazemann[3],
[1]UJF-Grenoble 1 / CNRS-INSU, Institut de Planétologie et d'Astrophysique de Grenoble UMR 5274, Grenoble,
[2]UJF-Grenoble 1 / CNRS-INSU, Institut des Sciences de la Terre, Grenoble. [3]Institut Néel, Grenoble, France.
45th Lunar and Planetary Science Conference, The Woodlands, Texas (17-21 Mars 2014) (abstract #1941)

[53] Nakato *et al.*, *LPSC 44th* (2013) *abstract* #2708. Quirico *et al.*, *Annu. Meet. Meteorit. Soc 76th* (2013) *abstract* #5132.
[54] Davidson J. et al. *Meteoritics & Planet. Sci.* **72** (2009) 5141. Beck P. et al. *Icarus* (submited). Briani G. et al. *Geochimica et Cosmochimica Acta* **122** (2013) 267.
[55] Bonal L. et al. *Geochimica et Cosmochimica Acta* **70** (2006) 1849

Biochemistry

Metal complexation in biological system

The LCIB at INAC/CEA Grenoble develops research focused on metal complexation at the interface with biology. One main area is dedicated to the rational design of efficient metal ligands for health applications, such as chelation therapy or imaging. Bio-inorganic chemistry approaches were successful in the design of chelators inspired from proteins known to efficiently chelate metals *in vivo*. For instance, intracellular copper chelators mimicking metallothioneins are currently proposed as drug candidates to treat copper overload in the rare Wilson disease. A second area is committed to toxicology and ecotoxicology with the objective of understanding the influence of metal speciation on their outcome and toxic impact in living organisms. This approach has for instance made possible the identification of mobile chemical complexes of uranium in plants, as well as immobilization forms. This provides new tools for the enhancement of uranium solubilisation and removal by plants from polluted soils, in a phytoremediation perspective.

Both fields gain crucial structural information about metal speciation using X-absorption spectroscopy at various edges. Indeed, the precise nature of the metal coordination sphere is a key-parameter for the stability of the metal complexes. Moreover speciation often determines the toxicity of metals and metallic nanoparticles. Fame is the relevant beamline to perform these studies since it combines an easy access to low temperature experiments and high sensitivity, which allow us to work in conditions that do not alter the metal speciation and at low metal concentration relevant to the biological medium.

Pascale Delangle & Marie Carrière
Laboratoire de Chimie Inorganique et Biologique, INAC, CEA-Grenoble

X-ray spectroscopy probes the chemical environment of metals in complexes of potential medical interest

The three pseudopeptides **L**$^{1\text{-}3}$, having three converging cysteine arms anchored on a nitrilotriacetic acid (NTA) scaffold have been demonstrated to be efficient Cu(I) and Hg(II) sulfur-based chelating agents. Such derivatives are currently proposed as drug candidates to treat copper (Cu) overload in the rare Wilson's disease or as detoxification agents for toxic mercury (Hg). Since the coordination of the metal ion is strongly related to the chelating ability – affinity and selectivity – of these potential drugs, we investigated in-depth the chemical environment of metal ions in the complexes with the pseudopeptides **L**$^{1\text{-}3}$. The Hg(II) thiolate complexes were fully characterized in water by acid-base titration and several spectroscopic methods, including UV, ^{1}H and ^{199}Hg NMR and Hg-L_{III} EXAFS. The formation of monometallic complexes was demonstrated with typical signatures of a trigonal HgS_3 coordination site, which is uncommon, as Hg(II) usually prefers a coordination number of two. The digonal HgS_2 structure is formed at acidic pH, where one cysteine group is protonated (HgLH complex).

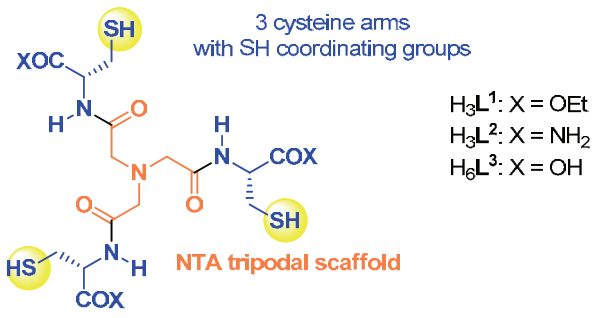

X-ray absorption spectroscopy and in particular EXAFS is the most efficient method to infer into the coordination sphere of metal ions. At alkaline pH, Hg-L_{III} EXAFS spectra at liquid Helium temperature are nearly identical for the three HgL complexes. Their analysis reveals asymmetrical HgS_3 binding environment with three S atoms at 2.38, 2.51 and 2.67 Å (Figure 25). This suggests that the C_3-symmetrical species detected by ^{1}H NMR at 298 K are averages of non-symmetrical complexes rapidly equilibrating on the NMR time-scale at ambient temperature. At acidic pH, Hg(II) is coordinated in a linear configuration to the two sulfur atoms from the thiolate groups at a distance of 2.36 Å, and in a T-shape geometry, to the third sulfur atoms from the protonated cysteine at 3.07 Å.

This work demonstrates that pseudopeptides derived from chemical scaffolds, which favor a tristhiolato HgS_3 coordination environment are interesting alternatives to design efficient water-soluble mercury-sequestering compounds. EXAFS studies are currently performed with the corresponding Cu(I) complexes to determine if their exceptionally high stability is related to the coordination environment of the Cu(I) ion.

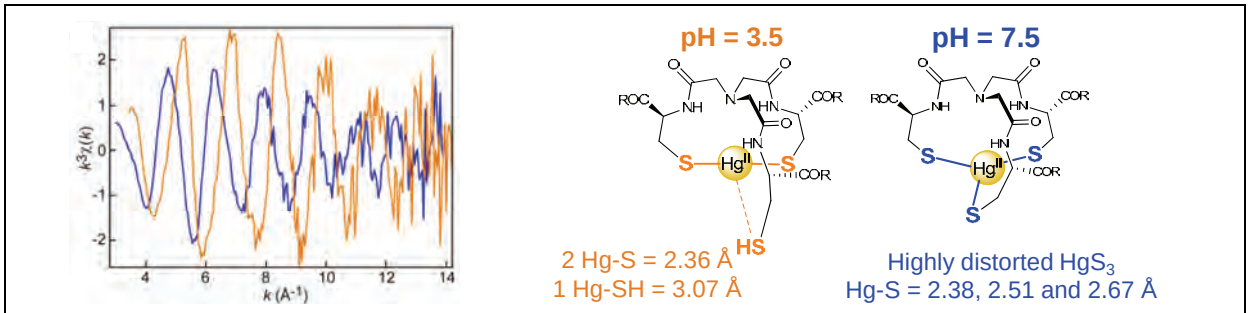

Figure 25. EXAFS spectra of HgL^3H complex with corresponding representations of the possible coordination modes

Authors and principal publication:
Pujol A. M.[1], Lebrun C.[1], Gateau C.[1], Manceau A.[2], Delangle P.[1], Mercury-Sequestering Pseudopeptides with a Tris(cysteine) Environment in Water, *European Journal of Inorganic Chemistry*, **24** (2012) 3835–3843.
[1] INAC, Service de Chimie Inorganique et Biologique, CEA, Grenoble / [2] ISTerre, UMR CNRS - UJF, Grenoble

Bioinspired Cu(I) chelators perfectly mimic metal-sequestering metallothioneins

Novel medicinal chemistry approaches may offer solutions to develop treatments for copper overload in Wilson's disease with a higher specificity than the systemic drug therapy used until now. Therefore we developed efficient intracellular Cu chelators to treat localized Cu overload in the liver, the main organ of Cu accumulation.

As the intracellular medium is a reducing environment, especially due to the high concentration of glutathione, the pool of Cu that can be mobilized is Cu(I). Cu(I) binding sites found in metallothioneins are good sources of inspiration to design high affinity Cu(I) chelators. Indeed, these small cysteine-rich proteins sequester Cu with a large affinity (Kd ~10^{-19}) in Cu(I)-thiolate clusters with a major CuS_3 coordination geometry. Pseudopeptides with three amino acids containing sulphur donors such as cysteines or D-Penicillamines have been demonstrated to form very stable Cu(I) complexes thanks to the preorganization of the chemical scaffold with a H-bond network in the upper cavity. Another crucial factor is thought to be their ability to promote CuS_3 coordination as metallothioneins.

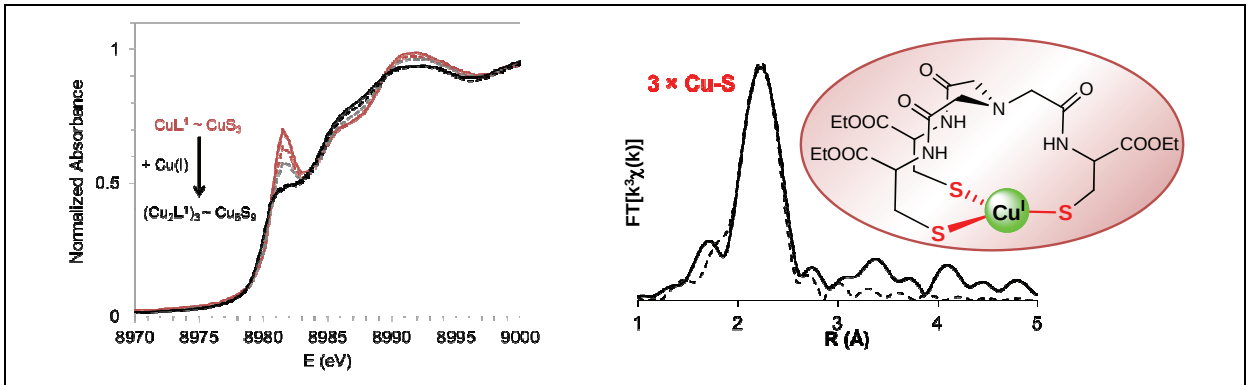

Figure 26. Left: Sensitivity of the Cu edge spectra to Cu(I) coordination – **Right**: Fourier transform of the k^3-weighted EXAFS experimental data and corresponding fit for one mononuclear Cu(I) complex

Cu K-edge X-ray Absorption Spectroscopy allowed us to probe the Cu(I) coordination sphere in these complexes. The X-Ray Absorption Near Edge Structure spectra shed light on the equilibrium between a mononuclear complex and a cluster for most of the sulphur ligands (Figure 26). Furthermore, XAS is a powerful method to quantify the equilibrium between the two Cu(I) environments, mononuclear ⇔ cluster and to determine the thermodynamic constants. The exclusive

symmetric CuS_3 geometry adopted in the mononuclear complexes (Cu-S ≈ 2.23 Å) was clearly demonstrated by the EXAFS analyses. They also proved that the clusters are organized on a symmetric CuS_3 core (Cu-S ≈ 2.26 Å), which interact with three nearby copper atoms (Cu---Cu ≈ 2.7 Å). These structural data confirm the formation of the Cu clusters characterized by PGSE-NMR spectroscopy: Cu_6S_9 for the cysteine derivatives and Cu_4S_6 for the D-Penicillamine compounds.

The bio-inspired Cu(I) chelators were demonstrated to perfectly reproduce the coordination sphere of Cu(I) found in the high affinity metal-sequestering metallothioneins, used by cells for the detoxification of excess Cu(I). This spectroscopic analysis thus provides useful guidelines for the design of efficient intracellular Cu(I) chelators.

Authors and principal publications:

Jullien A.-S.[1], Gateau C.[1], Lebrun C.[1], Kieffer I.[2,3], Testemale D.[2,4], Delangle P.[1], X-Ray Absorption Spectroscopy Proves the Trigonal Planar Sulfur-Only Coordination of Cu(I) with High Affinity Tripodal Pseudopeptides, *Inorganic Chemistry* **52** (2013) 9954-9961

Jullien A.-S.[1], Gateau C.[1], Kieffer I.[2], Testemale D.[3], Delangle P.[1], D-Penicillamine Tripodal Derivatives as Efficient Copper(I) Chelators, *Inorganic Chemistry* **53** (2014) 5229-5239

[1] INAC, Service de Chimie Inorganique et Biologique, CEA, Grenoble / [2] BM30B/FAME beamline, ESRF, Grenoble, France / [3] OSUG, UMS 832 CNRS, Grenoble, France / [4] Institut Néel, UPR CNRS, Grenoble, France

Uranium ecotoxicity and fate in environmental organisms

Weathering of uranium-containing natural minerals, industrial activities and the extensive use of phosphate fertilizers has resulted in a widespread uranium (U) contamination of the environment. Measurements showed that seepage waters, mine waters and tailing water contained up to 25 µM of U in some of these regions. Intense research is focused on the decontamination of such areas, particularly by using bacteria or plants, i.e. bio- or phyto-remediation, respectively. Depending on its chemical speciation, U can either be mobilized by these organisms, then bioaccumulated, or inversely it can be fixed on soil particles and minerals.

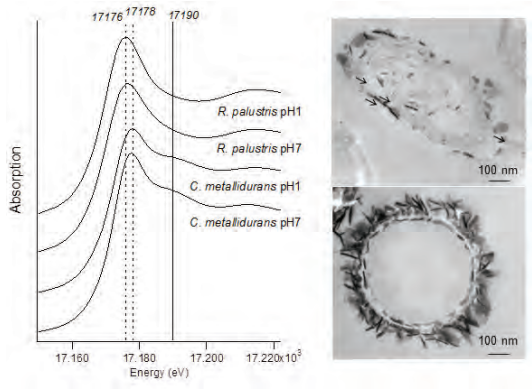

Figure 27. U L_{III}-edge XANES and TEM observations of bacteria exposed to U. *Cupriavidus metallidurans* CH34 is highly resistance to a variety of metals. *Rhodopseudomonas palustris,* can grow in aromatic compounds-polluted environments.

In an *in vitro* approach, we have investigated the bio- and phyto-remediation potential of several bacteria and plant species. Since most of the U-contaminated areas are co-contaminated with other metals, radionuclides or pollutants, only multi-resistant species can be used in a perspective of remediation. Our work thus focused on *Cupriavidus metallidurans* CH34 and *Rhodopseudomonas palustris*. Thanks to U L_{III}-edge XANES and TEM observation of U cellular distribution (Figure 27), coupled to ICP-MS measurement of U accumulation, we showed that both species can withstand high concentrations of U and immobilize it either through biosorption of U(VI)-phosphate or U(VI)-carboxylate on their outer membrane or through reduction of U(VI) to non-uraninite U(IV)-phosphate or U(IV)-carboxylate compounds.

In two traditional field crop higher plants species, sunflower (*Helianthus annuus*) and oilseed rape (*Brassica napus*), U complexation with endogenous phosphate residues leads to its precipitation as U(VI)-phosphate and fixation in plant roots, avoiding translocation to leaves (Figure 28). Conversely complexation in exposure solution with a strong ligand such as citrate circumvents this precipitation, and enhances root-to-shoot translocation, in a U(VI)-carboxylate complex form.

These results highlight correlations between U speciation in the environment and its mobility pattern in plants, which would help for phytoremediation purposes.

Main publications

I. Llorens, G. Untereiner, D. Jaillard, B. Gouget, V. Chapon, M. Carrière. Uranium interaction with three multi-resistant environmental bacteria: Cupriavidus metallidurans CH34, Deinococcus radiodurans R1 and Rhodopseudomonas palustris. *PLoS One* **7** (2012) e51783 / **Article 2012-17**

A. Khemiri, M. Carrière, N. Bremond, M.A. Ben Mlouka, L. Coquet, I. Llorens, V. Chapon, P. Cosette, C. Berthomieu. Escherichia coli response to uranyl exposure at low pH and associated protein regulations. *Plos One* **9** (2014) e89863 / **Article 2014-11**

J. Laurette, C. Larue, I. Llorens, D. Jaillard, PH. Jouneau, J. Bourguignon and M. Carrière. Speciation of uranium in plants upon root accumulation and root-to-shoot translocation: a XAS and TEM study. *Environmental and experimental botany* **77** (2012) 87-95 / **Article 2012-14**

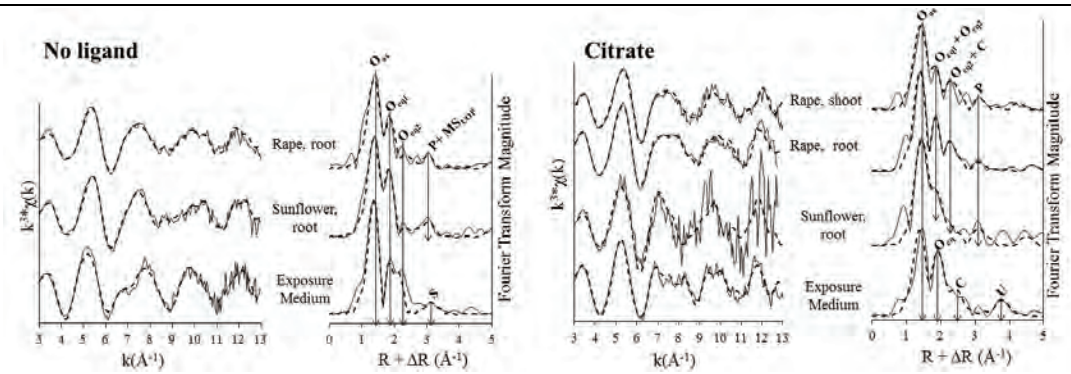

Figure 28. XAS signals of exposure medium and plant samples. EXAFS oscillations (left) and their corresponding FT (right) recorded on basic medium (left) and basic medium + citrate (right) @ pH4. Solid lines: experimental data; dashed lines: fits.

An original Cu(I)-coordination shell in a small bacterial metalloprotein identified by XAS and NMR spectroscopy

The combined use of X-ray Absorption Spectroscopy (XAS) and Nuclear Magnetic Resonance (NMR) spectroscopy enabled characterization of the three-dimensional structure and the metal-binding site of a small Cu(I)/Cu(II)-binding protein involved in bacterial heavy-metal resistance (Figure 29). This protein features a binding cooperativity with enhanced affinity for Cu(II) once Cu(I) is bound. NMR-derived data were used for the determination of the atomic coordinates of the protein moiety in solution while XAS yielded geometric information on the Cu(I) site which is coordinated by four sulphur atoms. This study represents the first example of a XAS characterization of a tetrathioether Cu(I) site in a protein in which copper is not part of a cluster. Knowledge of this new structure permits the understanding of the previously observed Cu(I) / Cu(II) binding cooperativity from a structural point of view.[56]

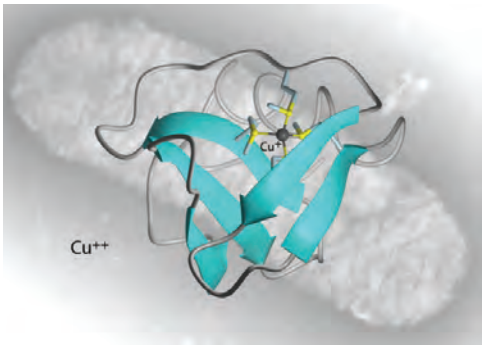

Figure 29. XAS and NMR studies of the CopK protein involved in bacterial copper resistance reveal a tetrathioether Cu(I)-site.

Living organisms are continuously exposed to environmental stress originating from sources such as toxic compounds, radiation and high temperature. During evolution, they have adapted to the specific environment in which they live and have developed resistance mechanisms to protect themselves against stress events. One well-known class of toxic products is formed by heavy metals that naturally occur in the environment but are also released in huge quantities through anthropogenic processes, especially since the beginning of industrialization. *Cupriavidus metallidurans* CH34 is a bacterium that was isolated from a Zn decantation tank in Belgium. It can resist high concentrations of many heavy metals. This strain became a model for studying metal resistance mechanisms in microorganisms. In our study we were interested in the molecular and metal binding properties of proteins involved in heavy metal resistance in this bacterium.

Many vital processes require copper as a redox-active cofactor but excess copper damages cells by catalyzing the production of free radicals. Therefore, several mechanisms have evolved which maintain a suitable level of intracellular copper and control its oxidation state. Copper resistance of *C. metallidurans* CH34 involves more than 19 proteins that are produced in response to excess copper.

[56] L.X. Chong, M. Ash, M.J. Maher, M.G. Hinds, Z. Xiao *et al.*, *J. Am. Chem. Soc.* **131**, 3549-3564 (2009)

One of these is CopK, a small periplasmic protein that is produced in abundance under copper stress. As a small metal binding protein probably involved in metal trafficking, it is called a metallochaperone. We have previously determined the solution structure of apo-CopK[57] and it has also been shown that CopK binds Cu(I) and Cu(II) in a cooperative way.[56]

We determine the solution structure of the Cu(I)-bound CopK protein and the characterization of its Cu(I)-site. A so far unique Cu(I) ligand sphere was discovered that is formed by 4 thioether groups belonging to four methionines from the same protein chain. Spectroscopic data obtained by NMR and XAS were combined for the detailed characterization of Cu(I)-CopK and its metal site (Figure 30). NMR provides information on intramolecular proton-proton distances that yield the atomic coordinates of the protein chain, the three-dimensional protein structure. However, the Cu(I) ion is NMR-silent and no geometric information on the metal site can be obtained. A cryo-cooled protein solution containing Cu(I)-CopK was therefore studied by XAS at Cu K-edge. The resulting spectra were in accordance with a ligand sphere formed by S atoms and the EXAFS fit suggested the presence of 4 S atoms in the Cu(I) site. This result was surprising as most small periplasmic bacterial Cu(I)-binding metallochaperones contain Cu(I) bound by S and N ligands. In addition, a tetrathioether Cu(I) site has so far only been observed in a single protein in which the Cu(I) ion belongs to a copper-molybdenum (MoS_2CuS_2Mo) cluster. However, a tetrathioether Cu(I) site was also in accordance with a Cu(I)-S distance of 2.31Å as determined by EXAFS. This distance is very untypical for a trigonal Cu(I) site. These findings were further corroborated by the observation of chemical shift differences in 1H-13C correlation NMR spectra occurring upon Cu(I)-binding. Four peaks, corresponding to methionine methyl groups were significantly affected by the addition of Cu(I) to the protein. This observation leads to the suggestion that the chemical shift of these carbon atoms is a new and interesting probe for the detection of methionine-bound Cu(I) and, most importantly, allows the sequence-specific identification of the Cu(I) ligands.

The structure of Cu(I)-CopK bridges the gap between what was previously known on the Cu(I) / Cu(II) binding cooperativity and the structures published beforehand. Knowledge of this new structure is the basis for the understanding of the observed Cu(I)/Cu(II) binding cooperativity from a structural point of view. We have demonstrated that the accommodation of Cu(I) in the tetrathioether site is associated with an important structural modification of the C-terminal part of the protein and propose that this reorientation is required for the formation of the Cu(II) specific site. This explains the much higher Cu(II) affinity of Cu(I)-CopK compared to apo-CopK.

Figure 30. Solution structure of Cu(I)-CopK. **Centre**: sidechains of the 4 methionines forming the Cu(I)-site are shown in detail (S atoms of the tetrathioether site in yellow, Cu(I) ion in green). The structure of apo-CopK is shown in light grey for comparison. **Left**: EXAFS FT data. Experimental data in black, simulations in magenta (modulus) and cyan (imaginary part). **Right**: NMR data - Comparison of the methionine-CH3 region of 1H,13C-HSQC spectra acquired on the apo protein (black) and Cu(I)-CopK (red). Peaks are annotated with the residue numbers. M28, M38, M44 and M54 form the Cu(I)-site.

Authors and principal publication:

G. Sarret[1], A. Favier[2], J. Covès[2], J.-L. Hazemann[3], M. Mergeay[4], B. Bersch[2], CopK from Cupriavidus metallidurans CH34 binds Cu(I) in a tetrathioether site: characterization by X-ray absorption and NMR spectroscopy, *J. Am. Chem. Soc.* **132**, 3770-3777 (2010) / **Article 2010-27**

1 LGIT, Grenoble / 2 IBS, Grenoble / 3 Inst. Néel, Grenoble / 4 SCK-CEN, Mol (Belgium)

[57] Bersch *et al.*, *J. Mol. Biol.* **380** (2008) 386-403

Catalysis & material energy

Collaboration between FAME, IRCELyon and IFPEn in heterogeneous catalysis

In the field of SR and more especially XAS, heterogeneous catalysis is a highly demanding domain. Considering the unique ranges of temperatures, pressures, concentrations as well as time resolutions that SR beamlines can provide and the deep need of understanding the behavior of nanoparticles under *in situ* or *operando* conditions, XAS becomes a unique technique for studying working catalysts. Synchrotron catalysis consortiums or sometimes beamlines owned or strongly supported by industrial actors demonstrate the importance of SR techniques for heterogeneous catalysis. IRCELyon has contributed to the early developments of this beamline and is still an active user. Similarly, IFPEn has always been a contributor to this field of research and had established many connections with XAS beamlines on several synchrotron sources.
The research topics related to XAS on BM30B during the period of 2009-2014 concerned mainly catalysis for hydrotreatments/ hydroconversion, photocatalysis and the reactivity of supported nanoclusters with H_2. (IFPEn). Most of the results presented in this report required either *in situ* context or characterization of low loading samples. Together with FAME team, we would like to thank Yves Joly (Institut Néel) for fruitful discussions related to XANES and his assistance with using the FDMNES code in several projects.

P. Afanasiev[1], J. Couble[1,] C. Geantet[1], A. Gorczyca[2,3], C. Legens[2], I. LLorens[1,4], V. Moizan-Basle[2], E. Puzenat[1]

[1] Institut de Recherches sur la Catalyse et l'Environnement, Villeurbanne France / [2] Institut Français du Pétrole Énergies Nouvelles, Solaize, France / [3] Institut Néel, Grenoble, France / [4] BM30B CRG-FAME, France

Catalysis for hydrotreatments and hydroconversion.

Hydrotreatments are major processes of refining industry. Sequential improvements in the activity of hydrotreating catalysts bring more efficient systems. Thus, specific preparation methods involving organic compounds constitute the last generation of catalysts. The understanding of the role of these additive on the activation (transformation of oxide state into active sulfide one) is a challenging task which deserves the use of XAS. QXAS demonstrates, as illustrated by Figure 31 and Figure 32, that the kinetic of sulfidation of a CoMo on alumina catalysts is drastically modified by the presence of an organic compound (TEG, triethylene glycol).

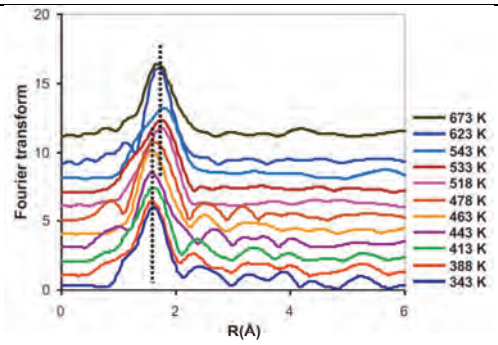

Figure 31. QEXAFS at Co K-edge during the sulfidation of CoMo on alumina catalyst doped with TEG.

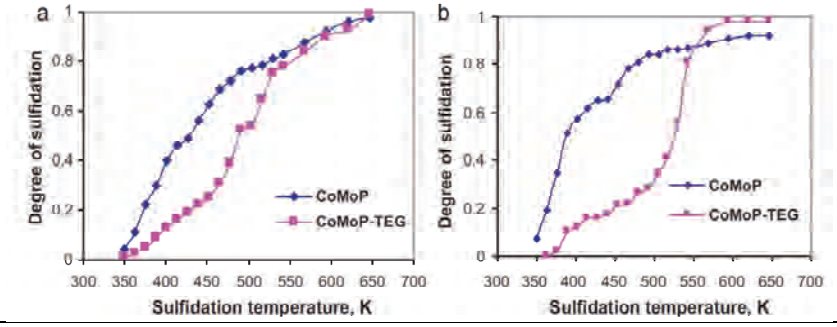

Figure 32. Evolution of the extent of sulfidation of Mo (**a**) and Co (**b**) during activation of a TEG promoted and non promoted HDT catalyst.

The presence of the organic compounds delays the sulfidation of both metals and finally brings more so called "CoMoS" active phase on the catalysts.

An alternative to supported catalysts is the use of highly dispersed unsupported active phases. Thus, a biogenic route has been developed to prepare highly divided MoS_2 with an interwoven tubular morphology. Cellulose fibers can be topotactically transformed to highly divided molybdenum sulfide by means of reflux in ethylene glycol in the presence of ammonium heptamolybdate and elemental sulfur. The product partially replicates the morphology features of the initial organic fibers (as illustrated by Figure 33) and possesses high specific surface area and developed mesoporosity.

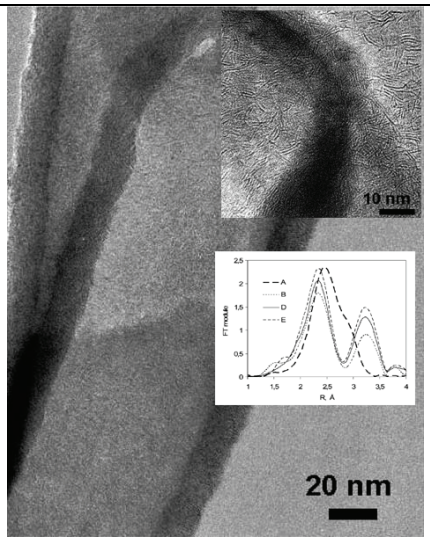

Figure 33. HRTEM image MoS_2 obtained from abiogenic route and FT of different stages of the synthesis.

Figure 34. Fourier transform Mo K- edge EXAFS spectra for the MoS_2 in the liquid and in the residual solid after AR hydroconversion at 450°C.

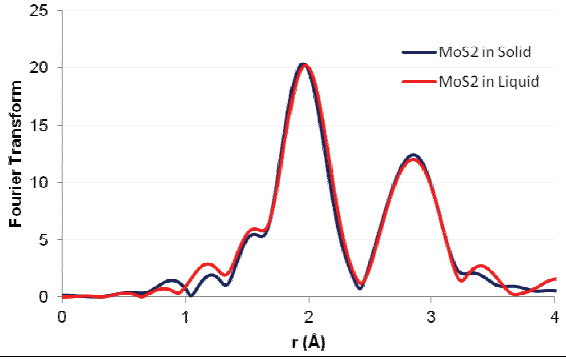

XAS was performed in order to describe the intermediate amorphous compounds obtained during the soft route synthesis (Figure 34).

Unsupported catalysts can also be generated in situ in for the conversion of heavy oils. Thus, 600 ppm of Mo introduced in a oil residue are sulfided under reaction conditions (430°C, 16 MPa H_2) into an active sulfide which allows to convert the heavy oil into valuable products. XAS has been used to characterize the activation of this element in the residue and demonstrate the similarity of the MoS_2 particles in the oil residuae and those recovered with traces of coke deposit.[58]

Principal publications:

Nguyen T.S., Loridant S., Lorentz C., Cholley T., Geantet C., "Effect of glycol on the formation of active species and sulfidation mechanism of CoMoP/Al_2O_3 hydrotreating catalysts", *Appl. Catal. B - Environ.* **107** (2011) 59-67 / **Article 2011-12**

Afanasiev P., Geantet C., Llorens I., Proux O., "Biotemplated synthesis of highly divided MoS_2 catalysts", *J. Mater. Chem.* **22** (2012) 9731-9737 / **Article 2012-1**

Photocatalysis

This project is a collaboration between the King Abdullah University of Science and Technology and IRCELYON (CADENCED project) which granted the post doc position of Isabelle Llorens.

1) Enhanced absortion with doped titania

TiO_2 photocatalysts have attracted extensive interest owing to their great advantages in the complete mineralization of organic pollutants in wastewater and contaminated air. One of the greatest challenges for TiO_2-based photocatalysis is extension of the photoresponse to the visible range with a high quantum yield over the whole light absorption range. It is generally considered that doping with transition metals brings recombination centers and is unfavorable for photocatalysis. However, a

[58] Nguyen T.S., Tayakout-Fayolle M., Lacroix M., Gotteland D., Aouine M., Bacaud R., Afanasiev P., Geantet C., **s**ubmitted to *Energy and fuels*

specific preparation method has been developed to promote visible light adsorption as illustrated by Figure 35 and XAS was used to characterize the state of low loading Cr dopant.

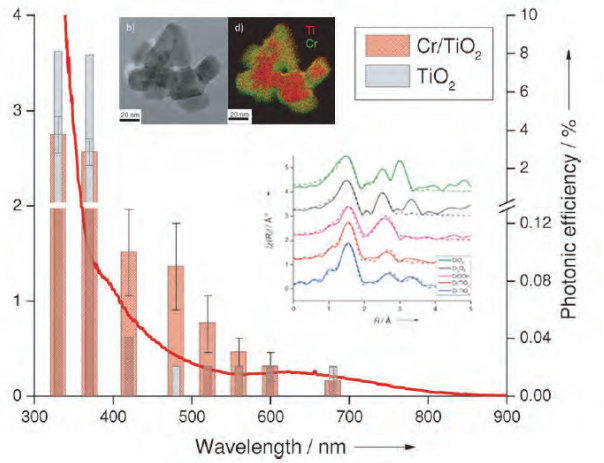

Figure 35. Action spectra with UV/vis of Cr/TiO_2 with 0.2 wt% Cr and FT of reference and Cr doped titania samples.

Principal publication:
Ould-Chikh S., Proux O., Afanasiev P., Khrouz L., Hedhili M., Anjum D., Harb M., Geantet C., Basset J.-M., Puzenat E., "Photocatalysis with Chromium-Doped TiO_2: Bulk and Surface Doping", *ChemSuschem* **7** (2014) 1361–1371 / **Article 2014-18**

2) Water splitting with bifunctional photcatalysts.

Researchers worldwide are struggling to find a simple affordable concept and technologies for H_2 production by solar water splitting. Among these concepts, photocatalysis is one of the most attractive since the reaction is performed at room temperature under soft conditions. We have developed *in situ* cells in order to study gas phase production of hydrogen from methanol or water (HER reaction, Figure 36). Pt L_{III} edge of low loading Pt/TiO_2 or Pt/C_3N_4 photocatalysts (from 0.3 to 1 wt %) were recording under illumination (or darkness). Effects of power intensity and wavelength of light were used in order to investigate the electron transfer induced from illuminated TiO_2 to Pt nanoparticles.

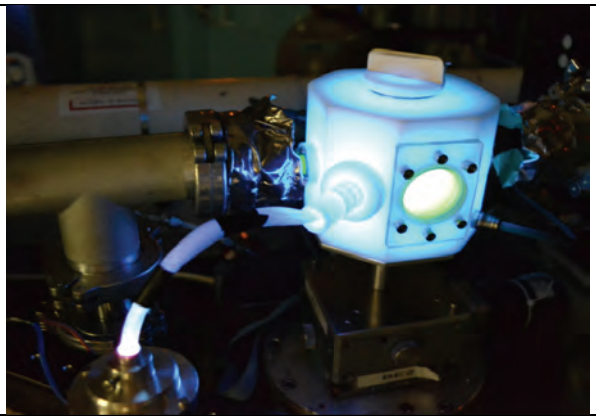

Figure 36. *in situ* photocatalytic cell for studying hydrogen evolution reaction from methanol or water reduction.

The sensitivity of Pt L_{III} XANES is illustrated on Figure 37 on reference compounds and photocatalytically reduced Pt/TiO_2 during oxidation/reduction cycles. XANES is a unique technique for probing the photoinduced effect on the Pt nanoparticles where two H atoms recombine. It gives a new insight on the mechanism of HER

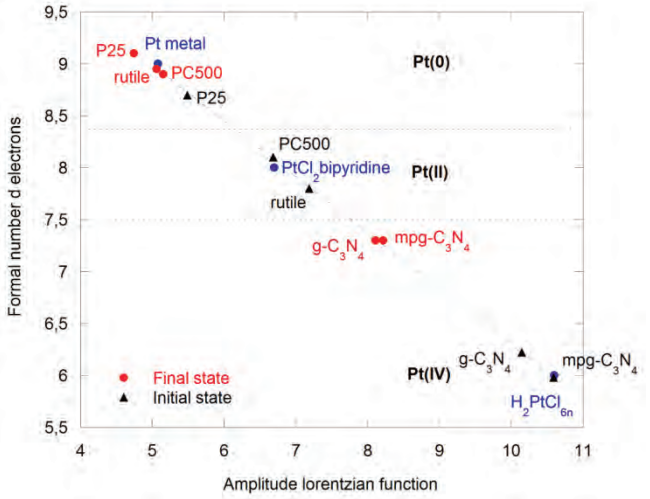

Figure 37. Relationship between WLA and formal d electron numbers for reference sample and initial and final Pt/TiO2 samples.

Monitoring morphology and hydrogen coverage of nanometric Pt/γ-Al_2O_3 particles by in situ HERFD-XANES and quantum simulations

Better knowledge of oxide supported metal nanoclusters is of paramount fundamental and technological importance especially in the field of energy. In particular, highly dispersed platinum nanoparticles supported on γ-alumina are widely used as heterogeneous catalysts.[59] Their reactivity and selectivity are intimately related to the local geometry and the electronic density of the active sites. As hydrogen is often present in the reactive medium, the metallic nanoparticles are in interaction with both the γ-alumina support and the reductive environment. On such catalysts, the sub-nanometric particles,[60] 13 atoms being a relevant model,[61] are highly dispersed, and the metal sites are even more sensitive to the chemical environment. Recent DFT studies suggest that Pt_{13} clusters are almost as stable on both main (100) and (110) γ-Al_2O_3 platelets faces in the absence of H_2.[62] A biplanar structure is preferred on the dehydrated (100) face, whereas a 3D cluster is favourable on the hydrated (110) face. For hydrogen contents higher than 20 hydrogen atoms per cluster, the morphology shifts from a biplanar one to a cuboctahedron.

We use X-Ray Absorption Near Edge Structure (XANES) experiments recorded in High Energy Resolution Fluorescence Detection (HERFD) mode to *in situ* characterize such systems at the atomic level. Models are provided by Density Functional Theory (DFT) Molecular Dynamics (MD) approach using the VASP package on both faces and for all possible hydrogen coverage. Obtained models were taken as input for the simulation of the XANES spectra and compared to the experiments performed at four operating conditions in terms of temperatures, T, and Hydrogen pressures, P (T = 25°C and 500°C and P = 0 and 1 bar).

XAS experiments were performed using a static quartz capillary *in situ* cell. The catalyst was transferred into the cell under inert atmosphere and a reduction treatment was done prior to other experiments. The crystal analyzer, set up with one spherically bent Ge (660) crystal (R=1000mm), was tuned to the $L\alpha_1$ (L_3-M_5) fluorescence line at 9442 eV (ΔE_{CAS} = 1.1 eV). XANES calculations were performed using the FDMNES code.[63]

In situ HERFD-XANES analysis coupled to DFT calculations allows then to discriminate different morphologies of nanoparticles and to quantify hydrogen coverage, as function of the temperature and hydrogen pressure, taking into account nanometric platinum clusters supported on the two main surfaces of γ-alumina (Figure 38).

[59] *a*) J. H. Sinfelt, in *Handbook of Heterogeneous Catalysis* (Eds.: G. Ertl, E. Knözinger, J. Weitkamp), Wiley, Weinheim, 1997, 1939-1955; *b*) G. A. Somorjai, H. Frei, J. Y. Park, *J. Am. Chem. Soc.* **131** (2009) 16589-16605.
[60] *a*) Cuenya *et al.*, *J. Am. Chem. Soc.* **132** (2010) 8747-8756; *b*) de Graaf *et al.*, *J. Catal.* **203** (2001) 307-321; *c*) Sanchez *et al.*, *J. Am. Chem. Soc.* **131** (2009) 7040-7054; *d*) Vaarkamp *et al.*, *J. Catal.* **163** (1996) 294-305.
[61] *a*) C. Mager-Maury, G. Bonnard, C. Chizallet, P. Sautet, P. Raybaud, *ChemCatChem* **3** (2011) 200-207; *b*) C. H. Hu, C. Chizallet, C. Mager-Maury, M. Corral-Valero, P. Sautet, H. Toulhoat, P. Raybaud, *J. Catal.* **274**, (2010) 99-110.
[62] C. Mager-Maury *et al.*, C. Chizallet, P. Sautet, P. Raybaud, *ACS Catal.* **2** (2012) 1346-1357.
[63] O. Bunău, Y. Joly, *J. Phys.: Condens. Matter* **21** (2009) 345501

This work gives unrivalled insights into the influence of hydrogen on morphology, surface structure and electronic properties of supported metallic nanoclusters, and also brings new methodologies to interpret XANES analysis, used in the characterization of many systems. It is difficult to have precise information about hydrogen coverage in given conditions by using DFT calculations alone, while it is even more difficult by using XAS experiments alone. Combining DFT-MD, HERFD-XANES simulations and dedicated experiments, more accurate insights are obtained on the morphologies and the mean hydrogen coverage of the catalyst. Hopefully this fine understanding of highly dispersed platinum particles will help for the better control of catalysts under reductive environment.

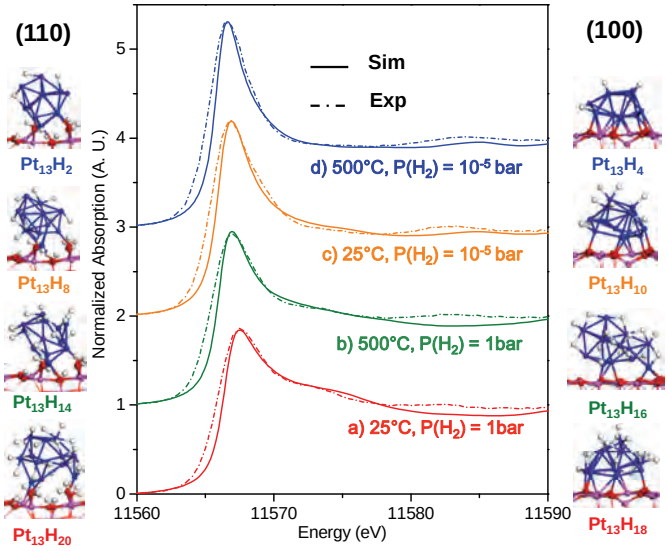

Figure 38. Pt-L_3 edge HERFD XANES spectra of Pt/Al_2O_3 catalysts recorded in different operating conditions reported on the figure (dashed line) and best simulated XANES spectra combining models on the (100) face (represented on right) and on the (110) face (represented on left) using the ratio (110)/(100) = 7/2.
γ-Al_2O_3 platelets exhibits two main faces: (100) (~20% of exposed surface) and (110) (~70%). The (111) surface (~10%) is neglected.

Authors and principal publication:
Gorczyca A.[1,2], Moizan V.[1], Chizallet C.[1], Proux O.[3], Delnet W.[3], Lahera E.[3], Hazemann J.-L.[2], Raybaud P.[1], Joly Y.[2], "Monitoring morphology and hydrogen coverage of subnanometric Pt/γ-Al_2O_3 particles by in situ HERFD-XANES and quantum simulations", *Angewandte Chemie International Edition* (2014), DOI: 10.1002/anie.201403585 / **Article 2014-9**
[1] IFP Energies nouvelles, 69360 Solaize, France/ [2] Institut Néel, UPR CNRS, Grenoble, France / [3] OSUG, UMS 832 CNRS, Grenoble, France

A surface science approach in aqueous phase used to rationalize the preparation of heterogeneous catalysts

The rational design of heterogeneous catalysts involves the implementation of model approaches, "surface science" being the best known. This approach aims to model a complex industrial catalyst using simple chemical systems most often presented in the form of plane monocrystalline supports capable of reproducing, at least in part, the physicochemical behavior of a metal particle or a pulverulent metal oxide with a large specific surface area.
This study focused on the study of catalysts using Ni on alumina (Ni/Al_2O_3), which can be found in many applications such as steam reforming (hydrogen production from hydrocarbons), hydrogenation and hydrotreating (removal of S, N, O and metals from petroleum fractions). To model the industrial γ-alumina oxide support (poorly crystalline and exhibiting many different crystallographic faces) we decided to use monocrystalline wafers of α-alumina in different crystallographic orientations in order to model the different surface groups (hydroxyl) of the industrial support.

The originality of this study lays in how the catalyst was synthesized. This was done in the aqueous phase (as done industrially) and the characterization was carried out under ambient conditions in contrast to more traditional surface science approaches, where the model catalyst is synthesized under ultra-high vacuum, industrially far less realistic.

The use of oriented monocrystals required the use of a characterization technique capable of providing molecular information for very low concentrations of active phase (Ni^{II} in this case)

deposited on the oxide surface. Grazing incidence EXAFS spectroscopy (Grazing-incidence XAS or GI-XAS) turned out to be a technique of choice in this regard. This technique has been implemented on several complementary beamlines during this study: FAME and GILDA at ESRF and DIFFABS and SAMBA at SOLEIL.

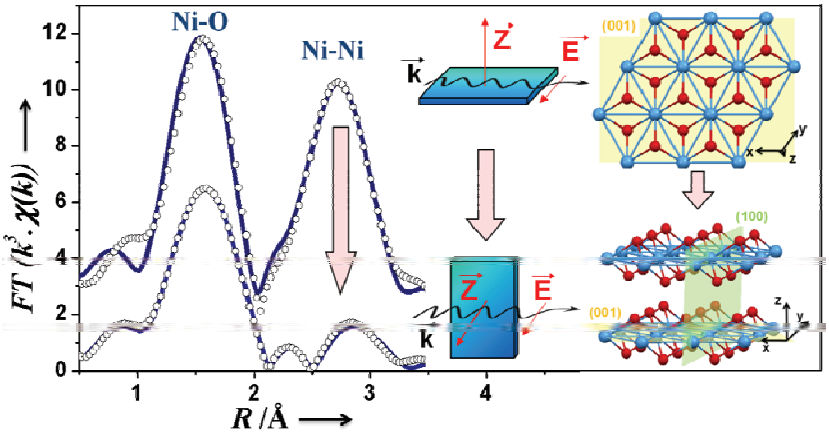

Figure 39 Fourier transforms of the Ni K -edge $k^3.\chi(k)$ EXAFS signal for parallel and perpendicular polarizations of the sample obtained by depositing Ni^{II} on the $(1\bar{1}02)$ surface of α-alumina. The solid blue line shows the experimental spectrum and the circle, refinement of the signal. The structure of the nickel hydroxide ($Ni(OH)_2$) is shown on the right as seen from the top or on the side with respect to the (001) basal plane.

The use of oriented monocrystals coupled with the polarization of the synchrotron beam yielded new information on the orientation of the supported active phase and showed that the crystalline orientation of the oxide support strongly governed speciation (chemical distribution) of the active phase. When Ni^{II} was adsorbed in the aqueous phase, Ni K-edge EXAFS revealed an oriented precipitation of nickel hydroxide ($Ni(OH)_2$) on the $(1\bar{1}02)$ surface of α-alumina. For example, Figure 39 shows the effect of polarization on the second peak in the Fourier transform of the EXAFS signal (Ni-Ni distances): this peak is very pronounced for a monocrystal orientation parallel to the electric field vector, $\vec{E}$, whereas the intensity of the same Ni-Ni peak decreases sharply when the sample is oriented perpendicular to the electric field vector $\vec{E}$. In contrast, for the (0001) surface of α-alumina, no Ni deposit was observed, which shows the importance of the type of surface group exposed by the oxide for controlling the adsorption of the active phase.

These results demonstrate at the molecular level that the oxide support does not merely act as a physical container of the active phase and that the nature of specific surface sites plays a key role in the formation and orientation of the nickel hydroxide precipitate. The fact that $Ni(OH)_2$ precipitated only on the $(1\bar{1}02)$ face can be explained by the minimization of surface energy between the alumina and the nickel hydroxide.

The use of a model system shows that the Ni dispersion on individual oxide particles is highly heterogeneous for an industrial catalyst as it will depend on the type of face exposed and therefore on the morphology of the oxide support. These findings also highlight the fact that each face of the alumina has a specific reactivity depending on which OH groups are exposed. Controlling the morphology of γ-alumina is therefore a key factor at the industrial scale in order to be able to control the deposition and dispersion of the active phase.

Authors and principal publication:

Tougerti A.[1], Llorens I.[2,3], D'Acapito F.[4], Fonda E.[4], Hazemann J. L.[2,6], Joly Y.[6], Thiaudiere D.[5], Che M.[1], & Carrier X.[1] (2012) "Surface Science Approach to the Solid–Liquid Interface: Surface-Dependent Precipitation of $Ni(OH)_2$ on γ-Al_2O_3 Surfaces" *Angewandte Chemie* **124** (2012) 7817–7821 / **Article 2012-28**

[1] UPMC, Laboratoire de Réactivité de Surface / [2] FAME Beamline, Grenoble / [3] CEA-INAC, Grenoble / [4] GILDA, ESRF, Grenoble / [5] Synchrotron Soleil, Gif-sur-Yvette / [6] Institut Néel, Grenoble, France

In-situ XRD and EXAFS investigation on layered Ni/Mn oxides in Lithium Ion Batteries

Li rich layered Ni/Mn oxides have a high capacity and were attractive candidates for Lithium Ion batteries,[64] whereby the processes of the first charge cycle are unclear and of certain interest for battery conditioning.[65] We synthesised $Li[Li_{0.2}Mn_{0.61}Ni_{0.18}Mg_{0.01}]O_2$ by solid state reaction of the corresponding carbonates. *In-situ* XRD and EXAFS experiments were performed on BM20-MRH and BM30b respectively.

On the first charge from $0.9<x<1.2$ a lattice shift in *a* and irreversible in *c* is observed (Figure 40, left). This parameter and the potential V remain constant until $x<0.2$, which is typical for a two phase process in such materials. Increased FWHM of reflection (0012) give hint to the existence of a second structural very similar crystal phase. EXAFS data reveal in the pristine material Ni to be very close to NiO and almost constant up to $x<0.9$ while Mn is oxidized to nominal +4 up to 4.4V (Figure 40, right). The subsequent discharge-charge plot shows the typical crystal lattice variation and oxidation state changes due to the charge state of the battery.

These experiments prove that the actual cathode material for the subsequent charge-discharge cycles is formed during the first charge in between $0.9<x<1.2$ by an irreversible phase transformation and corresponding oxidation of first Mn^{3+} and later Ni^{2+}.

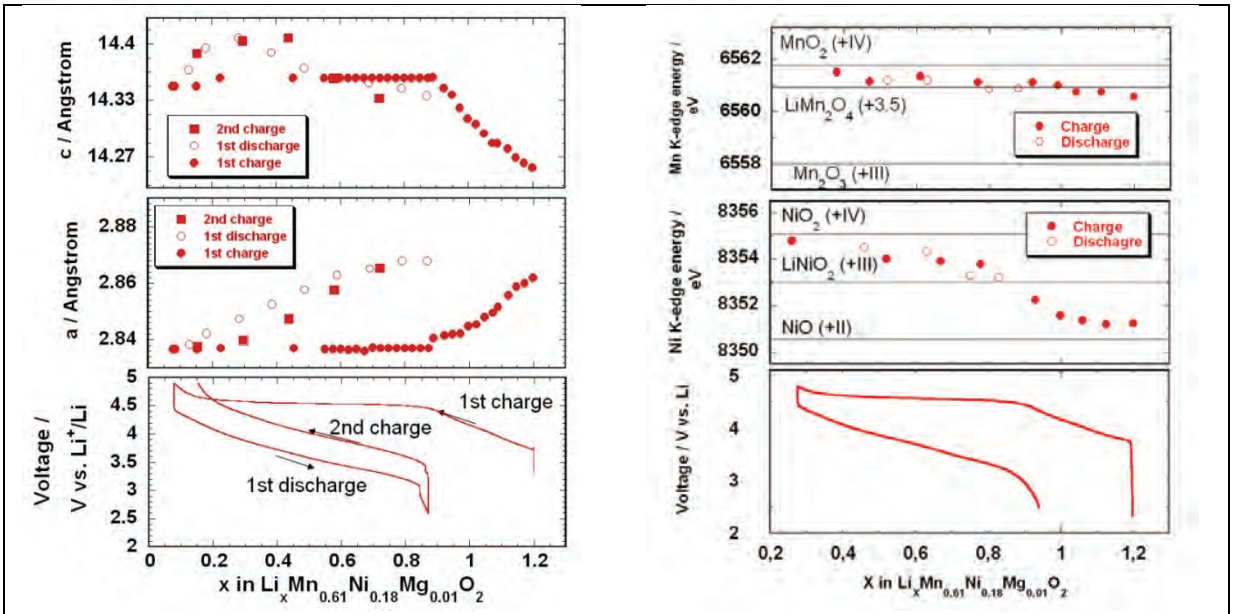

Figure 40. Evolution of the lattice parameter a and c during the first charge-discharge cycle (left), extracted by profile matching from diffraction data at 25 keV. Corresponding changes in the EXAFS data at the Mn and Ni-edge are displayed on the right.

Authors and principal publication:

Simonin L.[1], Colin J.-F.[1], Ranieri V.[2], Canévet E.[1], Martin J.-F.[1], Bourbon C.[1], Baehtz C.[3], Strobel P.[4], Daniel L.[1], Patoux S.[1], In situ investigations on a Li-rich Mn-Ni layered oxide for Li-ion battery, *Journal of Materials Chemistry* **22** (2012) 11316-11322 / **Article 2012-25**

[1] CEA-LITEN, Grenoble / [2] CEA-INAC, Grenoble & FAME Beamline, Grenoble, France / [3] ROBL beamline & Institute of Ion Beam Physics and Materials Research, Dresden / [4] Institut Néel, Grenoble, France

[64] M. M. Thackeray et al, *J. Mater. Chem.* **15** (2005) 2257
[65] F. La Mantia et al, *J. Electrochem. Soc.* **156** (2009) A823

List of selected experimental reports

Geochemistry and Environmental Sciences

Environment & biology

Proposal 30.02.1012 - Sarret G., Fate of Zn and Cd in dredged sediment deposits: Early stages and long term
Proposal 30.02.1049 - Isaure M.-P., Cd speciation in the symbiotic association *Anthyllis vulneraria* / *Mesorhizobium metallidurans* candidate for the phytostabilization of mine tailings

Environment & soils

Proposal 30.02.1008 - Schlegel M., Probing the molecular mechanim of Eu^{III} sorption on Fe-containing clay minerals by P-EXAFS spectroscopy
Proposal 30.02.1021 - Morin G., Arsenic speciation in flooded soils heavily impacted by Acid Mine Drainage
Proposal 30.02.1042 - Dublet G., Mechanisms of long term Co trapping in deeply weathered ultramafic rocks from New-Caledonia

Nano-ecotoxicology

Proposal 30.02.1052 - Tella M., Speciation of CeO_2-based nanocomposite within aquatic mesocosms
Proposal 30.02.1061 - Rose J., Cerium speciation in aquatic mesocosms using High Energy Resolution Fluorescence Detected X-ray Absorption Spectroscopy

Hydrothermal Fluids

Proposal EC-747 - Brugger J., XAS study of Mn^{II}-chlorocomplexing under hydrothermal conditions: octahedral to tetrahedral transitions as a driver for metal fractionation in hydrothermal systems
Proposal EC-755 - Pokrovski G., *In situ* XAS study of arsenic behavior in a fluid-mantle rock system: applications for the development of new geochemical traces of subduction-zone dynamics
Proposal 30.02.1004 - Cambon O., XAS *in-situ* studies on hydrothermal growth of FeO_4-based crytals
Proposal 30.02.1010 - Bazarkina E., Hydrothermal transport of palladium in near-and supercritical fluids
Proposal 30.02.1064 - Louvel M., Solubility and speciation of As, Cu and Fe in high temperature gas mixture: Implications for transport and deposition of metals and metalloids in magmatic-hydrothermal systems

Biochemistry

Proposal EC-748 - Carrière M., Interaction between bacteria and uranium in natural soils: population diversity and biotransformation mechanisms
Proposal SC-3455 - D'Angelo P., Structural investigation of the Cu^{II} and Cu^{I}-prion complex in human prion protein.
Proposal LS-2331 - Delangle P., Interaction of biological sulphur ligands with silver nanoparticles and relation with their toxicity

Catalysis & material energy

Proposal 30.02.1025 - Maillard F., Surface reactivity and durability of Pt_3Co/C nanoparticles in proton-exchange membrane fuel cells
Proposal CH-3815 - Gorczyca A., Characterisation of supported metal catalysts by XANES spectroscopy : high-resolution experiments supported by *ab initio* calculations
Proposal 30.02.1045 - Afanasiev P., *In-operando* XAS study of photocatalytic water splitting : state of catalytic sites as a function of irradiation and applied potential

Materials science

Proposal 30.02.1059 - Dupuis V., Anomalous structural distortion in mass-selected FeCo nanoalloys from X-ray chemical local probe
Proposal 30.02.1065 - Bordage A., *In situ* site-selective EXAFS investigation of the transformation of nanoconfined $Co^{II}Co^{III}$ Prussian Blue Analog into oxide

List of selected publications

Geochemistry and Environmental Sciences
Auffan M., Matson C. W., Rose J., Arnold M., Proux O., Fayard B., Liu W., Chaurand P., Wiesner M. R., Bottero J.-Y., Di Giulio R. T., "Salinity-dependent silver nanoparticle uptake and biotransformation in Atlantic killifish (*Fundulus heteroclitus*) embryos", *Nanotoxicology* **8** (2014) 167-176

Hydrothermal Fluids
Louvel M., Sanchez-Valle C., Malfait W. J., Testemale D., Hazemann J.-L., "Zr complexation in high pressure fluids and silicate melts and implications for the mobilization of HFSE in subduction zones", *Geochimica Cosmochimica Acta* **104** (2013) 281-299

Biochemistry
Sarret G., Favier A., Covès J., Hazemann J.-L., Mergeay M., Bersch B. "CopK from *Cupriavidus metallidurans* CH34 Binds Cu(I) in a Tetrathioether Site: Characterization by X-ray Absorption and NMR Spectroscopy", *Journal of the American Chemical Society* **132** (2010) 3770–3777

Catalysis & material energy
Gorczyca A., Moizan V., Chizallet C., Proux O., Delnet W., Lahera E., Hazemann J.-L., Raybaud P., Joly Y., "Monitoring morphology and hydrogen coverage of subnanometric Pt/γ-Al_2O_3 particles by in situ HERFD-XANES and quantum simulations", *Angewandte Chemie* (2014) DOI: 10.1002/anie.201403585 "Very Important Paper"

Materials science
Rodolakis F., Hansmann P., Rueff J.-P., Toschi A., Haverkort M.W., Sangiovanni G., Saha-Dasgupta T., Held K., Sikora M., Alliot I., Itié J.-P., Baudelet F., Wzietek P., Metcalf P. and Marsi M., "Inequivalent routes through the Mott transition in V_2O_3 explored by x-ray absorption spectroscopy: pressure vs. temperature and doping", *Physical Review Letters* **104** (2010) 047401

7. Scientific production 2010-2014

The complete list of the publications based on results obtained on the CRG-IF XAS station (BM32, until 2002) and then on the CRG-FAME (BM30B) beamline can be found on the beamline ESRF website, with the corresponding DOI links:
http://www.esrf.fr/UsersAndScience/Experiments/CRG/BM30B/Bibliographie/biblioSiteFame.html

Moreover, bibliometric information about these articles can be obtained on the ResearcherId page of the beamline : http://www.researcherid.com/rid/G-9313-2012

Articles

2014-1 Alexandratos V.G., Behrends T., Van Cappellen P., "Sulfidization of Lepidocrocite and its Effect on Uranium Phase Distribution and Reduction", *Geochim. Cosmochim. Acta* (2014) in press

2014-2 Afanasiev P., "Synthesis of finely divided molybdenum sulfide nanoparticles in propylene carbonate solution", *J. Solid State Chem.* **213** (2014) 158-164

2014-3 Auffan M., Matson C. W., Rose J., Arnold M., Proux O., Fayard B., Liu W., Chaurand P., Wiesner M. R., Bottero J.-Y., Di Giulio R. T., "Salinity-dependent silver nanoparticle uptake and biotransformation in Atlantic killifish (*Fundulus heteroclitus*) embryos", *Nanotoxicology* **8** (2014) 167-176

2014-4 Bazarkina E.F., Pokrovski G.S., Hazemann J.-L., "Structure, stability and geochemical role of palladium chloride complexes in hydrothermal fluids", *Geochim. Cosmochim. Acta* (2014) in press

2014-5 Brugger J., Tooth B., Etschmann B., Liu W., Testemale D., Hazemann J.-L., Grundler P. V., "Structure and Thermal Stability of Bi(III) Oxy-Clusters in Aqueous Solutions", *Journal of Solution Chemistry* **43** (2014) 314-325

2014-6 Collin B., Doelsch E., Keller C., Cazevieille P., Tella M., Chaurand P., Panfili F., Hazeman J-L., Meunier J.-D. "Copper distribution and speciation in bamboo exposed to a high Cu concentration and Si supplementation. First evidence on the presence of reduced copper bound to sulfur compounds in Poaceae", *Environmental Pollution* **187** (2014) 22-30

2014-7 Cutruzzola F., Arcovito A., Giardina G., della Longa S., D'Angelo P., Rinaldo S., "Distal–proximal crosstalk in the heme binding pocket of the NO sensor DNR", *Biometals* **27** (2014) 763-773

2014-8 Dauphas N., Roskosz M., Alp E.E., Neuville D.R., Hu M.Y., Sio C.K., Tissot F.L.H., Zhao J., Tissandier L., Médard E.,Cordier C., "Magma redox and structural controls on iron isotope variations in Earth's mantle and crust", *Earth and Planetary Science Letters* **398** (2014) 127-140

2014-9 Durst J., Lopez-Haro M., Dubau L., Chatenet M., Soldo-Olivier Y., Guétaz L., Bayle-Guillemaud P., Maillard F., "Reversibility of Pt-Skin and Pt-Skeleton Nanostructures in Acidic Media", *J. Phys. Chem. Lett.* **5** (2014) 434-439

2014-10 Gorczyca A., Moizan V., Chizallet C., Proux O., Delnet W., Lahera E., Hazemann J.-L., Raybaud P., Joly Y., "Monitoring morphology and hydrogen coverage of subnanometric Pt/γ-Al_2O_3 particles by in situ HERFD-XANES and quantum simulations", *Angewandte Chemie* (2014)

2014-11 Jullien A.-S., Gateau C., Lebrun C., Kieffer I., Testemale D., Delangle P., "D-Penicillamine Tripodal Derivatives as Efficient Copper(I) Chelators", *Inorg. Chem.* **53** (2014) 5229-5239

2014-12 Khemiri A., Carrière M., Bremond N., Ben Mlouka M. A. , Coquet L., Llorens I., Chapon V., Jouenne T., Cosette P., Berthomieu C., "*Escherichia coli* response to uranyl exposure at low pH and associated protein regulations", *Plos One* **9** (2014) e89863

2014-13 Klein S., Sommer A., Distel L., Hazemann J.-L., Kroener W., Neuhuber W., Muller P., Proux O., Kryschi C., "Superparamagnetic Iron Oxide Nanoparticles as Novel X-ray Enhancer for Low-dose Radiation Therapy", *J. Phys. Chem. B* **118** (2014) 6159–6166

2014-14 Leclere C., Katcho N.A., Tourbot G., Daudin B., Proietti M. G., Renevier H., "Anisotropic In distribution in InGaN core-shell nanowires", *J. Appl. Phys.* **116** (2014) 013517

2014-15 Le Pape P., Quantin C., Morin G., Jouvin D., Kieffer I., Proux O., Ganbaja J., Ayrault S., "Zinc speciation in the suspended particulate matter of an urban river (Orge, France): influence of seasonality and urbanization gradient", *Environmental Science and Technology* (2014) in press

2014-16 Liu W., Etschmann B., Testemale D., Hazemann J.-L., Rempel K., Müller H., Brugger J., "Gold transport in hydrothermal fluids: Competition among the Cl^-, Br^-, HS^- and $NH_{3(aq)}$ ligands", *Chem. Geol.* **376** (2014) 11-19

2014-17 Llorens I., Solari P.L., Sitaud B., Bès R., Cammelli S., Hermange H., Othmane G., Safi S., Moisy P., Wahu S., Bresson C., Schlegel M.L., Menut D., Béchade J.-L., Martin P., Hazemann J.-L., Proux O., Den Auwer C., "X-ray Absorption Spectroscopy Investigations on Radioactive Matter using MARS Beamline at SOLEIL Synchrotron", *Radiochimica Acta* (2014) in press

2014-18 Louvel M., Sanchez-Valle C., Malfait W. J., Cardon H., Testemale D., Hazemann J.-L., "Constraints on the mobilization of Zr in magmatic-hydrothermal processes in subduction zones from in situ fluid-melt partitioning experiments", *American Mineralogist* **99** (2014) 1616-1625

2014-19 Monnier J., Réguer S., Foy E., Testemale D., Mirambet F., Saheb M., Dillmann P., Guillot I., "XAS and XRD in situ characterisation of reduction and reoxidation processes of iron corrosion products involved in atmospheric corrosion", *Corrosion Science* **78** (2014) 293-303

2014-20 Ould-Chikh S., Proux O., Afanasiev P., Khrouz L., Hedhili M., Anjum D., Harb M., Geantet C., Basset J.-M., Puzenat E., "Photocatalysis with Chromium-Doped TiO_2: Bulk and Surface Doping", *ChemSuschem* **7** (2014) 1361–1371

2014-21 Pokrovski G.S., Akinfiev N.N., Borisova A.Y., Zotov A.V., Kouzmanov K. "Gold speciation and transport in geological fluids: insights from experiments and physical-chemical modeling", in: *Geological Society of London Special Publication* "Gold-transporting fluids in the Earth's crust" (eds. P. Garofalo, E. Ripley), **402** (2014) 9-70

2014-22 Riglet-Martial Ch., Martin Ph., Testemale D., Sabathier-Devals C., Carlot G., Matheron P., Iltis X., Pasquet U., Valot C., Delafoy C., Largenton R., "Thermodynamics of chromium in UO_2 fuel: a solubility model", *J. Nucl. Mat.* **447** (2014) 63-72

2014-23 Schreck E., Dappe V., Sarret G., Sobanska S., Nowak D., Nowak J., Stefaniak E. A., Magnin V., Ranieri V., Dumat C., "Foliar or root exposures to smelter particles: Consequences for lead compartmentalization and speciation in plant leaves", *Sci. Total Environ.* **476-477** (2014) 667-676

2014-24 Tella M., Auffan M., Brousset L., Issartel J., Kieffer I., Pailles C., Morel E., Santaella C., Artells E., Rose J., Thiéry A., Bottero J.-Y., "Transfer, transformation and impacts of ceria nanomaterials in aquatic mesocosms simulating a pond ecosystem", *Environmental Science and Technology* **48** (2014) 9004–9013

2014-25 Tian Y., Etschmann B., Mei Y., Grundler P., Testemale D., Hazemann J.L., Elliott P., Ngothai Y., Brugger J., "Speciation and thermodynamic properties of Manganese (II) chloride complexes in hydrothermal fluids: *in situ* XAS study", *Geochim. Cosmochim. Acta* **129** (2014) 77-95

2014-26 Trepreau J., Grosse C., Mouesca J.-M., Sarret G., Girard E., Petit-Haertlein I., Kuennemann S., Desbourdes C., de Rosny E., Maillard A. P., Nies D. H., Covès J., "Metal sensing and signal transduction by CnrX from Cupriavidus metallidurans CH34: role of the only methionine assessed by a functional, spectroscopic, and theoretical study", *Metallomics* **6** (2014) 263-273

2013-1 Adra A., Morin G., Ona-Nguema G., Menguy N., Maillot F., Bruneel O., Casiot C., Lebrun S., Juillot F., Brest J., "Arsenic scavenging by Aluminum-substituted Ferrihydrites in a circumneutral pH river impacted by acid mine drainage", *Environ. Sci. Technol.*, **47** (2013) 12784–12792

2013-2 Alies B., Sasaki I., Proux O., Sayen S., Guillon E., Faller P., Hureau C., "Zn impacts Cu coordination to amyloid-β, the Alzheimer's peptide, but not the ROS production and the associated cell toxicity", *Chem. Com.* **49** (2013) 1214-1216

2013-3 Bès R., Gaillard C., Millard-Pinard N., Gavarini S., Martin P., Cardinal S., Esnouf C., Malchère A., Perrat-Mabilon A., "Xenon behavior in TiN: a coupled XAS/TEM study", *J. Nucl. Mat.* **434** (2013) 56-64

2013-4 Blanc N., Diaz-Sanchez L. E., Ramos A. Y., Tournus F., Tolentino H. C. N., De Santis M., Proux O., Tamion A., Tuaillon-Combes J., Bardotti L., Boisron O., Pastor G. M., Dupuis V., "Element-specific quantitative determination of the local atomic order in CoPt alloy nanoparticles: Experiment and theory", *Phys. Rev. B* **87** (2013) 155412

2013-5 Cochain B., Pinet O., Richet P., "Diffusion of sodium ions driven by charge compensation as the rate-limiting step of internal redox reactions", *J. Non-Cryst. Solids* **365** (2013) 23-26

2013-6 Cochain B., Neuville D.R., de Ligny D., Malki M., Testemale D., Pinet O., P. Richet, "Dynamics of iron-bearing borosilicate melts: Effects of melt structure and composition on viscosity, electrical conductivity and kinetics of redox reactions", *J. Non-Cryst. Solids* **373-374** (2013) 18-27

2013-7 Couture R.-M., Rose J., Kumar N., Mitchell K., Wallschläger D., Van Cappellen P., "Sorption of Arsenite, Arsenate, and Thioarsenates to Iron Oxides and Iron Sulfides: A Kinetic and Spectroscopic Investigation", *Environ. Sci. Technol.* **47** (2013) 5652–5659

2013-8 Couture R.-M., Wallschläger D., Rose J., Van Cappellen P., "Arsenic binding to organic and inorganic sulfur species during microbial sulfate reduction: a sediment flow-through reactor experiment", *Environ. Chem.* **10** (2013) 285-294

2013-9 Duffy P., Cullen R. J., Jayasundara D. R., Murphy D. M., Fonda E., Colavita P. E., "Electroless deposition and characterization of Fe/FeOx nanoparticles on porous carbon microspheres: structure and surface reactivity", *J. Mater. Chem. A* **1** (2013) 6043-6050

2013-10 Dupuis V., Blanc N., Diaz-Sanchez L. E., Hillion A., Tamion A., Tournus F., Pastor G. M., "Specific local relaxation and magnetism in mass-selected CoPt nanoparticles", *Eur. Phys. J. B* **86** (2013) 83

2013-11 Garad H., Ortega L., Ramos A.Y., Joly Y., Fettar F., Auffret S., Rodmacq B., Diény B., Proux O., Erko A. I., "Competition between CoOx and CoPt phases in Pt/Co/AlO_x semi tunnel junctions", *J. Appl. Phys.* **114** (2013) 053508

2013-12 Glorieux B., Jubera V., Orlova A. I., Kanunov A.E., Garcia A., Pallier C., Oleneva T.A., "Phosphors Based on $NaZr_2(PO_4)_3^-$ Type Calcium and Strontium Phosphates Activated with Eu^{2+} and Sm^{3+}", *Inorg. Mater.* **49** (2013) 82–88

2013-13 Gonçalves Ferreira P., de Ligny D., Lazzari O., Jean A., Cintora Gonzalez O., Neuville D.R., "Photoreduction of iron by a synchrotron X-ray beam in low iron content soda-lime silicate glasses", *Chem. Geol.* **346** (2013) 106-112

2013-14 Grundler P.V., Brugger J., Etschmann B.E., Helm L., Liu W., Spry P.G., Tian Y., Testemale D., Pring A., "Speciation of aqueous tellurium(IV) in hydrothermal solutions and vapors, and the role of oxidized tellurium species in Te transport and gold deposition", *Geochim. Cosmochim. Acta* **120** (2013) 298-325

2013-15 Hillion A., Cavallin A., Vlaic S., Tamion A., Tournus F., Khadra G., Dreiser J., Piamonteze C., Nolting F., Rusponi S., Sato K., Konno T. J., Proux O., Dupuis V., Brune H., "Low Temperature Ferromagnetism in Chemically Ordered FeRh Nanocrystals", *Phys. Rev. Lett.* **110** (2013) 087207

2013-16 Jullien A.-S., Gateau C., Kieffer I., Testemale D., Delangle P., "X-Ray Absorption Spectroscopy Proves the Trigonal Planar Sulfur-Only Coordination of Cu(I) with High Affinity Tripodal Pseudopeptides", *Inorg. Chem.* **52** (2013) 9954–9961

2013-17 Louvel M., Sanchez-Valle C., Malfait W. J., Testemale D., Hazemann J.-L., "Zr complexation in high pressure fluids and silicate melts and implications for the mobilization of HFSE in subduction zones", *Geochim. Cosmochim. Acta* **104** (2013) 281-299

2013-18 Maillot F., Morin G., Juillot F., Bruneel O., Casiot C., Ona-Nguema G., Wang Y., Lebrun S., Aubry E., Vlaic G., Brown G. E. Jr, "Structure and reactivity of As(III)- and As(V)-rich schwertmannites and amorphous ferric arsenate sulfate from the Carnoulès Acid Mine Drainage, France: Comparison with biotic and abiotic model compounds and implications for As remediation", *Geochim. Cosmochim. Acta* **104** (2013) 310-329

2013-19 Manceau A., Simionovici A., Lanson M., Perrin J., Tucoulou R., Bohic S., Fakra S. C., Marcus M., Bedell J.P., Nagy K., "Thlaspi arvense binds Cu(II) as a bis-(L-histidinato) complex on root cell walls in an urban ecosystem", *Metallomics* **5** (2013) 1674-1684

2013-20 Proietti M.G., Coraux J., Renevier H., "Grazing Incidence Diffraction Anomalous Fine Structure in the study of structural properties of nanostructures", *Characterization of Semiconductor Heterostructures and Nanostructures* (2^{nd} Edition), ed. G. Agostini & C. Lamberti, (2013) 311–359

2013-21 Qian Q., Brugger J., Testemale D., Skinner W., Pring A., "Formation of As(II)-pyrite during

experimental replacement of magnetite under hydrothermal conditions", *Geochim. Cosmochim. Acta* **100** (2013) 1-10

2013-22 Ramos A. Y., Tolentino H. C. N., Soares M. M., Grenier S., Bunau O., Joly Y., Baudelet F., Wilhelm F., Rogalev A., Souza R. A., Souza-Neto N. M., Proux O., Testemale D., Caneiro A., "Emergence of ferromagnetism and Jahn-Teller distortion in $LaMn_{1-x}Cr_xO_3$ (x<0.15)", *Phys. Rev. B (Rapid Communication - Editor's suggestion)* **87** (2013) 220404

2013-23 Rueff J.P., Shukla A., "A RIXS cookbook: Five recipes for successful RIXS applications", *J. Electron Spectrosc.***188** (2013) 10-16

2013-24 Sarret G., Pilon Smits E.A.H., Castillo Michel H., Isaure M.P., Zhao F.J., Tappero R., "Use of Synchrotron-Based Techniques to Elucidate Metal Uptake and Metabolism in Plants", *Advances in Agronomy*, editor Donald L. Sparks, **119** (2013) 1-82

2013-25 Schlegel M.L., Manceau A., "Binding mechanism of Cu(II) at the clay-water interface by powder and polarized EXAFS spectroscopy", *Geochim. Cosmochim. Acta* **113** (2013) 113-124

2013-26 Tooth B., Etschmann B., Pokrovski G.S., Testemale D., Hazemann J.-L., Grundler P., Brugger J., "Bismuth Speciation in Hydrothermal Fluids: An X-ray Absorption Spectroscopy and Solubility Study", *Geochim. Cosmochim. Acta* **101** (2013) 156-172

2013-27 Vichery C., Maurin I., Proux O., Kieffer I., Hazemann J.L., Cortès R., Boilot J.P., Gacoin T., "Introduction of cobalt ions in γ-Fe_2O_3 nanoparticles by direct coprecipitation or post-synthesis adsorption: dopant localization and magnetic anisotropy", *J. Phys. Chem. C* **117** (2013) 19672–19683

2012-1 Afanasiev P., Geantet C., Llorens I., Proux O., "Biotemplated synthesis of highly divided MoS_2 catalysts", *J. Mater. Chem.* **22** (2012) 9731-9737

2012-2 Arcovito A., della Longa S., "Local structure and dynamics of hemeproteins by X-ray Absorption Near Edge Structure spectroscopy", *J. Inorg. Biochem.* **112** (2012) 93-99

2012-3 Auffan M., Rose J., Proux O., Masion A., Liu W., Benameur L., Ziarelli F., Botta A., Chaneac C., Bottero J.-Y., "Magnetic nanoparticles and metalloid co-contamination of human dermal fibroblasts: is there a Trojan horse effect", *Environ. Sci. Technol.* **46** (2012) 10789–10796

2012-4 Bali R., Soares M. M., Ramos A. Y., Tolentino H.C.N., Yildiz F., Boudot C., Proux O., De Santis M., Przybylski M., Kirschner J., "Magnetic and structural properties of the Fe layers in CoO/Fe/Ag(001) heterostructure", *Appl. Phys. Lett.* **100** (2012) 132403

2012-5 Brugger J., Etschmann B., Grundler P.V., Liu W., Testemale D., Pring A., "XAS evidence for the stability of polytellurides in hydrothermal fluids up to 599 °C, 800 bar", *Am. Mineral.* **97** (2012) 1519-1522

2012-6 Chevreux S., Llorens I., Solari P. L., Roudeau S., Devès G., Carmona A., Testemale D., Hazemann J.-L., Ortega R., "Coupling of Native IEF and Extended X-ray Absorption Fine Structure to Characterize Zinc Binding Sites from pI Isoforms of SOD1 and A4V Pathogenic Mutant", *Electrophoresis* **33** (2012) 1276–1281

2012-7 Chillemi G., De Santis S., Falconi M., Mancini G., Migliorati V., Battistoni A., Pacello F., Desideri A., D'Angelo P., "Carbon monoxide binding to the heme group at the dimeric interface modulates structure and copper accessibility in the Cu,Zn superoxide dismutase from Haemophilus ducreyi: in silico and in vitro evidences", *J. Biomol. Struct. Dyn.* **30** (2012) 269-279

2012-8 D'Angelo P., Della Longa S., Arcovito A., Mancini G., Zitolo A., Chillemi G., Giachin G., Legname G., Benetti F., "Effects of the pathological Q212P mutation on human prion protein non-octarepeat copper binding site", *Biochemistry* **51** (2012) 6068–6079

2012-9 Dublet G., Juillot F., Morin G., Fritsch E., Fandeur D., Ona-Nguema G., Brown G. E. Jr., "Ni speciation in a New Caledonian lateritic regolith: a quantitative X-ray absorption spectroscopy investigation", *Geochim. Cosmochim. Acta* **95** (2012) 119-133

2012-10 El Beze L., Rose J., Mouillet V., Farcas F., Masion A., Chaurand P., Bottero J.-Y., "Location and evolution of the speciation of vanadium in bitumen and model of reclaimed bituminous mixes during ageing: Can vanadium serve as a tracer of the aged and fresh parts of the reclaimed asphalt pavement mixture?", *Fuel* **102** (2012) 423-430

2012-11 Geantet C., Pichon C., "X-Ray Absorption Spectroscopy", Ch. 12 of *Characterization of Solid Materials and Heterogeneous Catalysts: From Structure to Surface Reactivity*, M. Che & J.

C. Védrine editors, Wiley-VCH Verlag (2012) 511–536

2012-12 Giannozzi P., Jansen K., La Penna G., Minicozzi V., Morante S., Rossi G., Stellato F., "Zn induced structural aggregation patterns of β-amyloid peptides by first-principle simulations and XAS measurements", *Metallomics* **4** (2012) 156-165

2012-13 Huguet S., Bert V., Laboudigue A., Barthès V., Isaure M.-P., Llorens I., Schat H., Sarret G., "Cd speciation and localization in the hyperaccumulator Arabidopsis halleri", *Environ. Exp. Bot.* **82** (2012) 54-65

2012-14 Laurette J., Larue C., Llorens I., Jaillard D., Jouneau P.-H., Bourguignon J., Carrière M., "Speciation of uranium in plants upon root accumulation and root-to-shoot translocation: a XAS and TEM study", *Environ. Exp. Bot.* **77** (2012) 87-95

2012-15 Liu W., Chaurand P., Di-giorgio C., De Meo M., Thill A., Auffan M., Masion A., Borschneck D., Chaspoul F., Gallice P., Botta A., Bottero J.Y., Rose J. C., "Influence of the length of imogolite-like nanotubes on their cytotoxicity and genotoxicity towards human dermal cells", *Chem. Res. Toxicol.* **25** (2012) 2513–2522

2012-16 Llorens I., Lahera E., Delnet W., Proux O., Braillard A., Hazemann J.-L., Prat A., Testemale D., Dermigny Q., Gelebart F., Morand M., Shukla A., Bardou N., Ulrich O., Arnaud S., Berar J.-F., Boudet N., Caillot B., Chaurand P., Rose J., Doelsch E., Martin P., Solari P. L., "High energy resolution five-crystal spectrometer for high quality fluorescence and absorption measurements on an X-ray Absorption Spectroscopy beamline", *Rev. Sci. Instrum.* **83** (2012) 063104

2012-17 Llorens I., Untereiner G., Jaillard D., Gouget B., Chapon V., Carrière M., "Uranium interaction with two multi-resistant environmental bacteria: *Cupriavidus metallidurans* CH34 and *Rhodopseudomonas palustris*", *PLoS One* **7** (2012) e51783

2012-18 Picard A., Testemale D., Hazemann J.-L., Daniel I., "The influence of high hydrostatic pressure on bacterial dissimilatory iron reduction", *Geochim. Cosmochim. Acta* **88** (2012) 120-129

2012-19 Pokrovsky O.S., Pokrovski G.S., Shirokova L.S., Gonzalez A.G., Emnova E.E., Feurtet-Mazel A., "Chemical and structural status of copper associated with oxygenic and anoxygenic phototrophs and heterotrophs: possible evolutionary consequences", *Geobiology* **10** (2012) 130-149

2012-20 Priadi C., Morin G., Ayrault S., Maillot F., Juillot F., Alliot I., Testemale D., Proux O., Brown Jr G. E., "EXAFS and SEM evidence for zinc sulphide solid phases in riverine suspended matter from the Seine River, France", *Environ. Sci. Technol.* **46** (2012) 3712–3720

2012-21 Pujol A.M., Lebrun C., Gateau C., Manceau A., Delangle P., "Mercury-Sequestering Pseudopeptides with a Tris(cysteine) Environment in Water", *Eur. J. Inorg. Chem.* **24** (2012) 3835–3843

2012-22 Ranieri V., Haines J., Cambon O., Levelut C., Le Parc R., Cambon M., Hazemann J-L., "An *in situ* X-ray absorption Spectroscopy study of $Si_{1-x}Ge_xO_2$ dissolution and Ge aqueous speciation under hydrothermal conditions", *Inorg. Chem.* **51** (2012) 414–419

2012-23 Rinaldo S., Castiglione N., Giardina G., Caruso M., Arcovito A., della Longa S., D'Angelo P., Cutruzzolà F., "Unusual Heme Binding Properties of the Dissimilative Nitrate Respiration Regulator, a Bacterial Nitric Oxide Sensor", *Antioxidants & Redox Signaling* **17** (2012) 1178-1189

2012-24 Rose J., Auffan M., Proux O., Nivière V., Bottero J.-Y., "Physical-chemical properties of nanoparticles in relation with toxicity", *Encyclopedia of Nanotechnology*, B. Bhushan editor, Springer **16** (2012) 2075-2085

2012-25 Simonin L., Colin J.-F., Ranieri V., Canévet E., Martin J.-F., Bourbon C., Baehtz C., Strobel P., Daniel L., Patoux S., "In situ investigations on a Li-rich Mn-Ni layered oxide for Li-ion battery", *J. Mater. Chem.* **22** (2012) 11316-11322

2012-26 Souleiman M. Cambon O. Haidoux A. Haines J. Levelut C., Ranieri V., Hazemann J.-L., "Study of Ga^{3+}-induced hydrothermal crystallization of a α-quartz type $Ga_{1-x}Fe_xPO_4$ single crystal by *in-situ* X-ray Absorption Spectroscopy (XAS)", *Inorg. Chem.* **51** (2012) 11811–11819

2012-27 Tella M., Pokrovski G.S., "Structure and stability of pentavalent antimony complexes with aqueous organic ligands", *Chem. Geol.* **292-293** (2012) 57-68

2012-28 Tougerti A., Llorens I., D'acapito F., Fonda E., Hazemann J.-L., Joly Y., Thiaudière D., Che

M., Carrier X., "Surface Science Approach to the Solid–Liquid Interface: Surface-Dependent Precipitation of $Ni(OH)_2$ on α-Al_2O_3 Surfaces", *Angewandte Chemie* **124** (2012) 7817–7821

2012-29 Volant A., Desoeuvre A., Casiot C., Lauga B., Delpoux S., Morin G., Personné J.C., Héry M., Elbaz-Poulichet F., Bertin P.N., Bruneel O., "Temporal variation in the arsenic-rich creek sediments of Carnoulès Mine, France", *Extremophiles* **16** (2012) 645-657

2012-30 Yang X., Gondikas A., Marinakos S. M., Auffan M., Liu J., Hsu-Kim H., Meyer J., "The mechanism of silver nanoparticle toxicity is dependent on dissolved silver and surface coating in *Caenorhabditis elegans*", *Environ. Sci. Technol.* **46** (2012) 1119–1127

2011-1 Alies B., Pradines V., Llorens-Alliot I., Sayen S., Guillon E., Hureau C., Faller P., "Zinc(II) modulates specifically amyloid formation and structure in model peptides", *J. Biol. Inorg. Chem.* **16** (2011) 333-340

2011-2 Arcovito A., Della Longa S., "Ligand Binding Intermediates of Nitrosylated Human Hemoglobin Induced at Low Temperature by X-ray Irradiation", *Inorg. Chem.* **50** (2011) 9423–9429

2011-3 Charlet L., Morin G., Rose J., Wang Y., Auffan M., Burnol A., Fernandez-Martinez A., "Reactivity at (nano)particle-water interfaces, redox processes, and arsenic transport in the environment", *Comptes Rendus Geoscience* **343** (2011) 123-139

2011-4 D'Angelo P., Zitolo A., Migliorati V., Bodo E., Aquilanti G., Hazemann J.-L., Testemale D., Mancini G., Caminiti R., "X-Ray absorption spectroscopy investigation of 1-alkyl-3-methylimidazolium bromide salts", *J. Chem. Phys.* **135** (2011) 074505

2011-5 Dupuis V., Blanc N., Tournus F., Tamion A., Tuaillon-Combes J., Bardotti L., Boisron O., "Local Order and Magnetic Properties in Mass-Selected L10 CoPt Nanoparticles", *IEEE Transactions on Magnetics* **47** (2011) 3358 - 3361

2011-6 Iadecola A., Joseph B., Puri A., Simonelli L., Mizuguchi Y., Testemale D., Proux O., Hazemann J.-L., Takano Y., Saini N. L., "Random alloy-like local structure of $Fe(Se,S)_{1-x}Te_x$ superconductors revealed by extended X-ray absorption fine structure", *J. Phys. Condens. Mat.* **23** (2011) 425701

2011-7 Le Bacq O., Machon D., Testemale D., Pasturel A., "Pressure-induced amorphization mechanism in $Eu_2(MoO_4)_3$", *Phys. Rev. B* **83** (2011) 214101

2011-8 Liu W., Borg S., Testemale D., Brugger J., Etschmann B., Hazemann J.-L., "Speciation and thermodynamic properties for cobalt chloride complexes in hydrothermal fluids at 35-440 C and 600 bar: an in-situ XAS study", *Geochim. Cosmochim. Acta* **75** (2011) 1227–1248

2011-9 Mondani L, Benzerara K., Carrière M., Christen R., Mamindy-Pajany Y., Février L., Marmier N., Achouak W., Nardoux P., Berthomieu C., Chapon V., "Influence of uranium on bacterial communities: a comparison of natural uranium-rich soils with controls", *PLoS One* **6** (2011) e25771

2011-10 Montes-Hernandez G., Sarret G., Hellmann R., Menguy N., Testemale D., Charlet L., Renard F., "Nanostructured calcite precipitated under hydrothermal conditions in the presence of organic and inorganic selenium", *Chem. Geol.* **290** (2011) 109-120

2011-11 Nagy K. L., Manceau A., Gasper J. D., Ryan J. N., Aiken G. R., "Metallothionein-Like Multinuclear Clusters of Mercury(II) and Sulfur in Peat", *Environ. Sci. Technol.* **45** (2011) 7298–7306

2011-12 Nguyen T.S., Loridant S., Lorentz C., Cholley T., Geantet C., "Effect of glycol on the formation of active species and sulfidation mechanism of $CoMoP/Al_2O_3$ hydrotreating catalysts", *Appl. Catal. B - Environ.* **107** (2011) 59-67

2011-13 Picard, A., Daniel, I., Testemale, D., Letard, I., Bleuet, P., Cardon, H., Oger, P., "Monitoring of microbial redox transformations under high pressure using in situ x-ray absorption spectroscopy", *Geobiology* **9** (2011) 196-204

2011-14 Rodolakis F., Rueff J.-P., Sikora M., Alliot I., Itié J.-P., Baudelet F., Ravy S., Wzietek P., Hansmann P., Toschi A., Haverkort M.W., Sangiovanni G., Held K., Metcalf P. and Marsi M., "Evolution of the electronic structure of a Mott system across its phase diagram: X-ray absorption spectroscopy study of $(V_{1-x}Cr_x)_2O_3$", *Phys. Rev. B* **84** (2010) 245113

2011-15 Stellato F., Spevacek A., Proux O., Minicozzi V., Millhauser G., Morante S., "Zinc ions modulate the Cu coordination mode in Prion protein octa-repeat subdomains", *Eur. Biophys. J.* **40** (2011) 1259-1270

2011-16 Testemale D., Pokrovski G.S., Hazemann J.-L., "Speciation of As^{III} and As^{V} in hydrothermal fluids by in situ X-ray absorption spectroscopy", *Eur. J. Mineral.* **23** (2011) 379-390

2011-17 Trepreau J., de Rosny E., Duboc C., Sarret G., Petit-Hartlein I., Maillard A. P., Imberty A., Proux O., Covès J., "Spectroscopic characterization of the metal-binding sites in the periplasmic metal-sensor domain of CnrX from *Cupriavidus metallidurans* CH34", *Biochemistry* **50** (2011) 9036–9045

2010-1 Arcovito A., Bonamore A., Hazemann J.-L., Boffi A., D'Angelo P., "Unusual proximal heme pocket geometry in the deoxygenated Thermobifida fusca: A combined spectroscopic investigation", *Biophys. Chem.* **147** (2010) 1-7

2010-2 Arcovito A., Ardiccioni C., Cianci M., D'Angelo P., Vallone B., Della Longa S., "Polarized X-ray Absorption Near Edge Structure spectroscopy of Neuroglobin and Myoglobin Single Crystals", *J. Phys. Chem. B* **114** (2010) 13223–13231

2010-3 Aurelio G., Fernandez-Martinez A., Cuello G.J., Roman-Ross G., Alliot I., Charlet L., "Structural study of selenium(IV) substitutions in calcite", *Chem. Geol.* **270** (2010) 249-256

2010-4 Bazarkina E. F., Pokrovski G. S., Zotov A. V., Hazemann J.-L., "Structure and stability of cadmium chloride complexes in hydrothermal fluids", *Chem. Geol.* **276** (2010) 1-17

2010-5 Benetti F., Ventura M., Salmini B., Ceola S., Carbonera D., Mammi S., Zitolo A., D'Angelo P., Urso E., Maffia M., Salvato B., Spisni E., "Cuprizone neurotoxicity, copper deficiency and neurodegeneration", *NeuroToxicology* **31** (2010) 509–517

2010-6 Borisova A.Y., Pokrovski G.S., Pichavant M., Freydier R., Candaudap F., "Arsenic enrichment in hydrous peraluminous melts: insights from femtosecond laser ablation – inductively coupled plasma – quadrupole mass spectrometry, and in situ X-ray absorption fine structure spectroscopy", *Am. Mineral.* **95** (2010) 1095-1104

2010-7 Cabaret D., Bordage A., Juhin A., Arfaoui M., Gaudry E., "First-principles calculations of X-ray absorption spectra at the K-edge of 3d transition metals: an electronic structure analysis of the pre-edge", *Phys. Chem. Chem. Phys.* **12** (2010) 5619–5633

2010-8 Camarillo-Ravelo D., Kaftandjian V., Duvauchelle P., "Accurate standard-based quantification of X-ray fluorescence data using metal-contaminated plant tissue", *X-Ray Spectrom.* **39** (2010) 391–398

2010-9 Collins R. N., Bakkaus E., Carrière M., Khodja H., Proux O., Morel J.-L., Gouget B., "Uptake, localization and speciation of cobalt in *Triticum aestivum L.* (wheat) and *Lycopersicon esculentum M.* (tomato)", *Environ. Sci. Technol.* **44** (2010) 2904–2910

2010-10 D'Angelo P., Zitolo A., Pacello F., Mancini G., Proux O., Hazemann J.-L., Desideri A., Battistoni A. "Fe-heme structure in Cu,Zn superoxide dismutase from Haemophilus ducreyi by X-ray Absorption Spectroscopy", *Arch. Biochem. Biophys.* **498** (2010) 43–49

2010-11 D'Angelo P., Della Longa S., Arcovito A., Anselmi M., Di Nola A., Chillemi G. "Dynamic Investigation of Protein Metal Active Sites: Interplay of XANES and Molecular Dynamics Simulations", *J. Am. Chem. Soc.* **132** (2010) 14901–14909

2010-12 Daval D., Testemale D., Recham N., Tarascon J.-M., Siebert J., Martinez I., Guyot F., "Fayalite (Fe_2SiO_4) dissolution kinetics determined by X-ray absorption spectroscopy", *Chem. Geol.* **275** (2010) 161-175

2010-13 Della Longa S., Arcovito A., "X-rays induced lysis of the Fe-CO bond in carbonmonoxy-myoglobin", *Inorg. Chem.* **49** (2010) 9958–9961

2010-14 Etschmann B., Liu W., Testemale D. Müller H., Proux O., Hazemann J.-L., Brugger J., "An in situ XAS study of copper transport in hydrothermal sulfuric solutions (25 °C to 600 °C, 600 to 180 bar): speciation and partitioning between vapor and liquid phases", *Geochim. Cosmochim. Acta* **74** (2010) 4723-4739

2010-15 Hollner S., Mirambet F., Rocca E., Réguer S., "Evaluation of new non-toxic corrosion inhibitors for conservation of iron artefacts", *Corros. Eng. Sci.Techn.* **45** (2010) 362-366

2010-16 Iadecola A., Joseph B., Simonelli L., Mizuguchi Y., Takano Y., Saini N. L., "Determination of the local structure in $FeSe_{0.25}Te_{0.75}$ single crystal by polarized EXAFS", *Europhys. Lett.* **90** (2010) 67008

2010-17 James-Smith J., Cauzid J., Testemale D., Liu W., Hazemann J.-L., Proux O., Etschmann B., Philippot P., Banks D., Williams P., Brugger J., "Arsenic Speciation in fluid inclusions using X-ray Absorption Spectroscopy", *Am. Mineral.* **95** (2010) 921–932

2010-18 Joly Y., "Interaction Matter-Polarized Light", in *Magnetism and Synchrotron Radiation*, Eric Beaurepaire, Hervé Bulou, Fabrice Scheurer, Jean-Paul Kappler (Ed.), Springer, (2010) 77-126

2010-19 Juhin A., Morin G., Elkaim E., Frost D. J., Juillot F., Calas G., "Structure refinement of a synthetic knorringite, $Mg_3Cr_2Si_3O_{12}$", *Am. Mineral.* **95** (2010) 59-63

2010-20 Legros S., Doelsch E., Masion A., Rose J., Borschneck D., Proux O., Hazemann J-L., Saint-Macary H., Bottero J-Y., "Combining size fractionation, scanning electron microscopy and X-ray absorption spectroscopy to probe Zn speciation in pig slurry", *J. Environ. Qual.* **39** (2010) 531-540

2010-21 Liscio F., Maret M., Meneghini C., Mobilio S., Proux O., Makarov D., Albrecht M., "Structural origin of perpendicular magnetic anisotropy in epitaxial $CoPt_3$ nanostructures grown on WSe_2(0001)", *Phys. Rev. B* **81** (2010) 125417

2010-22 Manceau A., Matynia A., "The Nature of Cu Bonding to Natural Organic Matter", *Geochim. Cosmochim. Acta* **74** (2010) 2556–2580

2010-23 Mirambet F., Reguer S., Rocca E., Hollner S., Testemale D., "A complementary set of electrochemical and X-ray synchrotron techniques to determine the passivation mechanism of iron treated in a new corrosion inhibitor solution specifically developed for the preservation of metallic artefacts", *Appl. Phys. A - Mater. Sci. Process.* **99** (2010) 341-349

2010-24 Petit-Hærtlein I., Girard E., Sarret G., Hazemann J.-L., Gourhant P., Kahn R., Coves J., "Evidence for conformational changes upon copper binding to Cupriavidus metallidurans CzcE", *Biochemistry* **49** (2010) 1913–1922

2010-25 Rodolakis F., Hansmann P., Rueff J.-P., Toschi A., Haverkort M.W., Sangiovanni G., Saha-Dasgupta T., Held K., Sikora M., Alliot I., Itié J.-P., Baudelet F., Wzietek P., Metcalf P. and Marsi M., "Inequivalent routes through the Mott transition in V_2O_3 explored by x-ray absorption spectroscopy: pressure vs. temperature and doping", *Phys. Rev. Lett.* **104** (2010) 047401

2010-26 Sammut M.L., Noack Y., Rose J., Hazemann J.-L., Proux O., Depoux M., Ziebel A., Fiani E., "Speciation of Cd and Pb in dust emitted from sinter plant", *Chemosphere* **78** (2010) 445-450

2010-27 Sarret G., Favier A., Covès J., Hazemann J.-L., Mergeay M., Bersch B. "CopK from *Cupriavidus metallidurans* CH34 Binds Cu(I) in a Tetrathioether Site: Characterization by X-ray Absorption and NMR Spectroscopy", *J. Am. Chem. Soc.* **132** (2010) 3770–3777

2010-28 Vespa M., Lanson M., Manceau A., "Natural Attenuation of Zinc Pollution in Smelter-Affected Soil", *Environ. Sci. Technol.* **44** (2010) 7814–7820

2010-29 Villain O., Galoisy L., Calas G., "Spectroscopic and structural properties of Cr^{3+} in silicate glasses: Cr^{3+} does not probe the average glass structure", *J. Non-Cryst. Solids* **356** (2010) 2228-2234

Conferences proceedings

2014-1 Dupuis V., Tamion A., "Atomic relaxation effects on magnetism in CoPt nanoalloys", *Journal of Physics: Conference Series* **521** (2014) 012001

2013-1 Dupuis V., Blanc N., Diaz-Sanchez L. E., Hillion A., Tamion A., Tournus F., Pastor G. M., Rogalev A., Wilhem F., "Finite size effects on structure and magnetism in mass-selected CoPt nanoparticles", *Eur. Phys. J. D* **67** (2013) 25

2013-2 Lay-Grindler E., Laurencin J., Villanova J., Kieffer I., Usseglio-Viretta F., Le Bihan T., Bleuet P., Mansuy A., Delette G., "Degradation study of the $La_{0.6}Sr_{0.4}Co_{0.2}Fe_{0.8}O_3$ solid oxide electrolysis cell (SOEC) anode after high temperature electrolysis operation", *ECS Trans.* **57** (2013) 3177-3187

2013-3 Tella M., Proux O., Hazeman J.-L., Briois V., Bravin M.N., Doelsch E., "Combining X-ray absorption spectroscopy (XAS) and diffusive gradients in thin films (DGT) to probe speciation and dynamic of heavy metals in soils amended with organic wastes", *15th Int. Conf. of the Research Network on Recycling of Agricultural and Industrial Residues in Agriculture*, Versailles (3-5 June 2013) Vallez, G.; Houot, S.; Formisano, S.; Cheviron, N.; Revallier, A.; Lepeuple, A.; Bacheley, H.; Cambier, P. (Ed.) S.02-3

2011-1 Laulhé C., Hippert F., Kreisel J., Pasturel A., Simon A., Hazemann J.-L., Bellissent R. & Cuello G. J. "Random local strain effects in the relaxor ferroelectric $BaTi_{1-x}Zr_xO_3$: experimental and theoretical investigation", *Phase Transitions* **84** (2011) 438-452

2011-2 Saffré D., Atinault E., Pin S., Renault J.-P., Hazemann J.-L., Baldacchino G., "In situ UV-visible spectrum acquisition of Br_3^-. Investigations of concentrated HBr aqueous solutions under 13-keV X-rays", *Journal of Physics: Conference Series* **261** (2011) 012013

2011-3 Soares M. M., Tolentino H. C. N., De Santis M., Ramos A. Y., Cezar J. C., "Highly anisotropic epitaxial L10 FePt on Pt(001)", *J. Appl. Phys.* **109** (2011) 07D725

Highlights

2014-1 Manceau A., Simionovici A., Lanson M., Perrin J., Tucoulou R., Bohic S., Fakra S. C., Marcus M., Bedell J.P., Nagy K., "Molecular form of copper in root cells of a non-hyperaccumulating plant grown in an urban setting", *ESRF Spotlight on Science* (2014)

2013-1 Andrault D., Antonangeli D., Dmitriev V., Filinchuk Y., Hanfland M., M. Hazemann J.L., Krisch M., Mayanovic R., Mezouar M., Monaco G., Pascarelli S., Rüffer R., Testemale D., Torchio R., "Science under Extreme Conditions of Pressures and Temperatures at the ESRF", *Synchrotron Radiation News* **26** (2013) 39-44

2013-2 Tougerti A., Llorens I., D'acapito F., Fonda E., Hazemann J.-L., Joly Y., Thiaudière D., Che M., Carrier X., "Surface Science Approach to the Solid–Liquid Interface: Surface-Dependent Precipitation of $Ni(OH)_2$ on α-Al_2O_3 Surfaces", *ESRF Highlights 2012* (2013) 117-118

2012-1 Goffé B., Christmann P., Vidal O., "La recherche pour l'utilisation durable des ressources minérales", *Géosciences* **15** (2012) 80-89

2011-1 Doelsch E., Auffan M., Bottero J.-Y., Chaurand P., Legros S., Levard C., Masion A., Rose J., "Déchets et nanomatériaux : valorisation, dépollution, impacts environnementaux et toxicologiques", *L'Actualité Chimique* **356-357** (2011) 91-96

2011-2 Faller P., Hureau C., "Impact of metallic ions in Alzheimer's disease: insights from XAS spectroscopy", *L'Actualité Chimique* **356-357** (2011) 88-90

2011-3 Picard, A., Daniel, I., Testemale, D., Letard, I., Bleuet, P., Cardon, H., Oger, P., "Why geobiology runs deeper", *ESRF Newsletter* **57** (2011) 7

2011-4 Sarret G., Favier A., Covès J., Hazemann J.-L., Mergeay M., Bersch B., "An original Cu(I)-coordination shell in a small bacterial metalloprotein identified by XAS and NMR spectroscopy", *ESRF Highlights 2010* (2011) 101-102

2010-1 Cotte M., Auffan M., Degruyter W., Fairchild I., Newton M.A., Morin G., Sarret G., Scheinost A.C., "Environmental Sciences at the ESRF", *Synchrotron Radiation News* **23** (2010) 28-35

2010-2 Doelsch E., "Nanotubes dépolluants", *La Nature comme modèle pour une intensification écologique de l'agriculture*, CIRAD (2010) 13

2010-3 Doelsch E., "Les imogolites, des nanoparticules qui piègent le nickel", *Le CIRAD en 2009* (2010) 66-67

2010-4 Sarret G., Favier A., Covès J., Hazemann J.-L., Mergeay M., Bersch B. "An original Cu(I)-coordination shell in a small bacterial metalloprotein identified by XAS and NMR spectroscopy", *ESRF Spotlight on Science* (2010)

2010-5 Huguet S., Sarret G., Bert V., Isaure M.-P., Proux O., Flank A.-M., Hammade V., Bulteel D., Laboudigue "La phytoextraction est-elle un traitement "vert" approprié pour les sédiments contaminés en métaux ?", *Revue Paralia* **3** (2010) 4.1–4.14

PhD thesis and french Habilitations à Diriger les Recherches

2014-1 Gorczyca A., " Caractérisation de catalyseurs métalliques supportés par spectroscopie XANES. Apports du calcul quantique dans l'interprétation des spectres expérimentaux", *PhD Institut National Polytechnique de Grenoble* (2014)

2014-2 Leonardo T., "Mécanismes d'accumulation et impact biologique de l'argent et du cobalt chez la micro-algue *Coccomyxa actinabiotis*", *PhD Univ. J. Fourier, Grenoble* (2014)

2013-1 Devineau S., "Adsorption des protéines sur les nanomatériaux. Biochimie et Physico-chimie d'un nouveau stress", *PhD Univ. Paris Sud* (2013)

2013-2 Dublet G., "Relation entre spéciation et distribution du nickel dans les couvertures d'altération latéritique des roches ultrabasiques de Nouvelle-Calédonie", *PhD P. et M. Curie, Paris* (2013)

2013-3 Jonchière R., "Solvatation supercritique de métaux précieux : apports de la simulation moléculaire", *PhD Univ. P. et M. Curie, Paris* (2013)

2013-4 Leclere Cédric, "Spectroscopies X et diffraction anomale de boîtes quantiques GaN et d'hétéro-structures III-N : inter-diffusion et ordre à courte distance", *PhD Institut National Polytechnique de Grenoble* (2013)

2013-5 NDiaye W., "Etude par photoémission résolue en angle et en spin de Mn_5Ge_3/Ge(111) en couches minces", *PhD Univ. Cergy-Pontoise* (2013)

2013-6 Schild F., "Caractérisation biochimique et l'implication dans la réponse au stress de la protéine Sélénium Binding Protein 1 (SBP1)", *PhD Univ. J. Fourier de Grenoble* (2013)

2013-7 Tooth B., "Geochemistry of Bismuth under hydrothermal conditions: constraining the bismuth collector model", *PhD Univ. Adelaide* (2013)

2013-8 Tian Y., "XAS studies of metal speciation in hydrothermal fluids ", *PhD Univ. Adelaide, school: Chemical Engineering* (2013)

2012-1 De Santis S., "Joined application of computational and experimental methods to the structural and dynamic study of proteins", *Dottorato di Ricerca in Scienze Chimiche, Università degli studi di Roma "la Sapienza"* (2012)

2012-2 Diot M.-A., "Etude du vieillissement et de l'altération de nanocomposites de la vie courante", *PhD Univ. Aix-Marseille* (2012)

2012-3 Durst J., "Etude du Vieillissement des Assemblages Membrane-Electrodes pour Piles à Combustible Basse Température", *PhD Institut National Polytechnique de Grenoble* (2012)

2012-4 Garad H. M., "L'anisotropie magnétique perpendiculaire induite par oxydation et recuit thermique : De la structure au magnétisme", *PhD Univ. J. Fourier, Grenoble* (2012)

2012-5 Le Pape P., "Etude de la dynamique, des sources et de la spéciation des éléments traces dans le bassin versant de l'Orge (Essonne, France)", *PhD Univ. Paris Sud* (2012)

2012-6 Puri A., "Experiments on strongly correlated materials under extreme conditions", *Dottorato di Ricerca in Scienza dei Materiali, Università degli studi di Roma La Sapienza* (2012)

2012-7 Sibert E., "Étude de l'interface électrochimique à l'aide de surfaces monocristallines caractérisées *in situ*", *Habilitation à Diriger des Recherches, Univ. J. Fourier de Grenoble* (2012)

2012-8 Vichery C., "Procédé de recuit protégé appliqué à des nanoparticules d'oxyde de fer: étude des relations structure / propriétés magnétiques", *PhD Ecole Polytechnique* (2012)

2012-9 Volant A., "Etude des communautés microbiennes (bactéries, Archaea et eucaryotes) et leurs variations spatiotemporelles dans la mine de Carnoulès fortement contaminée en arsenic", *PhD Univ. Montpellier II* (2012)

2011-1 Collin B., "Rôle du silicium sur la tolérance au cuivre et la croissance des bambous", *PhD Univ. P. Cézanne* (2011)

2011-2 Gotteland D., "Procédé d'hydroconversion par catalyse dispersée des résidus lourds pétroliers", *PhD Univ. C. Bernard Lyon 1* (2011)

2011-3 Iadecola A., "Local structural studies of Fe-based superconductors", *PhD. in Material Science, Università degli studi di Roma "la Sapienza"* (2011)

2011-4 Laurette J., "Rôle de la spéciation de l'uranium sur sa bioaccumulation, son transport et sa toxicité dans les plantes. Application à la phytoremédiation", *PhD AgroParisTech* (2011)

2011-5 Lenoir T., "Mécanismes de rétention du cuivre dans les sols: évaluation statistique des approches macroscopiques et spectroscopiques", *PhD Univ. J. Fourier de Grenoble* (2011)

2011-6 Louvel M., "Partition coefficient of trace elements between fluids and silicate melts at high pressure - high temperature : Implications for magma genesis in subduction zones", *PhD of Institute of Geochemistry and Petrology, ETH Zurich* (2011)

2011-7 Maillot F., "Structure local des nano-oxyhydroxydes de fer (III) de type ferrihydrite et

schwertmannite", *PhD Univ. P. et M. Curie, Paris* (2011)

2011-8 Mei Y., "Metal Mobility in Hydrothermal Fluids: Insights from Molecular Dynamics Simulations", *PhD Univ. Adelaide, school: geochemistry and geology* (2011)

2011-9 Michel A., "Etude du comportement des gaz de fission dans le dioxyde d'uranium : mécanismes de diffusion, nucléation et grossissement des bulles", *PhD Univ. de Caen* (2011)

2011-10 Quian G., "Formation of Fe sulfides via dissolution-reprecipitation reactions", *PhD Univ. Adelaide* (2011) *lan Wark Research Institute Medal* (2011)

2011-11 Saffré D., "Radiolyse de l'eau dans des conditions extrêmes de température et de TEL. Capture de HO^+ par les ions Br^-", *PhD Univ. Paris Sud* (2011)

2011-12 Soares M., "Croissance, structure et magnétisme dans les systèmes à décalage d'échange FM / AFM : approche fondamentale par la physique des surfaces", *PhD Univ. J. Fourier, Grenoble* (2011)

2011-13 Trepreau J., " Perception du stress métallique (nickel/cobalt) par le système de signalisation transmembranaire Cnr chez Cupriavidus metallidurans CH34", *PhD Univ. J. Fourier, Grenoble* (2011)

2010-1 Bes R., "Comportement thermique du xénon dans le nitrure de titane fritté matrice inerte d'intérêt des RNR-G", *PhD Univ. C. Bernard Lyon 1* (2010)

2010-2 Doelsch E., " Étude du comportement des éléments majeurs et traces à l'interface eau-sol-plante: une approche multi-technique et multi-échelle", *Habilitation à Diriger des Recherches, Univ. P. Cézanne* (2010)

2010-3 Juillot F., "Apport d'une approche combinant la cristallochimie et la géochimie isotopique à la compréhension du comportement des éléments traces métalliques dans les environnements continentaux", *Habilitation à Diriger des Recherches, Univ. Paris 7* (2010)

2010-4 Priadi C. R., "Caractérisation des phases porteuses : Métaux particulaires en Seine", *PhD Univ. Paris Sud* (2010)

2010-5 Stellato F., "X-ray Absorption Spectroscopy: a powerful tool for structural studies of molecules involved in the pathogenesis of neurodegenerative diseases", *Dottorato di Ricerca in Fisica, Università degli studi di Roma Tor Vergata* (2010)